ESCUELA TÉCNICA SUPERIOR DE INGENIEROS INDUSTRIALES Y DE TELECOMUNICACIÓN

Titulación :

INGENIERO INDUSTRIAL

Título del proyecto:

EXPERIMENTAL STUDY OF THE PERFORMANCE OF MICROTABS FOR LOAD ALLEVIATION IN WIND TURBINES

Asier Herrero Barandica

Tutor: Pablo Sanchís Gúrpide

Pamplona, 23 de Julio de 2012

upna Universidad Pública de Navarra Nafarroako Unibertsitate Publikoa
Todos los derechos reservados
Eskubide guztiak erresalbatu dira

ESCUELA TÉCNICA SUPERIOR DE INGENIEROS INDUSTRIALES Y DE TELECOMUNICACIÓN

Titulación :

INGENIERO INDUSTRIAL

Título del proyecto:

EXPERIMENTAL STUDY OF THE PERFORMANCE OF MICROTABS FOR LOAD ALLEVIATION IN WIND TURBINES

Iñigo Solana Arocena

Tutor: Pablo Sanchís Gúrpide

Pamplona, 23 de Julio de 2012

This Project was accomplished in the Erasmushogeschool Brussel and is the result of the Erasmus student exchange program and the relationship between Universidad Pública de Navarra and Erasmushogeschool Brussel. The development of the project was carried out by Asier Herrero Barandica and Iñigo Solana Arocena, who collaborated in this work.

Pamplona, July 23rd, 2012.

upna Universidad Pública de Navarra Nafarroako Unibertsitate Publikoa
Todos los derechos reservados
Eskubide guztiak erresalbatu dira

EXPERIMENTAL STUDY OF THE PERFORMANCE OF MICROTABS FOR LOAD ALLEVIATION IN WIND TURBINES

Academic year 2011 - 2012

Asier Herrero Barandica

Iñigo Solana Arocena

Promoter: Dr. Ing. Tim De Troyer

Master thesis proposed for the degree of Master in Industrial Sciences

- Electromechanics -

upna Universidad Pública de Navarra Nafarroako Unibertsitate Publikoa
Todos los derechos reservados
Eskubide guztiak erresalbatu dira

Acknowledgments:

The accomplishment of this thesis would not have been possible without the invaluable help of many people who have supported us along this experience. It is not only our duty but a pleasure to thank all of them for their help.

First of all, we would like to express our most sincere gratitude to our families, who have stayed by our side during our lives, making our dreams and needs come true. Without them we would not be who we are. And also thank our girlfriends, Arantza and Anabel, who have been patient in the distance and shared the best and the worst moments.

Thanks to our promoters; Tim De Troyer, who has been guiding us during the thesis, and has given us meaningful advice, and Pablo Sanchís, as our promoter in the Universidad Pública de Navarra.

Thanks also to the people of the FabLabXL in the Erasmushogescool Brussel, especially to Lieven Standaert, Serge Kubera, Stijn De Mil and Ronald van Ham, who have introduced us into new manufacturing techniques, helped us to find solutions and made the hours spent in the lab enjoyable.

We are also grateful to Mario Carbonaro from the Von Karman Institute, who shared his knowledge about wind tunnel testing.

We do not want to forget the universities. Thanks to the Erasmushogeschool Brussel, especially to the Department of Aerodynamics, for giving us the chance of learning and researching in such an interesting area. And thanks also to the Universidad Pública de Navarra, our alma mater, for forming us as engineers and taking us into maturity.

Last, but not least, we would like to thank our friends and colleagues, for all the support that they have given us during these months. Thanks to the friends that we have met as Erasmus students, for making the experience something unique that we will always remember. And thanks to our friends in Pamplona, with whom we have shared our lives and have shaped the path which has taken us here.

Thank you very much.

upna Universidad Pública de Navarra Nafarroako Unibertsitate Publikoa
Todos los derechos reservados
Eskubide guztiak erresalbatu dira

Index

upna Universidad Pública de Navarra Nafarroako Unibertsitate Publikoa
Todos los derechos reservados
Eskubide guztiak erresalbatu dira

upna Universidad Pública de Navarra Nafarroako Unibertsitate Publikoa
Todos los derechos reservados
Eskubide guztiak erresalbatu dira

upna Universidad Pública de Navarra Nafarroako Unibertsitate Publikoa
Todos los derechos reservados
Eskubide guztiak erresalbatu dira

Preface

The goal of this thesis is to carry out an experimental study of the performance of smart blades reducing extreme and/or cyclic loads for their use in wind turbines.

First of all, theoretical research about wind turbines and smart blades was done. Some of this information is explained in the thesis in order to set the background and make it more readable and understandable (*Chapters 1 to 3*). At the same time, the available wind tunnel was studied, in order to know its characteristics, decide whether it was appropriate for the experiments that would take place, and make the improvements needed for better results (*Chapter 4*).

The next step was to choose a blade profile that would fit well the requirements of the experiments and the manufacture of the set up. Besides, one of the possible smart devices had to be chosen according to its expected performance and its feasibility. It had to be taken into account the technologies and tools that could be used for the construction of the set up, and the characteristics of the set up itself. Therefore, the main features of the set up had to be thought at this point, even though the final design was not decided.

Before starting the experiments, theoretical calculations were accomplished in order to have information to compare with the results that would be obtained. These calculations made also possible the choice of the measuring devices, and to have an approximate idea of the pressures that the blade would have to face (*Chapter 5*). By doing the calculations before, the materials and the design of the set up would be perfectly able to carry out the tests.

After all the preceding work, the set up was defined and built (*Chapter 6*). It consisted in a GU25(5)8-11, a profile designed by the University of Glasgow that is quite thick, and has a C_L graph quite linear. The core was made out of foam to make it light, and covered with fiberglass and epoxy, in order to give it stiffness. For the pressure readings, holes were drilled on its surface. These holes go into tubes that run inside the wing, and exit from one side to be connected with the desired pressure measuring device. The wing was mounted in a test section, with a controller for the angle of attack and a protractor. The accuracy of the controller was 0.1 degrees.

The experiments (*Chapter 7*) consisted in measuring the pressure distribution over the wing with and without microtab for different angles of attack, with a solidity ratio of 100%. Also different speeds were tested, as the behavior of the profile changes extremely depending on the Reynolds number. Two different microtabs were tried, a metal cylinder of 2 mm of diameter, and a wooden rectangular prism with section of

upna Universidad Pública de Navarra Nafarroako Unibertsitate Publikoa
Todos los derechos reservados
Eskubide guztiak erresalbatu dira

2.5 x 4 mm, using the 4 mm as height. Besides, the microtab was placed in three different positions. Firstly, in order to study the load alleviation, microtabs were installed in the suction side at 90% and 95% of the chord. Secondly, they were also tested in the pressure side, at 95% of the chord, obtaining measurements of the lift enhancement produced by the device. This last position was tried in order to have a reference of the effect of microtabs in both sides.

upna Universidad Pública de Navarra Nafarroako Unibertsitate Publikoa
Todos los derechos reservados
Eskubide guztiak erresalbatu dira

1. Introduction

1.1. Global warming

Before the industrial revolution, earth's atmosphere contained 280 ppm of CO_2. By the middle 50s this proportion had raised up to 315. Nowadays, there are about 380 ppm and the concentration keeps rising around 2 parts per million every year (J. Ripa, 2009 [7]). The increase of CO_2 in the atmosphere is one of the factors that are leading to global warming. The most visible signs of this problem are the decrease of North and South Poles surface, and the gradual extinction of more than half of the glaciers on Earth.

Never before on Earth's history there has been such an increase of CO_2 concentration with the same characteristics. Denying the influence of humankind's activity is one of the biggest parts of this issue. This activity produces gas emissions (such as methane, carbon dioxide, nitrogen oxide, etc.) which are the cause of the so called greenhouse effect. Burning fossil fuels for energy production is the main cause of this phenomenon, with a much bigger impact than transport emissions. As long as there is not a global feeling of the necessity of solving the problem, this will become more and more serious. It is our duty to make ours, and future generations conscious of this huge menace, so that the fight against it persists.

Without any doubt, the solution lies in the restriction of the emissions. And it is at this point that renewable energies come into scene. The development and increase of the efficiency in these sources is the key to settle a sustainable model of energy consumption.

1.2. Renewable energies in Europe and wind power

Due to the serious environmental issues described in the previous chapter the European Commission is trying to push the renewable energies, emphasizing the promotion of the wind power. According to this, there are some guidelines whose main goal is to obtain the 20% of the European electricity production from a renewable source by the year 2020. This target rises till 100% of the electricity production by the end of the year 2050 (European Wind Energy Association, 2012 [2]).

upna Universidad Pública de Navarra Nafarroako Unibertsitate Publikoa
Todos los derechos reservados
Eskubide guztiak erresalbatu dira

This fact makes the wind power one of the most interesting in the area of energy production at this moment. The statistics of the European Wind Energy Association show the exponential growth of the wind sector in the last years and its relevance between the electricity generating installations built in the last years.

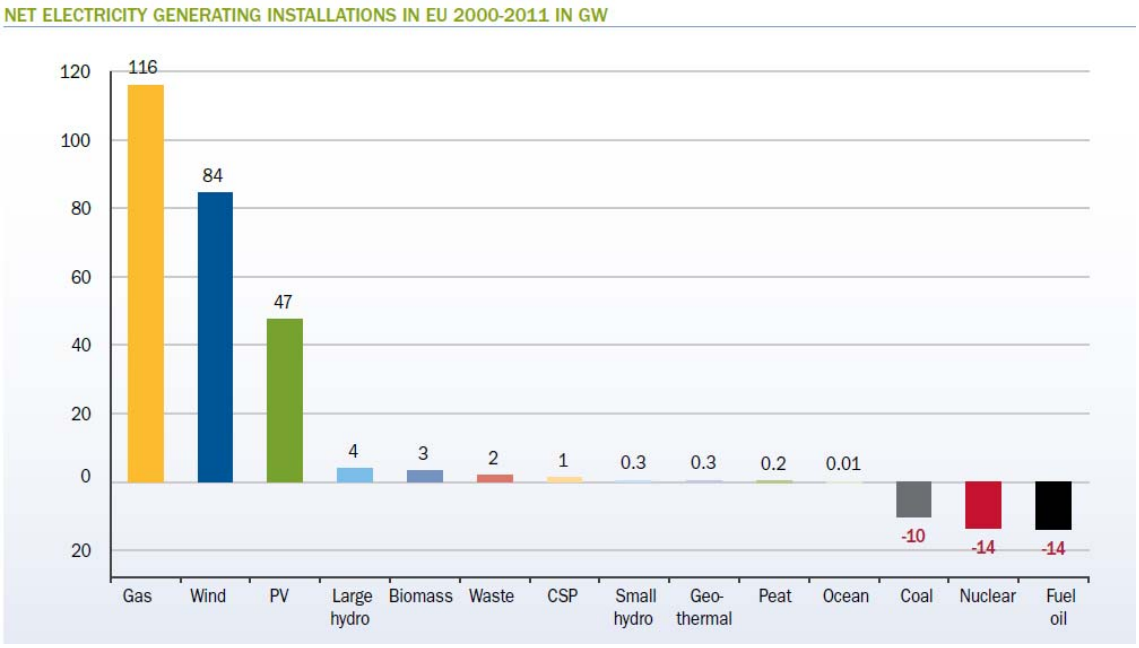

Figure 1.1. Net electricity generating installations in EU 2000-2011 in GW [2].

Knowing the relevance of this type of power, the research involving wind turbines has become very important and several institutions and enterprises are trying to improve the effectiveness and the efficiency of these machines. A good evidence of this fact is the work amount gathered in the department of aerodynamics in the Erasmushogeschool Brussel and also the necessity of the master thesis that is being read as well as the large quantity of other thesis linked to this area of research.

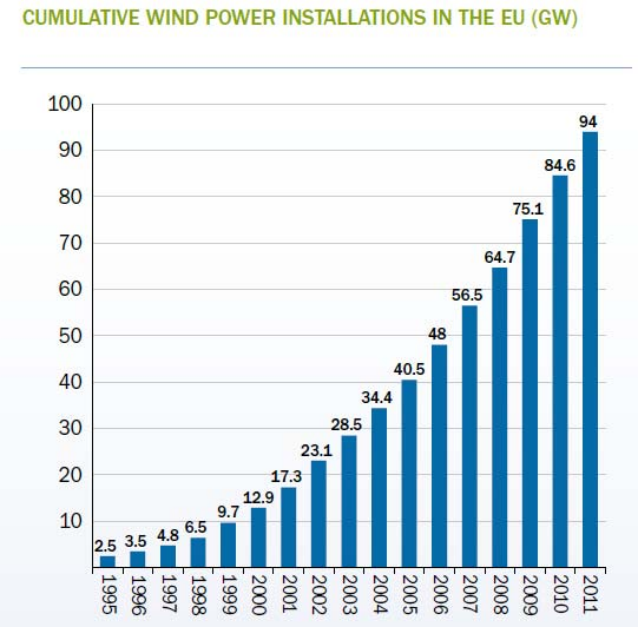

Figure 1.2. Cumulative wind power installations in the EU (GW) [2].

upna Universidad Pública de Navarra Nafarroako Unibertsitate Publikoa
Todos los derechos reservados
Eskubide guztiak erresalbatu dira

1.3. Wind turbine types

The pros and cons of the models are not a concern of this project, but a general classification will be done to give an idea of the background in the research done.

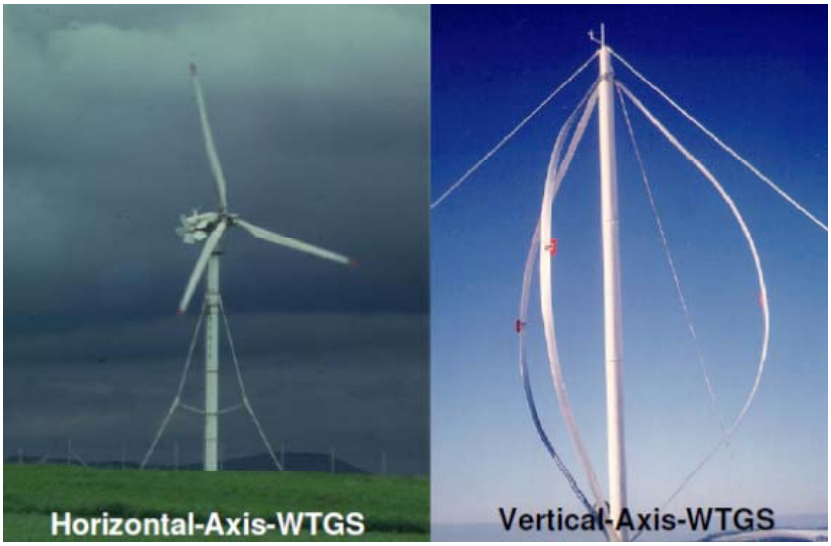

Figure 1.3. Horizontal and vertical axis wind turbines [7].

Nowadays we can classify the wind turbines in two big groups: turbines with horizontal axis and turbines with vertical axis. The ones with horizontal axis are used more often, and within this group two different types are built: with the rotor to leeward or to windward, being these last ones much more used. Also the wind turbine can be built with or without gearbox. Although the gearbox is a critical part, the benefits earned make it worthy of consideration, and it is usually installed (J. Ripa, 2009 [7]).

The number of blades used can also change, but the three blade model is the most developed. After the good results obtained with this kind of turbines on the ground, now a new field of development, consisting in settling the wind mills in the sea, is being explored. Wind conditions in this emplacement are much better, so great achievements can be expected.

Figure 1.4. Offshore wind turbines.

upna Universidad Pública de Navarra Nafarroako Unibertsitate Publikoa
Todos los derechos reservados
Eskubide guztiak erresalbatu dira

To sum up, the most developed type of wind mill is the turbine with horizontal axis, gearbox, rotor to windward and three blades. So the research made in this project is related with blades and devices that could be used to improve the performance of these machines.

1.4. Research

There are two main reasons for the accomplishment of this master thesis. First of all, according to the actual situation of the energy requirements and its production, it is clear that the existing systems need a change and improvements. A change, needed to make it possible getting rid of the dependence on fossil fuels, to make the energetic model sustainable and that may allow leaving a habitable world for future generations and ensure the subsistence of the welfare state. And improvements in the green energy technologies that will make possible to build larger and more efficient devices, which will produce more energy at lower costs, helping the change to become real and feasible. Within the improvements, the control systems play a leading role, as they give to the wind turbines the ability of adapting to the wind conditions in order to optimize the production of electricity, and alleviate the loads that they suffer in order to make their lifetime longer. Therefore, the research and development of smart devices becomes an extremely interesting issue.

Besides in the Erasmushogeschool, where this thesis was written, there were many numerical studies related with this issues taking place. As theoretical calculations and simulations do not always resemble perfectly to reality, it is useful to complement them with experimental studies. This will allow proving the reliability of the previous studies, and/or make the corresponding corrections. Furthermore, other experimental studies related with the issue of this thesis had taken place before and were taking place at the moment of beginning it. Therefore, the thesis will take part in a wide set of investigations.

upna Universidad Pública de Navarra Nafarroako Unibertsitate Publikoa
Todos los derechos reservados
Eskubide guztiak erresalbatu dira

2. Wind Turbines

2.1. Cost of energy (COE)

Nowadays the massive use of energy that takes place all over the world and the necessity that people have of consuming electricity, require low cost of the energy in its generation. Actually the rising of the fuel price is becoming a problem and this is one of the main reasons to improve the technology involving wind turbines. Keeping the wind energy economically competitive against the traditional ways of electricity generation and other renewable energies is absolutely important for the success of this energy field. There is a ratio called cost of energy (from now on COE) that is very useful to measure the cost of the energy delivered by a wind turbine (Johnson *et al.*, 2010 [5]). It is based on three variables:

- ✓ The energy capture of the wind turbine over its lifetime
- ✓ The capital cost of the wind turbine
- ✓ The operation and maintenance cost (scheduled and unscheduled)

$$COE = \frac{\text{Capital Cost} + \text{O\&}M\ Cost}{\text{Lifetime Energy Capture}}$$

Equation 2.1. Cost of Energy [5].

Of course, the target is to decrease as much as possible the COE, so that the profit made by the installation of the wind turbine rises. There are several ways to decrease this cost of energy and they are quite easy to imagine, just by looking the equation above. The first idea is to increase the lifetime of the wind turbine, and this can be done by increasing the reliability of the machine. Nevertheless, it is important to realize that by doing this, the capital cost of the turbine would rise.

Another way to decrease the COE can be to do all the installation cheaper, reducing the capital cost of the wind mill. The research of new technologies can help to reduce the manufacturing and material cost during the fabrication of the machine.

Even though all costs would increase, growing the size of the wind mill is also another option to reduce the COE as far as it gets more energy from the wind. But the huge size of the modern wind mills have some problems, like the difficulty of

upna Universidad Pública de Navarra Nafarroako Unibertsitate Publikoa
Todos los derechos reservados
Eskubide guztiak erresalbatu dira

controlling them and the problems due to extreme loads, that makes nearly impossible to follow this way of improvement.

This engineering challenge has led to intensive research around the way to improve the efficiency of the modern wind turbines. In order to achieve this, passive and active control techniques in wind turbines become very interesting, as they allow adapting the mill performance to the wind conditions.

2.2. Wind turbines theory

In order to set a background and to make the reading of this document easier, some main concepts of aerodynamics, wind turbines and wind turbines loads will be described in this section (Anderson, 2008 [1] and J. Ripa, 2009 [7]).

The main target of a wind mill is to produce as much electric energy as possible in each situation, optimizing its performance for all the different wind circumstances. The wind turbine extracts the kinetic energy present in an air stream, converting firstly to mechanical energy in the rotor and afterwards converting it to electricity through the generator. To do so, they use the aerodynamic forces created by the air stream in their blades. At this point, the design of the aerodynamics becomes very interesting. Unfortunately, it is not possible to design a mill that delivers nominal power rate at every wind speed. Each design should be done to optimize the amount of energy that can be extracted according to previous studies that show the wind's behavior in the area where the wind turbine will be installed.

2.2.1. Lift and drag

In order to understand the performance of a wind turbine, we should firstly understand the phenomenon that takes place in each blade, as it is the component that takes advantage of the wind to produce movement in the rotor.

When the wind hits the blade two different forces are produced. The lift (L) and the drag (D) as it can be appreciated on *figure 2.1*. The first one is normal to the wind direction, and is the result of the pressure difference between the suction side or extrados and the pressure side or intrados. The second one is parallel to the wind direction and is due to the resistance of the profile to the wind. The sum of both gives a resultant (R), which we can be divided into two forces according to the effect on the wind turbine (J. Ripa, 2009 [7]).

upna Universidad Pública de Navarra Nafarroako Unibertsitate Publikoa
Todos los derechos reservados
Eskubide guztiak erresalbatu dira

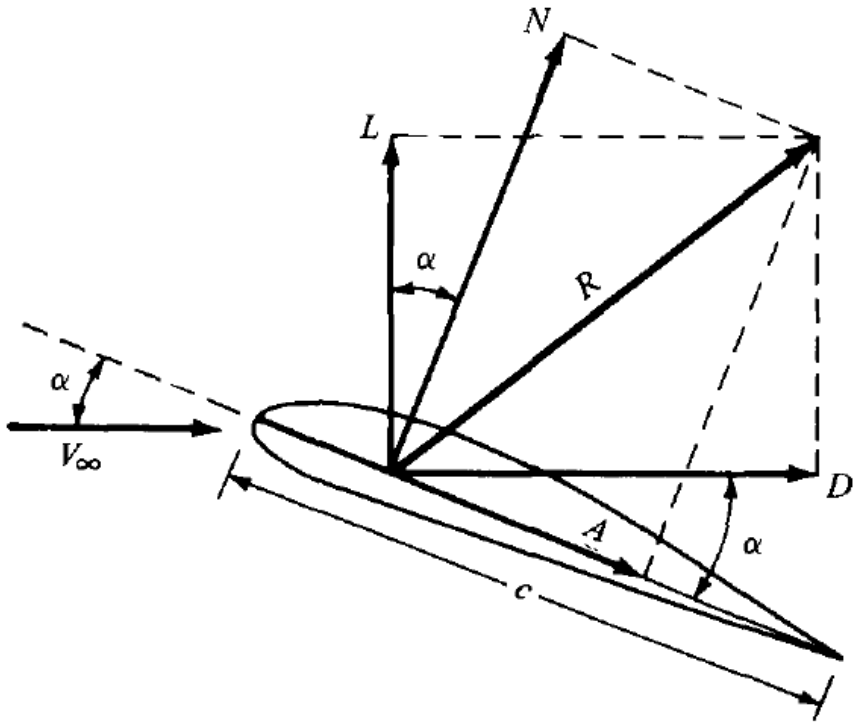

Figure 2.1. Aerodynamic forces [1].

The two forces are:

- ✓ The tangential that is located in the rotation surface.
- ✓ The axial, that is perpendicular to that surface.

To develop the equation of both in the following lines, the angle of inclination (φ) is used. It is the sum of the angle of attack (α), from now on AoA, and the angle of step (angle between the chord of the blade and the rotation surface). According to this, the forces can be written with the following expressions (J. Ripa, 2009 [7]).

$$dF_{tan} = dLsin\varphi - dDcos\varphi = \frac{\rho w^2 c}{2}(C_L sin\varphi - C_D cos\varphi)dR$$

Equation 2.2. Tangential force [7].

$$dF_{ax} = dLcos\varphi + dDsin\varphi = \frac{\rho w^2 c}{2}(C_L cos\varphi + C_D sin\varphi)dR$$

Equation 2.3. Axial Force [7].

Where w is the wind speed, ρ the air density, c the cord, C_L the lift coefficient, and C_D the drag coefficient. To obtain the final expression, it should be done the integral between 0 and the length of the blade.

The axial force pushes the whole tower, causing a torque that tries to knock over the structure. So it should be considered for the calculations of the wind mill. It is obvious that the best case would be a wind turbine with null axial force, as it only

upna Universidad Pública de Navarra Nafarroako Unibertsitate Publikoa
Todos los derechos reservados
Eskubide guztiak erresalbatu dira

causes problems. Unfortunately that is not possible, but a decrease can be achieved by both decreasing the lift or the drag. The lift is the one that makes the wind turbine work, so the only option is to reduce the drag.

The tangential force produces the moment that makes the rotor spin. According to the *equation 2.2* the lift makes this force grow and the drag makes it smaller. So once again it is interesting to reduce the drag in order to improve the performance of the mill.

Taking into account these reasoning, it is interesting to develop devices that allow increasing the lift in those conditions where the optimum is not reached. But not only that, it is also useful to create mechanisms that make possible to operate the wind mill at speeds further than its original cut-out speed (this concept is explained in the next point), by reducing the lift and therefore the extreme loads in the turbine. By achieving this, the nominal energy could be produced in wider ranges of speed.

Using these devices could also affect the drag, which has also to be taken into account, as the higher it is, the stronger the structure should be and the more it will decrease the tangential force. Stronger structure means a more expensive wind mill, and the reduction of the tangential force means a decrease in the efficiency of the machine.

2.2.2 Power curve and performance coefficient (C_p)

The relationship between the wind speed and the power that a turbine can get is fundamental. As a consequence one of the most important plots for every wind turbine is the power curve, in which the power output of the turbine is represented as a function of the wind speed. In *figure 2.2* is shown a typical power curve with its most important points and zones (Johnson *et al.*, 2008 [4]).

upna Universidad Pública de Navarra Nafarroako Unibertsitate Publikoa
Todos los derechos reservados
Eskubide guztiak erresalbatu dira

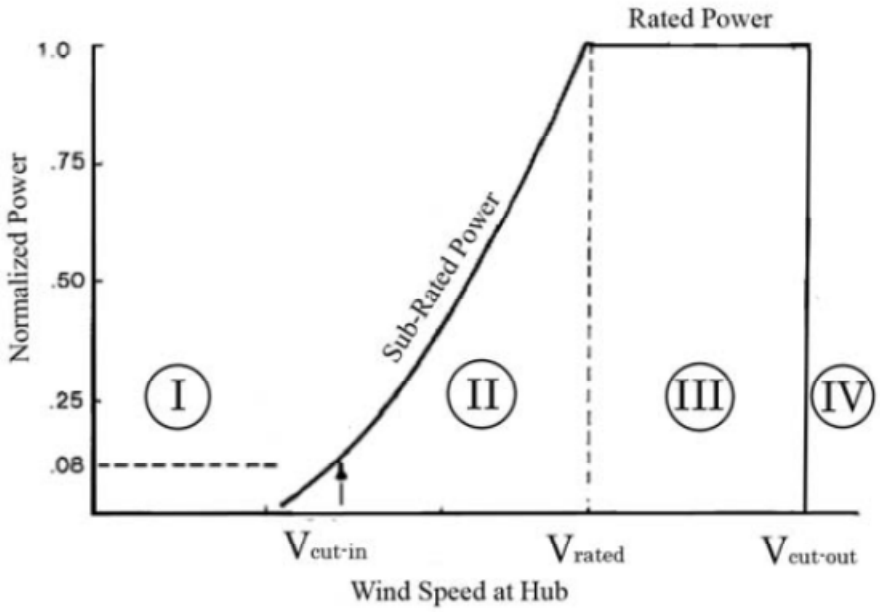

Figure 2.2. Typical power curve of a wind turbine [4].

At very low wind speeds, there is insufficient torque exerted by the wind on the turbine blades to make them rotate. However, as the speed increases, the wind turbine will begin to rotate and generate electrical power. The speed at which the turbine first starts to rotate and generate power is called the cut-in speed.

As the wind speed rises above the cut-in speed, the level of electrical output power rises rapidly as shown (the power is proportional to the speed cubed). However, due to the wind speed increase the power output of the turbine can reach the limit of the electrical generator. This limit of the generator output is called the rated power output and the wind speed at which it is reached is called the rated wind speed. At higher wind speeds, the design of the turbine is arranged to limit the power to this maximum level and there is no further rise in the output power. There are two typical ways in wind turbines to keep the rated power at a constant level, by controlling the pitch angle or by controlling the stall.

Even though the rated power can be controlled above the rated wind speed, there is a critical wind speed in which the turbine must stop, as the generated forces can damage the turbine structure and induce the collapse of the mill. This is called cut-out speed.

The efficiency or, as it is more commonly called, the performance coefficient, C_p, of the wind turbine is simply defined as the power delivered divided by the available power.

$$C_p = \frac{Delivered\ power}{Available\ power} = \frac{P}{\frac{1}{2}\rho S V^3}$$

Equation 2.4. Performance coefficient [7].

upna Universidad Pública de Navarra Nafarroako Unibertsitate Publikoa
Todos los derechos reservados
Eskubide guztiak erresalbatu dira

2.2.3 Available wind power

It is very important to know how much energy is in the wind that can go through a turbine. Imagine a mass flow crossing a control volume that represents the rotor (*figure 2.3*). The mass flow crosses the control volume (dV), which is a disk of area S and depth dL, with speed U (notice that U is used instead of V for velocity in order not to mix with volume). Applying the continuity equation of fluid mechanics and physics it can be determined the power of the air stream crossing the disk (J. Ripa, 2009 [7]).

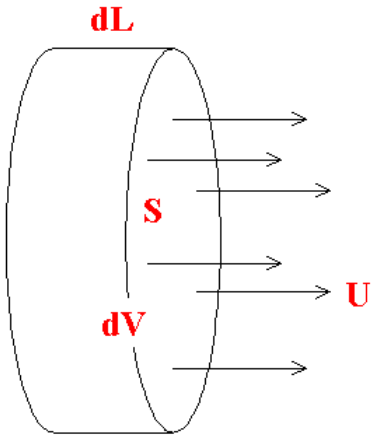

Figure 2.3 Mass flow crossing control volume.

$$\dot{m} = mass\ flow = \frac{dm}{dt} = \frac{d(\rho V)}{dt} = \rho\frac{dV}{dt}$$

$$dV = SdL = SUdt$$

$$\dot{m} = \rho SU$$

$$E_c = \frac{1}{2}mU^2$$

$$P = \frac{dE_c}{dt} = \frac{1}{2}\dot{m}U^2$$

$$P = \frac{1}{2}\rho SU^3 \quad [W]$$

Equation 2.5. Wind power [7].

The kinetic energy per unit time (or the power of the flow) is given by the equation above. There are three important conclusions that can be made from this:

- ✓ The wind power is proportional to the density of the air. This implies that the location of the wind mill is important as the air density depends on it, for example it is bigger in the sea level than in the high mountains.

- ✓ Power from the wind is proportional to the area swept by the rotor or the rotor's radius squared. So the bigger the rotor is the bigger the power that can be obtained will be. The effect of the rotor diameter increase is more important than the air density effect, due to the radius squared proportion.

- ✓ The wind power is also proportional to the wind velocity cubed. Obviously, this is the most relevant parameter because a little variation in the air velocity means a big difference in the obtained power. Again the importance

upna Universidad Pública de Navarra Nafarroako Unibertsitate Publikoa
Todos los derechos reservados
Eskubide guztiak erresalbatu dira

of the wind mill location is shown, and this is the reason why long-term wind data from the location is studied before installing any wind turbine.

The kinetic energy per unit time calculated in the previous equation is not the maximum that can be obtained from wind by a turbine. This is the power that the wind has, but it is impossible to take advantage of all this energy with a wind mill.

2.2.4 Betz limit

There is a theory about the maximum possible energy that can be delivered by a "hydraulic wind engine", or wind turbine, that is called Betz's law. Decades before the arrival of the modern 3-blade wind turbines used to generate electricity, Betz's law was developed, in 1919, by the German physicist Albert Betz. According to Betz's law, no turbine can transform more than 59.3 percent of the kinetic energy in wind (J. Ripa, 2009 [7]).

In order to calculate the maximum theoretical efficiency of an ideal rotor (for example a wind mill), it has to be replaced by a thin disc that withdraws energy from the fluid that goes through it. The upstream flow has higher velocity (V_1) than the one in the rotor section (V), and at certain distance behind the rotor section the fluid flows with a smaller velocity (V_2). These velocities are represented in the *figure 2.4*.

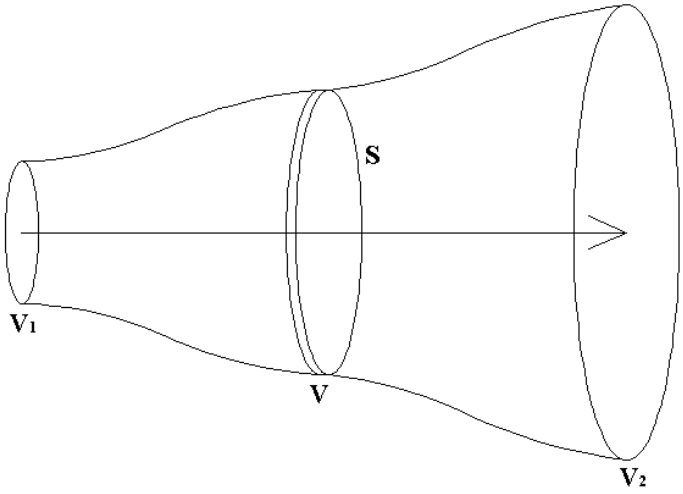

Figure 2.4. Scheme of the wind velocities distribution.

upna Universidad Pública de Navarra Nafarroako Unibertsitate Publikoa
Todos los derechos reservados
Eskubide guztiak erresalbatu dira

To describe Betz's theory we need to do some assumptions:

- ✓ First of all the rotor is considered without the hub. It is an ideal rotor, with an infinite number of blades which have no drag. Any resulting drag would only lower this idealized value.

- ✓ In addition, the flow into and out of the rotor is axial. This is a control volume analysis, and to obtain a solution the control volume must contain all the flow going in and out (not taking into account the whole flow would violate the conservation equations).

- ✓ The flow is considered incompressible. The density remains constant, and there is no heat transfer from the rotor to the flow or vice versa.

Once those assumptions are done, the expression that describes the power in a wind turbine based on kinetic energy can be achieved *(appendix 1)*:

$$P = \frac{\Delta E}{\Delta t} = \frac{1}{4}\rho S {V_1}^3 \left[1 - \left(\frac{V_2}{V_1}\right)^2 + \left(\frac{V_2}{V_1}\right) - \left(\frac{V_2}{V_1}\right)^3\right]$$

Equation 2.6. Power based on kinetic energy [7].

If we optimize this formula, it is shown that the maximum value for the power happens when:

$$\frac{V_2}{V_1} = \frac{1}{3}$$

Substituting these values in the power expression we obtain the maximum power in function of the air density, the rotor area and the upstream wind velocity cubed. This equation is the same as the *equation 2.5* multiplied by a number that represents the coefficient of performance.

This German physicist proved in his theory that the coefficient of performance has a maximum value of $C_{p,optimus} = \frac{16}{27} = 0.593$. According to this, the maximum power that can be obtained by an ideal wind turbine is:

$$P = \frac{16}{27} \cdot \frac{1}{2}\rho S V^3 \quad [W]$$

Equation 2.7. Maximally theoretical usable wind power [7].

In the *figure 2.5* the differences between the available power in the wind, the theoretical maximum usable power and the real power curves in conventional stall controlled and pitch controlled turbines are shown.

upna Universidad Pública de Navarra Nafarroako Unibertsitate Publikoa
Todos los derechos reservados
Eskubide guztiak erresalbatu dira

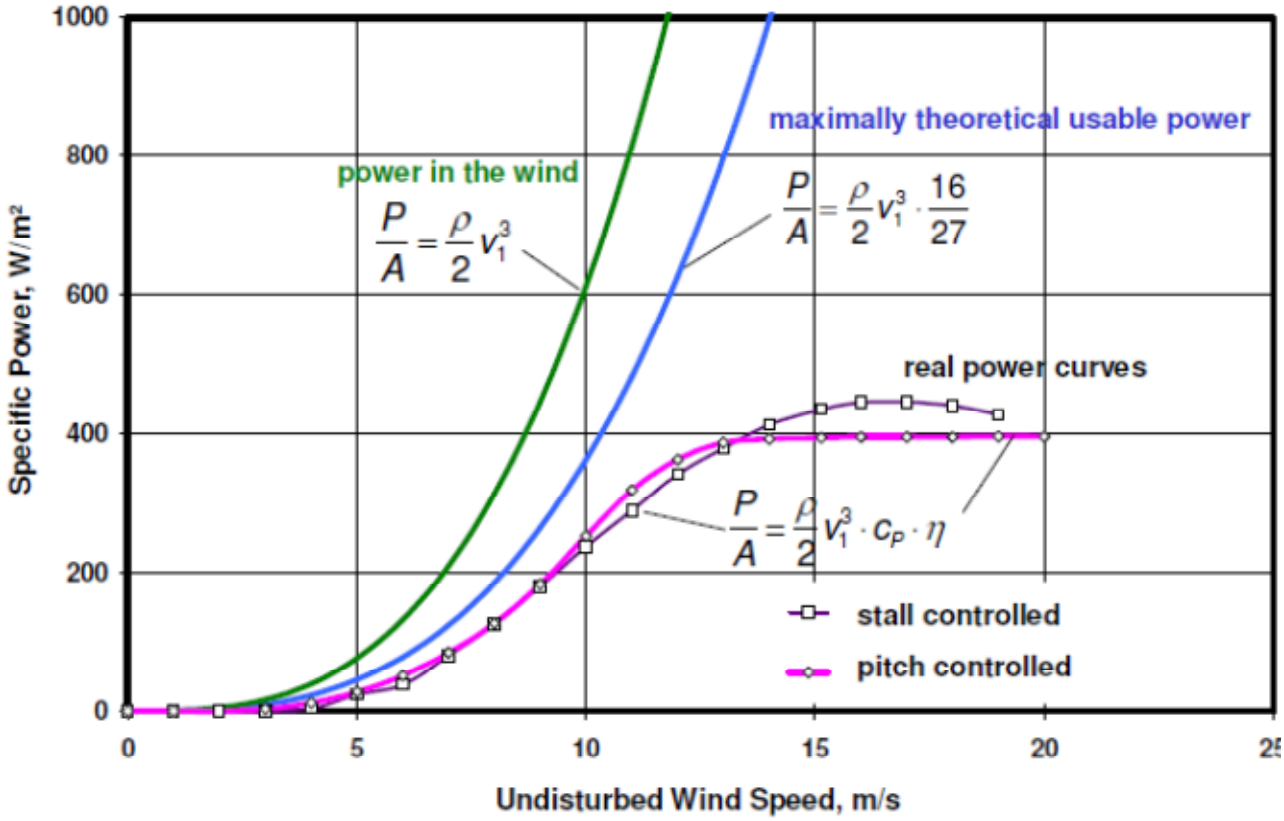

Figure 2.5. Power curves [7].

2.3. Loads in a wind turbine

When a wind turbine is on service, several loads appear due to the wind and the movements of the machine, and also the structural loads are involved in the stress suffered by the mill. The fundamental loads can be classified into four main groups (Johnson et al., 2008 [4]):

1) *Tower base:* the tower is the main structure that holds all the assembly. It has to withstand its weight and torques and forces due to wind and windmill operation.

2) *Tower top:* at the top of the tower the nacelle is engaged to the tower, transmitting the loads due to the blades, the rotor, and the movement when the mill is orientated to the wind direction. One of the critical loads comes from the "shadow effect" produced by the tower. When one of the blades is in the lower position, the tower influence in the wind flow makes the loads due to wind in that blade fall, and therefore the wind mill suffers a fast change of load, like a hit.

upna Universidad Pública de Navarra Nafarroako Unibertsitate Publikoa
Todos los derechos reservados
Eskubide guztiak erresalbatu dira

3) *Rotor:* all the loads due to the spin of the turbine go through it. In the wind mills built with gear box, this element is one of the most problematic and difficult to maintain.

4) *Blades:* they bend and twist when the wind blows. Its performance is similar to the wings of a plane.

Over the last decades, these machines have increased in size and weight, in order to reduce the cost of the energy and produce a bigger amount of energy with every mill. This growth has meant more difficulties for controlling them (reaching the point of making them impossible to control passively) and higher loads and fatigue for the structure. Extreme loads make the designs more expensive, which is against the main principle of building bigger turbines. Therefore, the reduction of the loads by using new load control techniques is crucial for making large machines feasible or getting higher energy production with smaller wind mills. The shadow effect produces a cyclic load that is one of the most relevant loads that affect the mill. It could be alleviated by developing the right devices making the lifetime longer.

In the analysis of the lift equation for the blades of a mill, the main areas of influence in the rotor power control can be found.

$$L = \int_{r=0}^{b} \frac{1}{2}\rho[C_{L_\alpha}(\alpha + \theta_{pitch} - \alpha_0)\{V_{wind}^2 + (2\pi nr)^2\}c]dr$$

Equation 2.8. Lift equation for a wind turbine blade [4].

The first area is the incidence angle (θ_{pitch}). It can be controlled in two different ways: by turning the blade itself along its length axis or by designing the blade in such a way that it twists according to the wind speed. Of course both can be used at the same time.

The second one is the flow velocity (n), which can be fixed and changed by using a rotor that allows variable speed. Both techniques are developed on modern machines.

The third area is the size of the blades (b). Achieving the construction of a blade with variable length (which means obtaining a variable diameter for the rotor) would allow adjusting the size of the rotor to the wind conditions in every moment. If the wind is slow, a bigger diameter can be used in order to improve the power production, otherwise, if the wind is too fast, the diameter can be reduced to protect the wind mill from extreme loads.

The fourth and last area, involves controlling the blade section, which has an impact in the aerodynamics (C_{L_α}, α_0). In this project, this area will be researched by studying the implementation of devices that allow active flow control (AFC).

upna Universidad Pública de Navarra Nafarroako Unibertsitate Publikoa
Todos los derechos reservados
Eskubide guztiak erresalbatu dira

3. Smart blades for wind turbines

In the previous chapter some basic wind turbine theory, with special emphasis on the loads of a turbine, has been explained. In this chapter we describe how smart blades can be used to alleviate these loads. Nowadays, as the researches in new materials and size growth of the turbines are reaching levels that are not economically sustainable, the area of the smart blades research is growing.

3.1. Concept of smart blade

Smart blades are those that are controlled actively and can adapt their performance so that the power can be obtained more efficiently and in a wider range of wind conditions. There are several goals that can be achieved using this type of blades:

- ✓ To settle the cut-in speed at lower wind speeds.
- ✓ To settle the cut-out speed at higher wind speeds.
- ✓ Reduce some of the extreme and cyclic loads in turbines.
- ✓ Decrease the size of mills.
- ✓ Increase the power output for the same size of machines.

Usually smart blades are like the classic blades used for turbines but with a sort of devices installed to improve the performance. These devices are groups of sensors that are able to measure the working conditions and through a software analysis give the optimal response to some actuators also installed in the blade. The actuators change the performance of the blades, and indeed, the performance of the whole turbine, raising its effectiveness.

Another type of smart blades is the one in which intelligent materials are used in the manufacture. This allows the blades modifying their profile depending on the wind conditions. Normally blades of this kind are not controlled actively; in fact, they are classified as passive control blades. For a deeper analysis in smart blades it is necessary to study the way that wind turbines are controlled.

upna Universidad Pública de Navarra Nafarroako Unibertsitate Publikoa
Todos los derechos reservados
Eskubide guztiak erresalbatu dira

3.2. Evolution of control techniques in wind turbines

In this section the control techniques in wind turbines will be discussed. To do so, concepts of "*SANDIA*" (Johnson *et al.*, 2008 [4]) and *"An Overview of Active Load Control Techniques for Wind Turbines with an Emphasis on Microtabs"* (Johnson *et al.*, 2008 [5]) reports will be summarized.

The turbine control is divided into two main groups: passive control turbines and active control turbines. Concerning to the classification of control types, when the control over the blade is done without any external energy support is called passive control. Some well known passive controls are the yaw movement, which allows orientating the mill against the wind direction, and the aeroelastic blade twist, which increases the performance all along the blade.

If an external energy support is needed for the control of the turbine, it is said that active control is being used. Notice that additional power is used to improve the performance and obtain higher power output. Therefore, further studies are required when this kind of controls are installed, in order to assure that the power gain due to this control is bigger than the power input done. It is also important to realize that operating and maintenance cost will increase with this kind of regulation. Pitch angle control and variable rotor speed control are examples of active control. In the following figure is shown the classification of different control types.

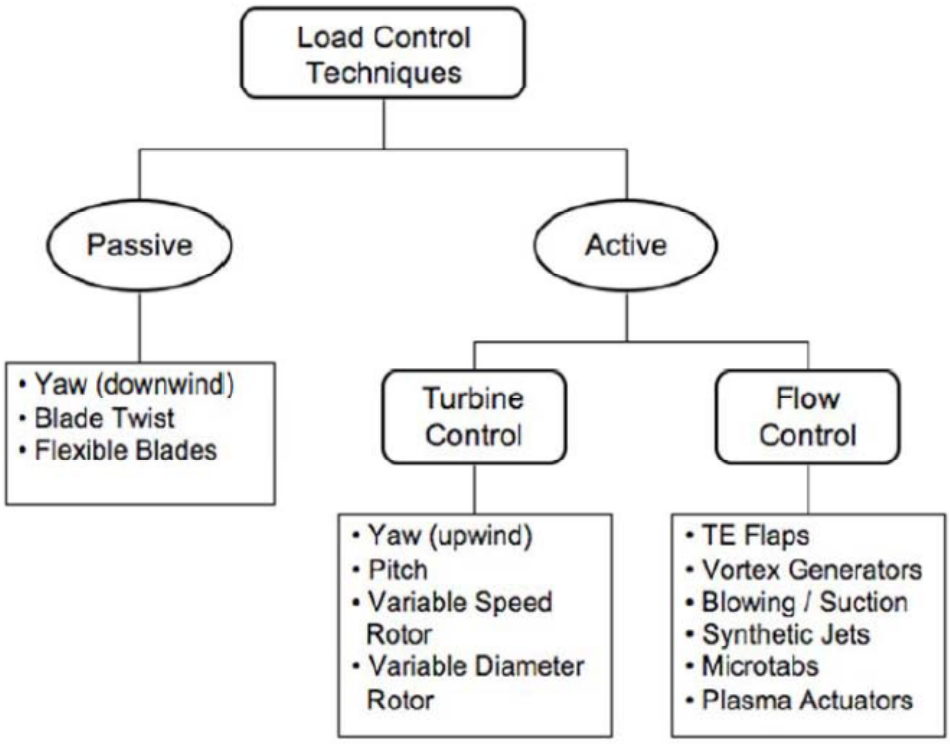

Figure 3.1. Load control techniques [4].

upna Universidad Pública de Navarra Nafarroako Unibertsitate Publikoa
Todos los derechos reservados
Eskubide guztiak erresalbatu dira

The goal of wind turbine control is to balance the following requirements:

- ✓ Setting upper bounds on and limiting the torque and power experienced by the drive train in order to prevent the mill from collapse.

- ✓ Minimizing the fatigue from the rotor drive train and other structural components due to changes in wind direction, speed (including gusts), and turbulence, as well as start-stop cycles of the wind turbine.

- ✓ Maximizing energy production.

In the beginning the described active and passive control systems were used. But the need to increase the power production pushed engineers to design new systems to improve the effectiveness of mills and also to make higher size growth feasible. In these new huge machines it is sometimes very difficult to handle the control of oscillatory loads that cause fatigue in the structure. These loads occur as a result of rotor yaw errors, wind shear, wind upflow, shaft tilt, wind gusts, shadow effect and turbulence in the wind flow. For this purpose it is not enough with the pitch controlled or variable rotor speed wind turbines used until now and more complex controls are required. The following several control methods are able to handle this kind of problems.

3.2.1. Advanced pitch control

Traditional pitch control is based on rotating all the blades around its spanwise axis. That way the AoA is modified and the generated lift changes. It is used to limit the peak power in order to prevent the generator from powers above the rated one, optimize the rotor efficiency and also slow down the rotor.

By comparison, the advanced pitch control technique allows each blade to rotate independently. This means that some oscillatory loads can be alleviated. For instance, fatigue loads due to rotor tilt and yaw errors can be reduced by pitching the blades in this way.

The goal of this advanced control is to assembly both systems , where collective pitch is used to keep the power at a desired level (adjusting pitch based on the mean wind speed) while the individual pitching is used to modify this pitch angle independently for each blade to minimize fatigue loads without affecting the power output. This kind of control is already used in helicopters, so the development is done, only the adaptation to wind turbines and its effects have to be studied.

upna Universidad Pública de Navarra Nafarroako Unibertsitate Publikoa
Todos los derechos reservados
Eskubide guztiak erresalbatu dira

3.2.2. Blade twist control

This advanced passive control is nowadays possible thanks to the great advances done in the last years in the modern composite materials field. The implementation of these new materials allowed creating aeroelastic tailored blades. These elastic blades are able to modify their twist distribution along the blade depending on how much they are bended as a consequence of the aerodynamic loads, reducing fatigue loads. In addition to this, the temporary loads caused by wind gusts are also mitigated with this control system. At the same time the pitch activity is reduced.

However the blade twist control has some negative issues that should be noticed. First of all, the blade which includes these materials has a reduced energy capture. Secondly, the capital cost increases as a result of the use of more complex materials. In addition to this the blade integrity becomes weaker, affecting the maintenance costs also. Anyway, studies (Lobitz *et al.*, 2001 [9]) done in Albuquerque show that this type of blades can lead to a reduction of 70% in fatigue loads damage, and another research (General Electric, 2009 [10]) also predicts that a reduction up to 6% in COE can be obtained.

3.2.3. Variable diameter control

As it has been explained before in this document, the energy capture in a wind turbine depends on the size of the rotor area. It means that making the rotor blades larger or smaller changes the power output. Under such circumstances, there are some designs done about systems that allow the blade to increase its size obtaining variable diameter turbines. This implies that energy capture can be improved for low wind speeds and also the extreme loads in high wind conditions can be reduced. In this kind of turbines the power curve shows that the machines are able to get power from wind for a wider range of wind velocities.

upna Universidad Pública de Navarra Nafarroako Unibertsitate Publikoa
Todos los derechos reservados
Eskubide guztiak erresalbatu dira

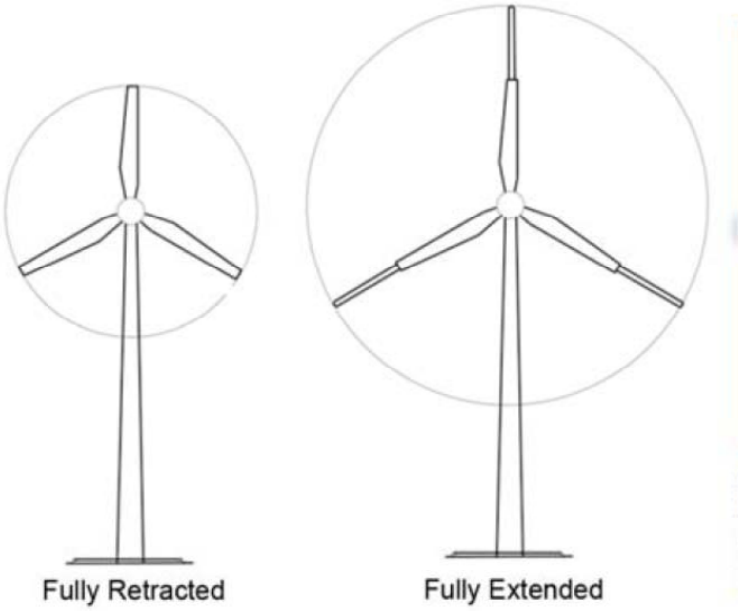

Figure 3.2. Scheme of a rotor with variable diameter [4].

Of course there are several engineering challenges to solve before this type of turbines become economically feasible. Problems due to complex control strategies, reliability of the machine or maintaining the aerodynamic efficiency for both sizes of blade, make difficult for these systems to be marketable at the moment.

3.2.4. Active flow control (AFC)

One way to improve the performance of the turbine is to control the airflow that surrounds the blades. This technique allows also decreasing extreme loads and fatigue loads, as both of them take place due to the action of the wind in high speed wind conditions. This is the main goal of the AFC, and in order to achieve it, the blades must be provided with sensors that recognize changes in the local flow and actuators that react in response to the readings of the sensors, counter striking the conditions that cause the loads.

More specifically, what the flow control devices do is to delay or advance the transition between laminar and turbulent regime, to suppress or enhance turbulence and prevent or promote boundary layer separation. The effects pursued with the use of the devices in order to reach the goal are: lift enhancement, drag reduction, heat transfer enhancement, flow-induced noise reduction and mixing augmentation. It has to be taken into account that improving one of these objectives may interfere with one of the others, so it is the responsibility of the engineer to find a balanced solution.

upna Universidad Pública de Navarra Nafarroako Unibertsitate Publikoa
Todos los derechos reservados
Eskubide guztiak erresalbatu dira

Besides, installing AFC systems can result into secondary effects that can be very beneficial. Bigger rotors can be built as the AFC allows reducing loads, which means that more wind energy can be transformed by one wind mill. They also can make the mill more productive in low speed winds conditions, and make the turbine able to work in higher values of the lift curve. Besides, if the flow is kept in laminar regime the noise will be reduced and the aerodynamic performance improved.

The methods used can be organized as the load control ones, in passive and active. Passive techniques involve geometry manipulation or fixed mechanical devices, which work regardless of the conditions. Active technique can be divided into predetermined or interactive, as shown in *figure 3.3*.

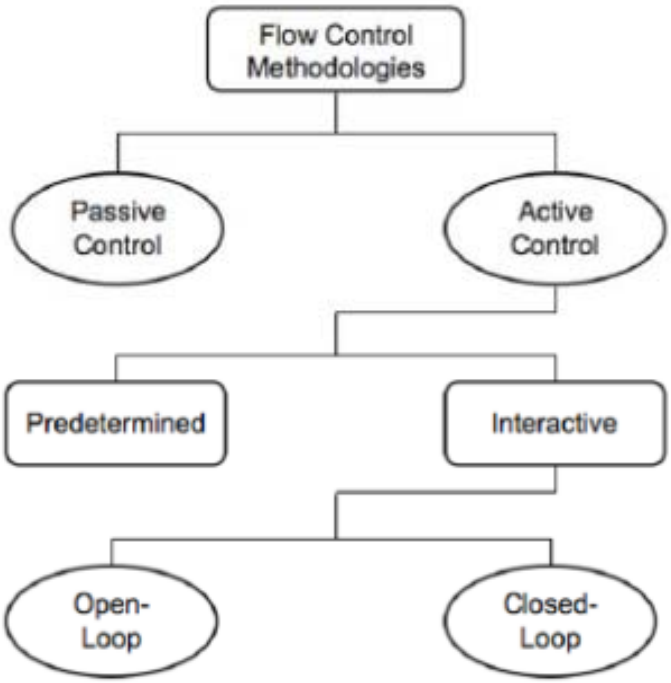

Figure 3.3. Flow control methodologies [5].

Predetermined means that the system has two positions, “on” and “off”, so it works depending on the wind conditions, but it always works in the same way. An interactive system is the ensemble of a sensor, an actuator and a controller, therefore the response is given according to every condition. Open loop means that the effect of the response is not measured, so the system cannot correct itself, while close loop does. The best way to reach the objectives accurately is a close loop system without any doubt.

upna Universidad Pública de Navarra Nafarroako Unibertsitate Publikoa
Todos los derechos reservados
Eskubide guztiak erresalbatu dira

To end up the analysis of the AFC, it has to be said that it is composed by three categories:

1) *Control and sensors:* the sensors give the controller the information about the operational conditions. The info stream is continuous, so that the controller can adjust the operation in every moment.

2) *Actuators and devices:* actuators receive orders from the controllers, and their mission is to deploy the devices, which produce the effect in the air flow.

3) *Flow phenomena:* the interaction with the devices produces a change on the flow. This change is registered by the sensors, and then the loop is closed and starts again.

According to what explained in this point, different solutions have been found and researched, in order to mitigate loads and improve the performance of the turbines. In the next pages, different types of AFC systems will be analyzed making possible the choice of the best one for the study considered in this project.

3.3. Smart devices

This compilation of devices and the way to separate them into categories is based on the *SANDIA* Report: "*Active Load Control Techniques for Wind Turbines*" (Johnson et al., 2008 [4]).

Before starting the analysis of the devices, a little further explanation is needed, so that it will be easier and faster to understand how each one works. Four different points will be explained, for the classification of the systems:

1) *Actuation:* there are two different kinds, geometric (G) / fluidic (F). The geometric devices are those who move an external section of the blade in order to change the shape of the profile and achieve air flow attachment. The fluidic ones blow or suction air from the air flow to modify it. Some devices can be considered from both types, or not included in this classification.

2) *Location:* according to the location of the device, it will be considered near the leading edge (LE), in the mid-chord (MC), or near the trailing edge (TE).

upna Universidad Pública de Navarra Nafarroako Unibertsitate Publikoa
Todos los derechos reservados
Eskubide guztiak erresalbatu dira

3) *Lift curve adjustment:* this curve is moved in two different ways by the deployment of the AFC systems. Firstly, the curve can be lifted up or down. When is lifted up, it is called increasing lift (I) and the opposite is called decreasing (D). If a device is able to do both it will be marked with (I/D). Secondly, the lift curve can be extended so that it goes into stall at higher AoAs, which is called delay stall (DS).

4) *Movement:* if the device operates in a specific position, it is called steady (S) and if it has continuous movement it will be considered unsteady (U).

Even though each system has different characteristics and fundamentals in its way of working, there are some points to take into account in every device to obtain worthy results.

- ✓ The size of each device has to be as small as possible, so that it can be installed along part of the span to obtain different control depending on the section. It also has to be scalable, so that it can work properly no matter how long the chord of the section is.

- ✓ Fast activation speed is needed, to provide the capacity of countering oscillating loads regardless of the frequency.

- ✓ The energy consumed by the activation of the device must be low; therefore the activation forces must be low, as well as the power requirements. The energy consumed must be lower than the energy gain, or at least equal.

- ✓ The system has to be reliable and dependable, so that the turbine maintains operation if one or more devices fail.

- ✓ The system has to be able to support the environment surrounding the turbine, and the lifetime has to be similar to the lifetime of the turbine and its components.

- ✓ The device has to be easy to integer in the manufacture, assembly and maintenance of the turbine blade.

- ✓ It has to be able to reduce the cost of energy, as it is the main factor behind the research of these devices.

upna Universidad Pública de Navarra Nafarroako Unibertsitate Publikoa
Todos los derechos reservados
Eskubide guztiak erresalbatu dira

Now, several types of devices will be explained to proceed to the selection of the most interesting for this project.

- ✓ ***Traditional Trailing-Edge Flaps:*** *(G,TE,I/D,S)* These well known devices are commonly used in aircraft technology and they can be also used for wind turbines. They are surfaces located in the trailing part of the wing that can deflect towards the pressure or the suction side. This control method has a slow response, implies big actuators and as a consequence there is an important increase of the weight. The created aeroacustic noise is also another problem for this kind of actuator. The targets of these devices are usually aerodynamic braking and load control.

- ✓ ***Nontraditional Trailing-Edge Flaps:*** *(G,TE,I/D,S/U)* They are very similar to the previous ones, but these introduce newer materials and technologies, such as small piezoelectric devices and flexible materials. They are shorter, faster, lighter and sometimes even there are not gaps between the flap and the blade and their main purpose is to counter the extreme loads and the fatigue loads. Compact Trailing-Edge Flaps, Adaptive Trailing-Edge Geometry and Adaptive Compliant Wing are inside this group.

- ✓ ***Microtabs:*** *(G,TE,I/D,S/U)* They are very small tabs located near to the trailing edge of the wing and deployed perpendicular to the surface. This devices are located inside the airfoil and when needed they are able to slide out in the wing surface. These smart devices will be deeply studied later in this document because of their interesting performance in load control.

- ✓ ***Miniature Trailing-Edge Effectors (MITE's):*** *(G,TE,I/D,S/U)* They are very similar to microtabs, but in this case they are located in the trailing edge of the wing. They are able to slide up or down with a translational movement. The effect of this device is to enhance or mitigate the lift.

Figure 3.4. Miniature Trailing-Edge Effectors [4].

upna Universidad Pública de Navarra Nafarroako Unibertsitate Publikoa
Todos los derechos reservados
Eskubide guztiak erresalbatu dira

- ✓ ***Microflaps:*** *(G,TE,I/D,S/U)* Again they are very similar to Microtabs and MITE's. In these devices the movement instead of a translational is rotational but the achieved effect is the same.

- ✓ ***Active Stall Stripes:*** *(G,LE,D,S)* They are another kind of very small tabs that can slide out perpendicularly to the wing. The difference is that they are located near to the leading edge of the wing and that they promote the flow separation.

- ✓ ***Vortex Generators:*** *(G,LE,DS,S)* Active vortex generators are very small solid tabs mounted on the airfoil surface. Their main goal is to delay the stall by mixing the airflow in the boundary layer. They increase the lift but also the drag in blades.

- ✓ ***Blowing and Suction:*** *(F,LE/TE,DS,S/U)* The main idea of blowing and suction is to introduce some properly located slots in the airfoil surface (it can be near to leading or trailing edge). Thus, a high momentum (in blowing devices) or low momentum (in suction devices) are introduced or removed from the boundary layer through these slots. The target is to delay the boundary layer separation.

- ✓ ***Circulation Control:*** *(F,TE,I/D,S)* The circulation control is derived from blowing and suction theory. Basically they are very small jets introducing high momentum air tangentially to the rounded trailing edge of an airfoil. This device increases the circulation and as a result the lift, but it needs to install air ducts inside the blade making them much more complex and also the trailing edge has to be rounded which increases the noise and drag.

- ✓ ***Plasma Actuators:*** *(P,LE,DS,S/U)* This non fluidic device allows to create a high momentum air stream converting electricity into kinetic energy. An "electric wind" stream is created between an anode and a cathode guided by the electric field when applying a large voltage difference. That way the boundary layer airflow is modified and the separation point of the flow can be delayed.

- ✓ ***Vortex Generator Jets:*** *(F,LE,DS,S/U)* It consists in jets of air. The air comes out through the airfoil surface, and it hits a cross flow, that is the air running along the surface. The result is a dominant streamwise vortex. The characteristics of the vortices can be controlled, allowing modifying the flow in different ways.

- ✓ ***High-Frequency Micro Vortex Generators:*** *(G,LE,DS,U)* Conceptually is a mechanical element which oscillates in high frequency, inside the boundary layer thickness. The frequency is settled to a certain value, so that it

upna Universidad Pública de Navarra Nafarroako Unibertsitate Publikoa
Todos los derechos reservados
Eskubide guztiak erresalbatu dira

generates periodic vortices. The result is high-momentum streamwise air that has to be focused into the surface, in order to give more energy to the boundary layer and reduce its separation.

- ✓ ***Synthetic Jets:*** *(G/F,LE,DS,U)* The purpose of this device is to create streamwise vortices similar to the ones obtained with the PVGJs. Instead of using compressed air, the vortices are created by the movement of a diaphragm inside the airfoil. It sucks and ejects air from the airflow periodically, creating vortices that interact with it. The jet is generated by the interaction and advection of the vortices, and it moves the streamlines producing the same effect as a change of shape in the airfoil. Significant lift increase can be reached.

- ✓ ***Active Flexible Wall:*** *(G,LE,DS,U)* It can detect when the boundary layer starts to separate, and disturb it to avoid separation. It is an assembly of transducers embedded in a flexible housing, which has a thickness of microns. Thanks to this, it does not affect the airflow when it is not activated. When boundary layer separation is detected, the transducers vibrate to counter it. The device is able to decide which transducers need to vibrate to obtain the wished result. Stall can be delayed and the lift increased a little bit.

- ✓ ***Shape Change Airfoil:*** *(G,MC,I,S/U)* This setup consists in some piezoelectric actuators assembled inside the airfoil, covered with a latex membrane to make the surface of the airfoil continuous and avoid seams. When the system is deactivated, the shape of the profile is the regular one. When activated, the actuators push the upper side of the airfoil, changing the shape and thus generating a change of camber and vortices in the flow. The movement is adaptive and fast. Higher lift coefficients and smaller flow separation area can be obtained.

After this quick analysis, the decision of which device will be studied can be made. Due to the complexity of some of the setups, and the impossibility of acquiring certain materials or technologies and working with them, the best decision is to work on one of the geometric devices of which performance relies in simple mechanisms. Between these, the choice is to study the microtabs for several reasons. First of all, the benefits obtained with this device are very interesting in order to alleviate loads and improve the performance of a wind turbine. Besides, it can be studied in steady positions and the results will be useful anyway, and even though it has to be installed near the trailing edge the assembly is acceptable. So finally, this will be the object of study in this project.

upna Universidad Pública de Navarra Nafarroako Unibertsitate Publikoa
Todos los derechos reservados
Eskubide guztiak erresalbatu dira

3.4. Microtabs

As it has been explained before in this document, microtabs are geometrical devices that are located near to the trailing edge of a blade. The tabs are very small in height (usually around the boundary layer thickness) and they can be as long as the blade allows. Thanks to a translational movement they can be deployed perpendicularly to the wing surface modifying its aerodynamic performance. The tabs can be installed in both, the suction and the pressure sides of a blade, in order to achieve different aerodynamic performances. Controlling the device actively means that the tab can be inside the airfoil (maintaining the original airfoil shape), can be totally deployed or also in an intermediate position depending on the wind conditions, and that it needs to use some energy supply.

The implementation of this small device causes a very important change in the aerodynamics of an airfoil. When located in the pressure side of the airfoil, the flow separation point changes from the trailing edge to the end of the smart device (it changes the Kutta condition). Altering the flow separation and changing effectively the camber result into modification of the lift coefficient. Experimental studies done in 2000 (Yen *et al,*. 2000 [11]) show that a 30-50% increase in the lift coefficient can be achieved, using a microtab with a height of 1% of the chord and located in the pressure side. Lift enhancement is achieved by deploying the tab on the pressure (lower) surface and lift mitigation is achieved by deploying the tab on the suction (upper) surface. In *figure 3.5* it is shown how the flow separation is displaced to the microtab, representing the flow streamlines over an airfoil.

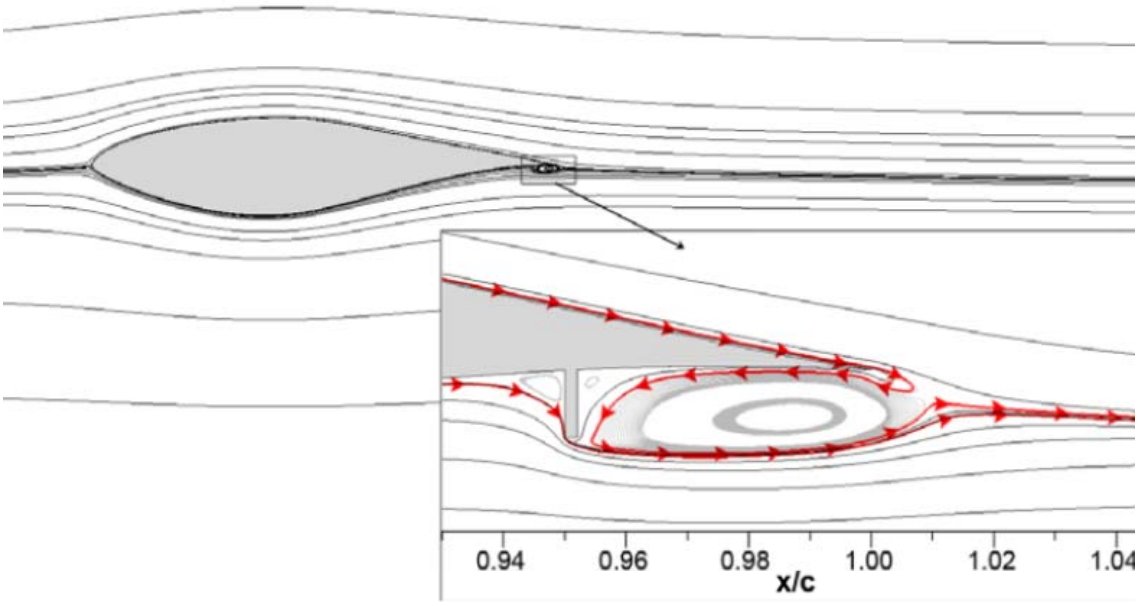

Figure 3.5. Flow separation detail in a microtab located at 95% of the chord [4].

upna Universidad Pública de Navarra Nafarroako Unibertsitate Publikoa
Todos los derechos reservados
Eskubide guztiak erresalbatu dira

The aforementioned studies related with microtabs show the importance of the size and location of these devices. In them, it is indicated that the best compromise between size and location is a height of 1-2% of the chord located at 95% of the chord in the pressure side, and at 90% of the chord in the suction side, so that the balance between lift, drag and volume constrains is optimal. Moreover, the space covered by the tab along the spanwise of the blade it is also important for the microtab effectiveness. The conclusion of the study done was that tab effectiveness is reduced as the gap size between the microtabs is increased. The amount of gap can be identified with a solidity ratio, defined as:

$$SR = \frac{span\ covered\ by\ tabs}{total\ span\ of\ the\ model}$$

Equation 3.1. Solidity radio [4].

The results said that it is highly recommended to maintain an 85% solidity ratio or higher for a proper effectiveness. In case of a 75% solidity ratio, the gaps between microtabs allow the flow to reattach in the trailing edge and it causes a big reduction of the blade performance.

In conclusion, microtabs can be used for load alleviation in wind turbines and lift enhancement. Modification of the lift and drag coefficients when needed can remove, or at least alleviate, some cyclic loads in turbines. For instance, the fatigue loads due to the shadow effect could be alleviated by installing a smart microtab in the suction side and deploying it every time the blade passes in front of the tower. This will smoothen the lift variation.

The main advantage of microtabs for their implementation is that they are able to do big changes in lift. The abovementioned studies (Yen *et al,*. 2000 [11]) report lift increases up to 22% when deployed in the pressure side and lift decrease up to 30% when deployed in the suction side. These lift modifications are only comparable to ones obtained by much more larger flaps, but the microtabs need less external power to be deployed and they are also faster. In the other hand the main problem of these smart devices are the gaps created between the tabs and the airfoil surface. The air leakage going through them affects negatively to the blade performance and it also generates aeroacoustic noise.

upna Universidad Pública de Navarra Nafarroako Unibertsitate Publikoa
Todos los derechos reservados
Eskubide guztiak erresalbatu dira

4. Wind tunnel

The experiments accomplished for the study of the microtabs took place in the wind tunnel of the Erasmushogeschool Brussel. But before developing them, the performance of this tunnel had to be improved, in order to take better advantage of it. Besides, it was important to know it well, so that the setup could be built regarding to its characteristics, and results could be better understood.

4.1. Introduction

4.1.1. Description

The wind tunnel used for the experiments is an old tunnel donated by the VUB to the Erasmushogeschool. Although the actual equipment available in the VUB is bigger and with higher potential, the one used was enough to reach good results in the tests designed. Besides, the tunnel in the Erasmushogeschool aerodynamics lab was less used at that moment, so the opportunity to perform the experiments and work on it was also interesting.

This machine works in open circuit and subsonic regime; in a range of speeds from 0 up to 22 m/s. It means that the air comes from the outside and goes out again, without having control of the characteristics of the incoming air. This will result in a possible variation of the results, related with the atmospheric conditions, any variation in the speed rate of the fan or possible alterations in the air due to human activity. Therefore, the conditions in every experiment have to be known in order to correct the effect of the environmental conditions in all the measurements and adapt them to obtain comparable results.

The original system consists in a fan, and a wooden tunnel with three different sections: a diffuser, a settling chamber and a contraction cone.

- ✓ *Diffuser:* it slows down the air speed, the pressure of the air is decreased and the airflow expands. All this makes easier for the air to occupy the whole section of the tunnel, and for the flow to be more homogeneous.

- ✓ *Settling chamber:* here the flow has a quiet area after the expansion that helps it to increase homogeneity.

upna Universidad Pública de Navarra Nafarroako Unibertsitate Publikoa
Todos los derechos reservados
Eskubide guztiak erresalbatu dira

✓ *Contraction cone:* it speeds up again the airflow, without adding turbulence to the stream. Thanks to this we can achieve speeds closer to the original ones in the exit of the fan but with better conditions in the airflow.

In *figure 4.1* it is shown a scheme of the components with the main size measures. Likewise in *figure 4.2* it is shown a real picture of the wind tunnel.

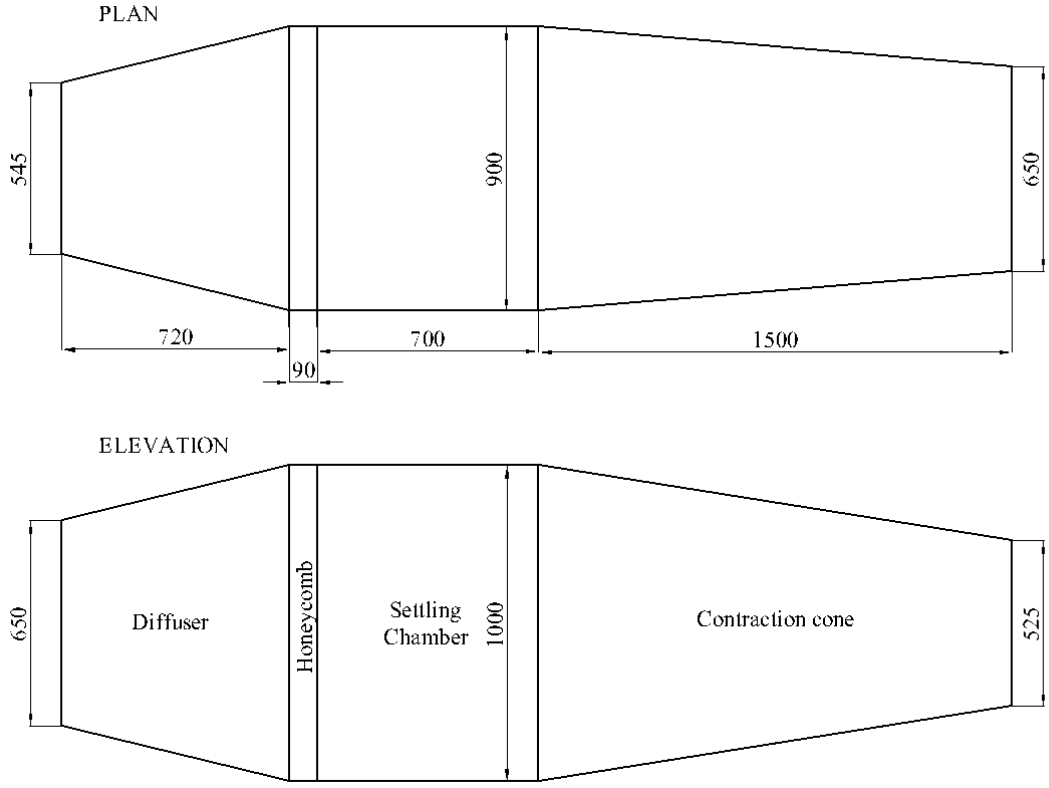

Figure 4.1. Scheme of the wind tunnel.

Figure 4.2. Wind tunnel at the Erasmushogeschool Aerodynamics lab.

upna Universidad Pública de Navarra Nafarroako Unibertsitate Publikoa
Todos los derechos reservados
Eskubide guztiak erresalbatu dira

To provide control of the spin velocity in the fan, it is linked to a computer. A controller has been implemented with the software LabView 2010 (*figure 4.3*). It allows controlling the fan speed, in a range from 0 to 5, where 0 means that the fan is stopped, and 5 is the maximum velocity. Although the accuracy of the control device is up to 6 digits (figure 4.4), it does not mean that this level of accuracy can be reached for the wind speed control inside the tunnel. The wind gusts and fluctuations produced by the fan make impossible to reach that level of accuracy in the airflow velocity. Apart from the fan inaccuracy, the controller cannot be settled numerically and it has to be done moving a wheel so it could be difficult to set the income power by the user at a certain value (*figure 4.4*). An interesting improvement would be to change the scale of the controller to wind speed instead of levels, and to develop a closed loop control, although it will not be extremely accurate according to what has been explained.

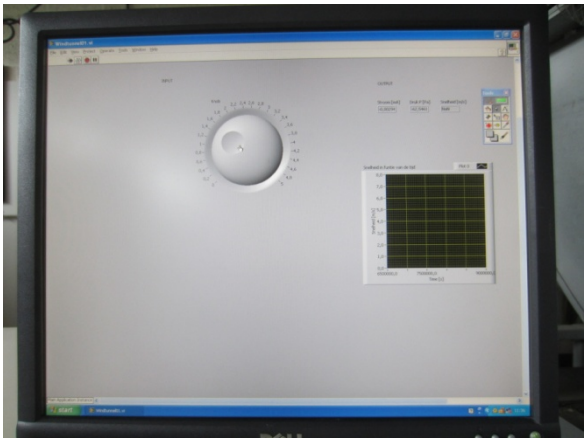

Figure 4.3. LabView 2010 interface.

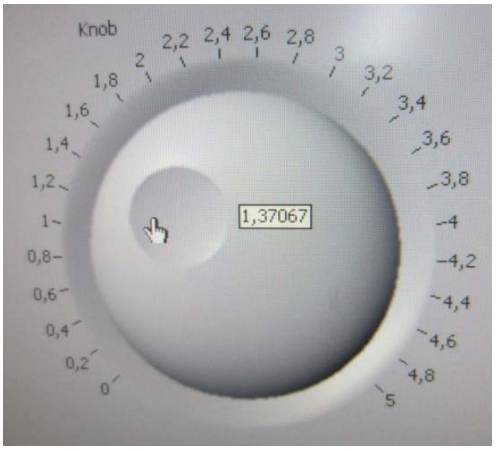

Figure 4.4. LabView 2010 controller.

4.1.2. Characteristics of the airflow with the original setup

In order to know the performance of the wind tunnel and orientate further improvement paths, the airflow had to be measured. For this task, a hot wire anemometer was used. This device allows us to measure the speed of the airflow. To do so, a wire is heated, and the heat transference due to the interaction with the air stream is measured and translated into wind speed. The anemometer used for the measurements (*figure 4.5*) gives also the environmental temperature, which is very useful data as far as measurements made in different days need to be compared.

upna Universidad Pública de Navarra Nafarroako Unibertsitate Publikoa
Todos los derechos reservados
Eskubide guztiak erresalbatu dira

Figure 4.5. Hot wire anemometer.

The speed tests were made at levels 1, 2, 3, 4 and 5 of power. The exit section was divided with a grid of 5 lines and 5 columns, to organize the measures, and set defined areas for them so that they are taken more or less in the same place in each experiment or test. The grid was formed by 13 cm wide and 10 cm high rectangles. This division is also useful in order to obtain a quick idea of the speed distribution in the exit area, just by writing the measured speeds in a grid. For each level of power the 25 areas were measured with the anemometer (*figure 4.6*) in the center of each rectangle, obtaining the following readings:

Figure 4.6. Grid at the wind tunnel exit.

upna Universidad Pública de Navarra Nafarroako Unibertsitate Publikoa
Todos los derechos reservados
Eskubide guztiak erresalbatu dira

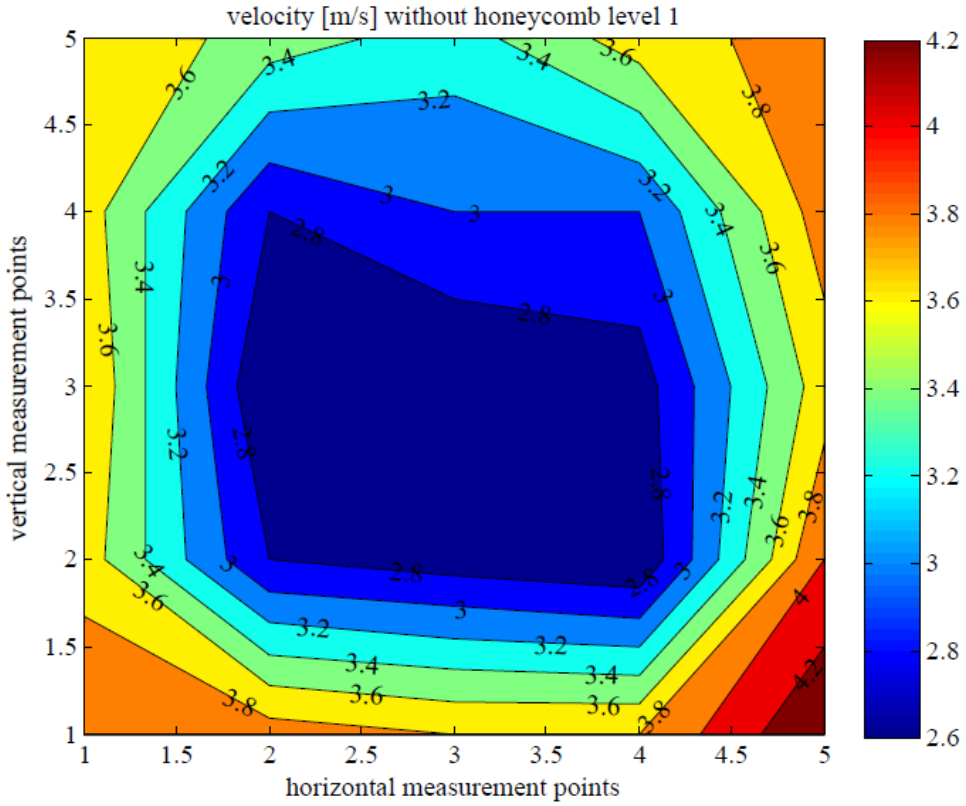

Figure 4.7. Velocity distribution, level 1.

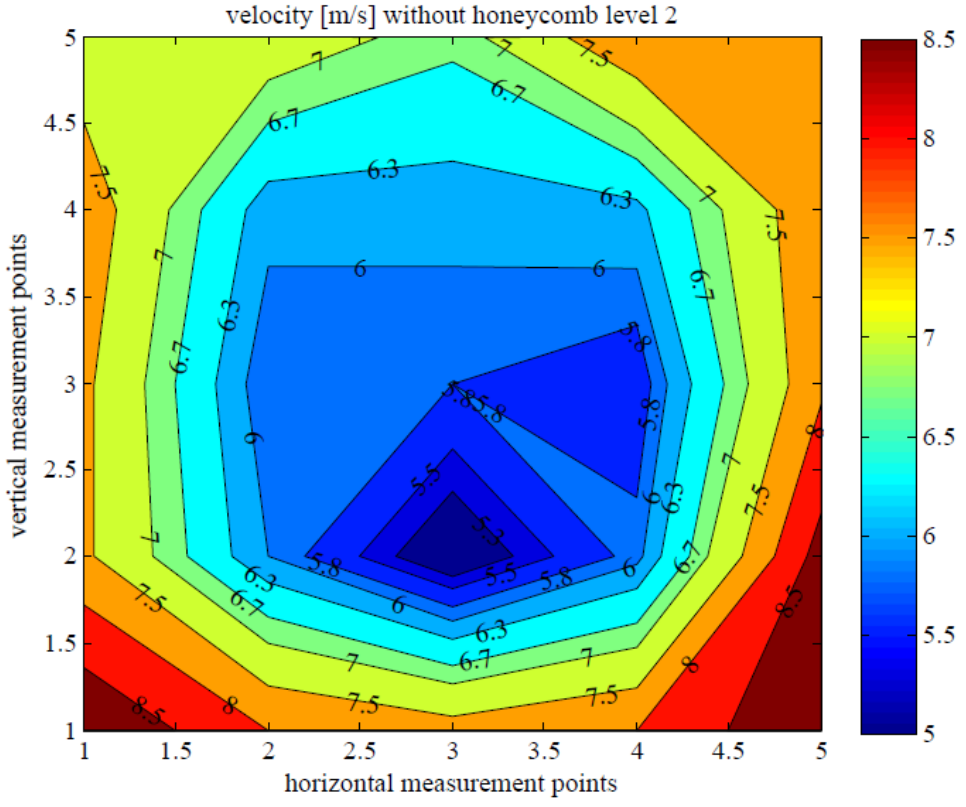

Figure 4.8. Velocity distribution, level 2.

upna Universidad Pública de Navarra Nafarroako Unibertsitate Publikoa
Todos los derechos reservados
Eskubide guztiak erresalbatu dira

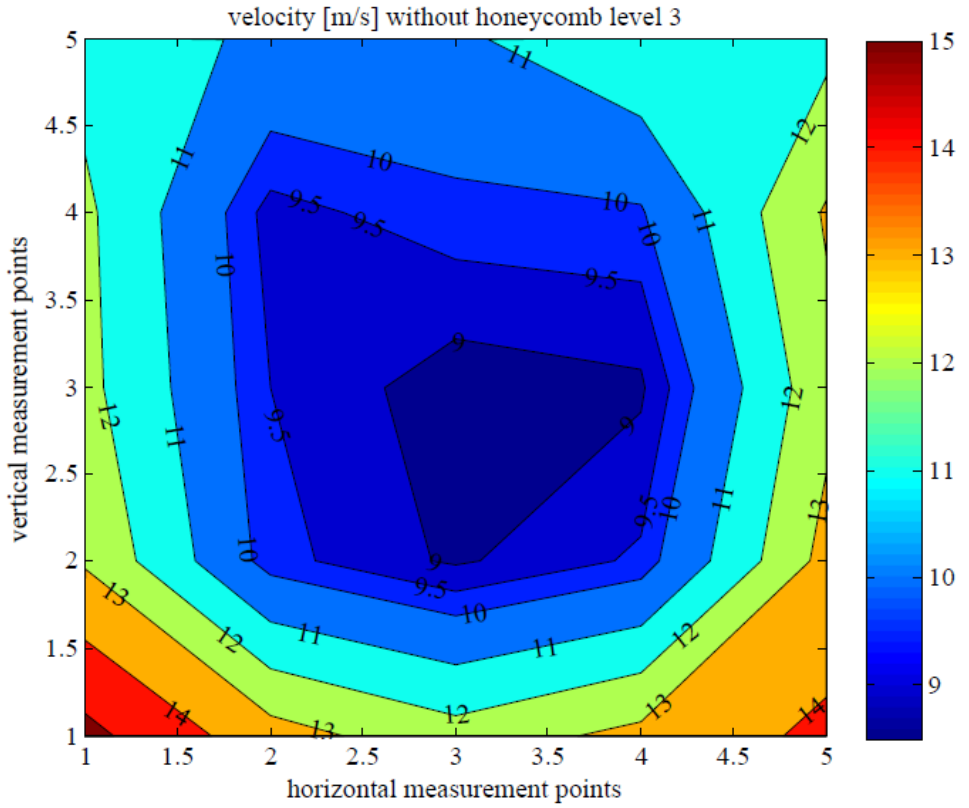

Figure 4. 9. Velocity distribution, level 3.

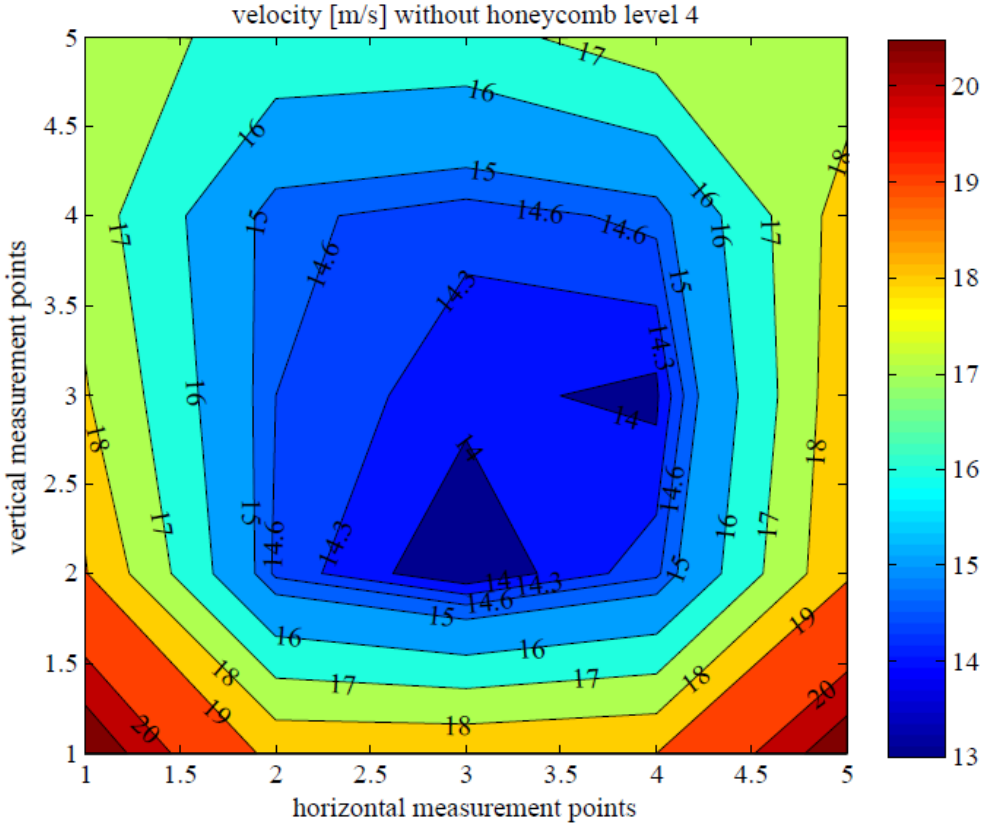

Figure 4.10. Velocity distribution, level 4.

upna Universidad Pública de Navarra Nafarroako Unibertsitate Publikoa
Todos los derechos reservados
Eskubide guztiak erresalbatu dira

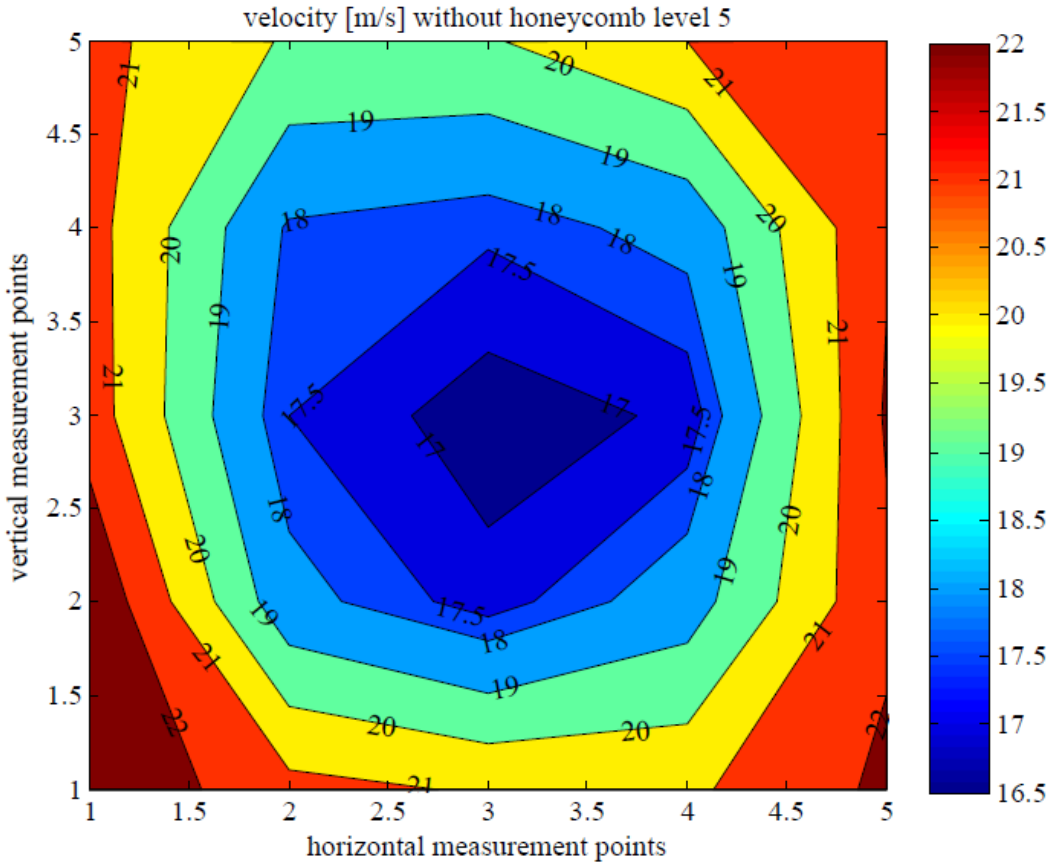

Figure 4.11. Velocity distribution, level 5.

Two main issues can be appreciated from the results:

- ✓ The first one is that the flow is not highly homogeneous. It is truth that in the center of the wind tunnel the speeds are more equal, but in close sections there are speed jumps up to 2-3 m/s (e.g. *figure 4.10* in the lower half, or *figure 4.11* left and right). The increase of the homogeneity would allow to develop more accurate experiments, and to use a bigger area of the wind tunnel section. Anyway, it has to be taken into account that the closer that any device is to the walls of the tunnel, the bigger their influence will be.

- ✓ The second one is that the lowest wind speeds (dark blue) are located in the centre of the exit section. If highest speeds can be focused in this area, then the range of speeds available for the experiments will be wider, and the potential of the machine will be increased.

upna Universidad Pública de Navarra Nafarroako Unibertsitate Publikoa
Todos los derechos reservados
Eskubide guztiak erresalbatu dira

4.2. Improvements done in the wind tunnel

4.2.1. Honeycomb

The first trial to improve the wind tunnel performance was to install a honeycomb between the diffuser and the settling chamber. In order to make the assemblage of the honeycomb possible, it is mounted in a wooden frame. The frame is strength enough to support loads without damaging the grid, and thanks to this, it can be held between the two sections just by using clamps or similar fixations (*figure 4.12*).

Figure 4.12. Honeycomb installed in the wind tunnel.

The expected result is that the movement of the air that arrives to the honeycomb will have a smaller transverse component once it has passed through it. This would cause a reduction of the turbulence within the stream, improving the characteristics of the airflow and making the axial component of the air predominant. Highest speeds may also be focused in the central area due to the turbulence decrease.

After fixing the honeycomb to the structure of the tunnel, the tests performed with the original setup were repeated.

The results are shown in *figures 4.13* to *4.17*.

upna Universidad Pública de Navarra Nafarroako Unibertsitate Publikoa
Todos los derechos reservados
Eskubide guztiak erresalbatu dira

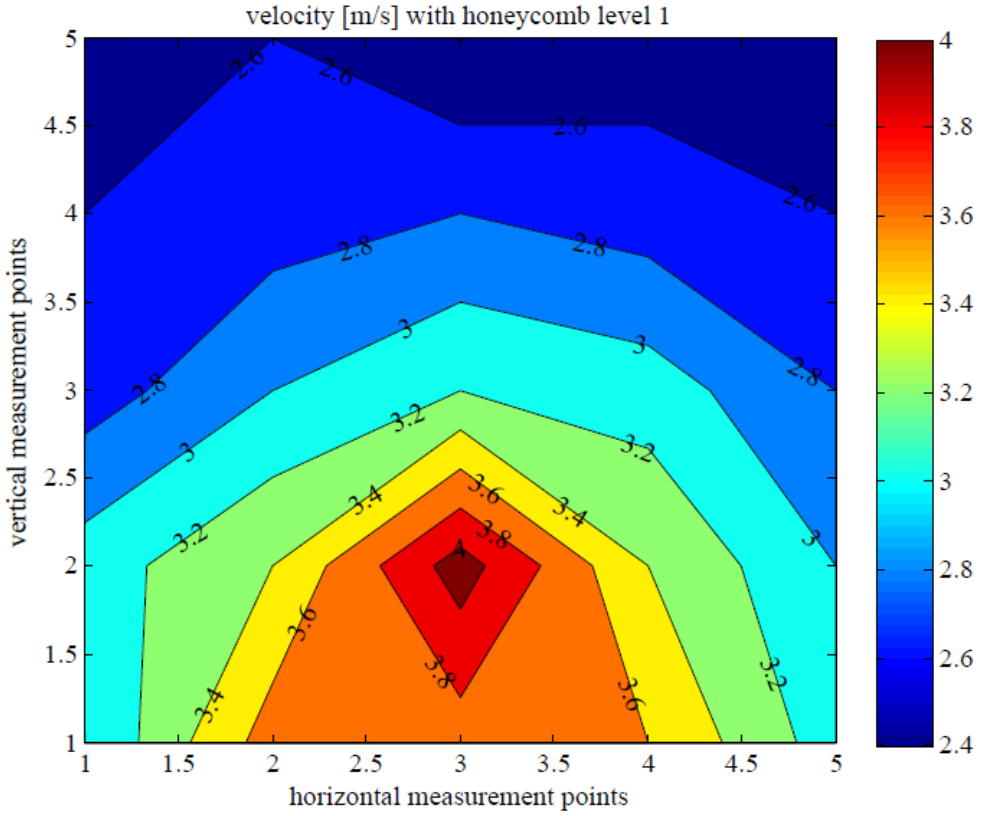

Figure 4.13. Velocity distribution with honeycomb, level 1.

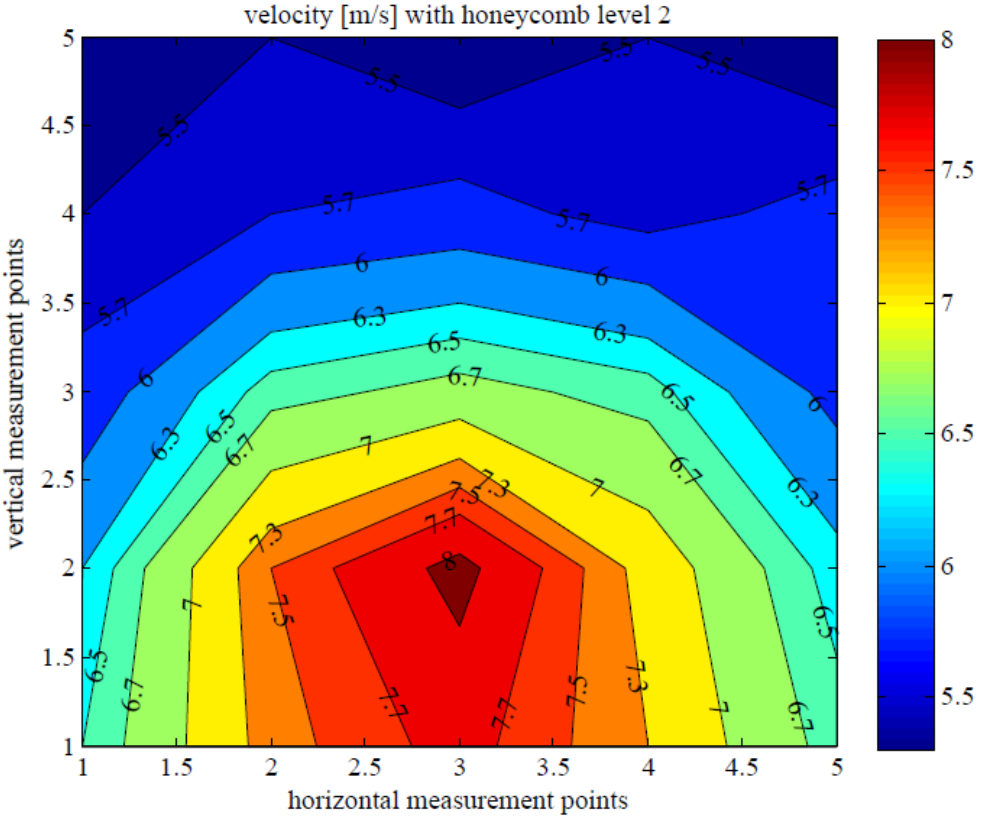

Figure 4.14. Velocity distribution with honeycomb, level 2.

upna Universidad Pública de Navarra Nafarroako Unibertsitate Publikoa
Todos los derechos reservados
Eskubide guztiak erresalbatu dira

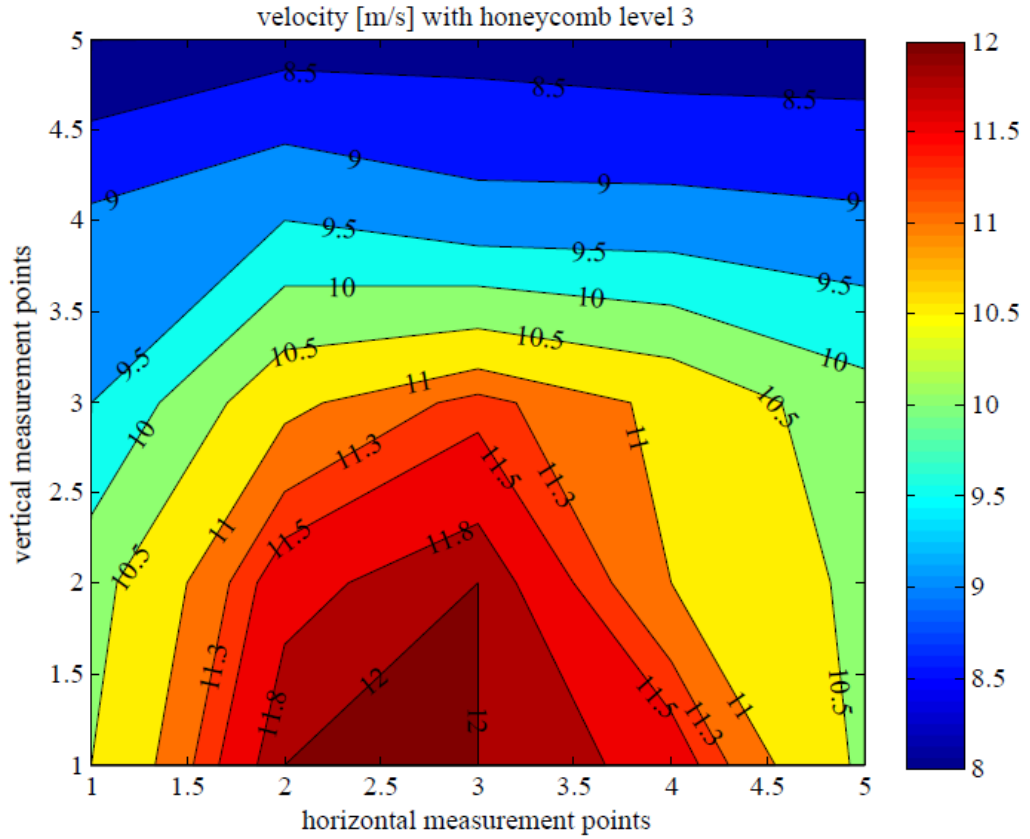

Figure 4.15. Velocity distribution with honeycomb, level 3.

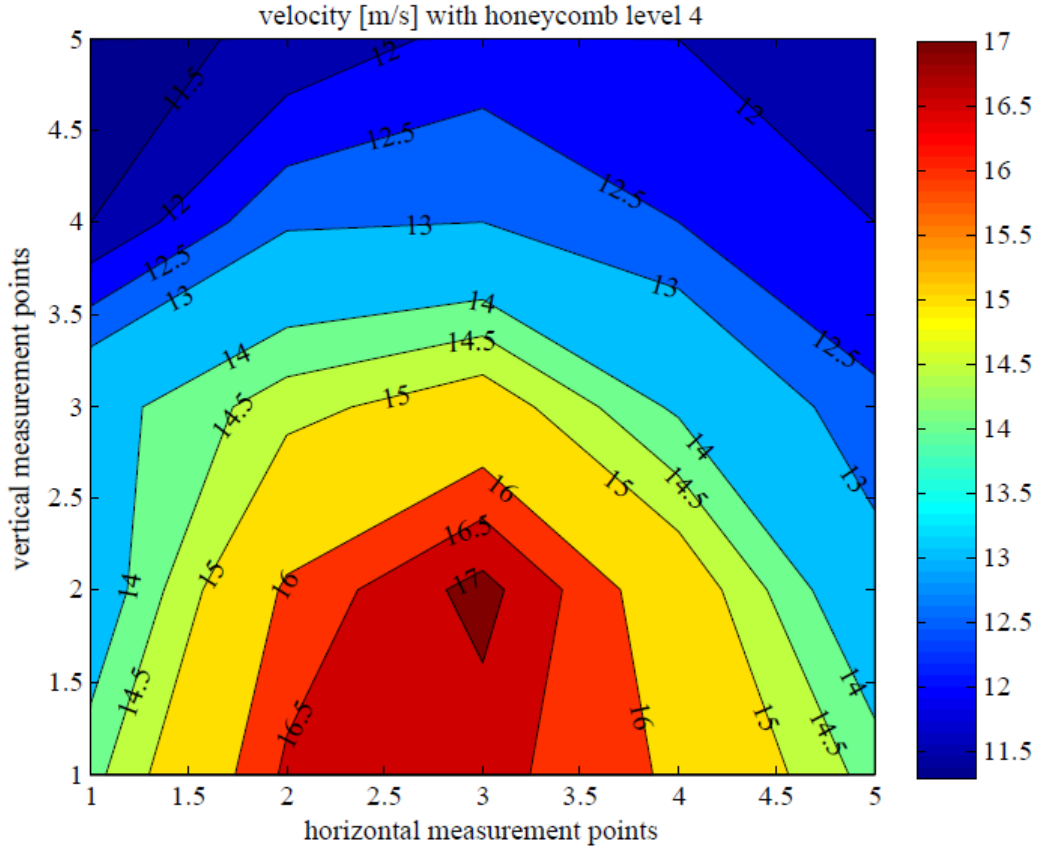

Figure 4.16. Velocity distribution with honeycomb, level 4.

upna Universidad Pública de Navarra Nafarroako Unibertsitate Publikoa
Todos los derechos reservados
Eskubide guztiak erresalbatu dira

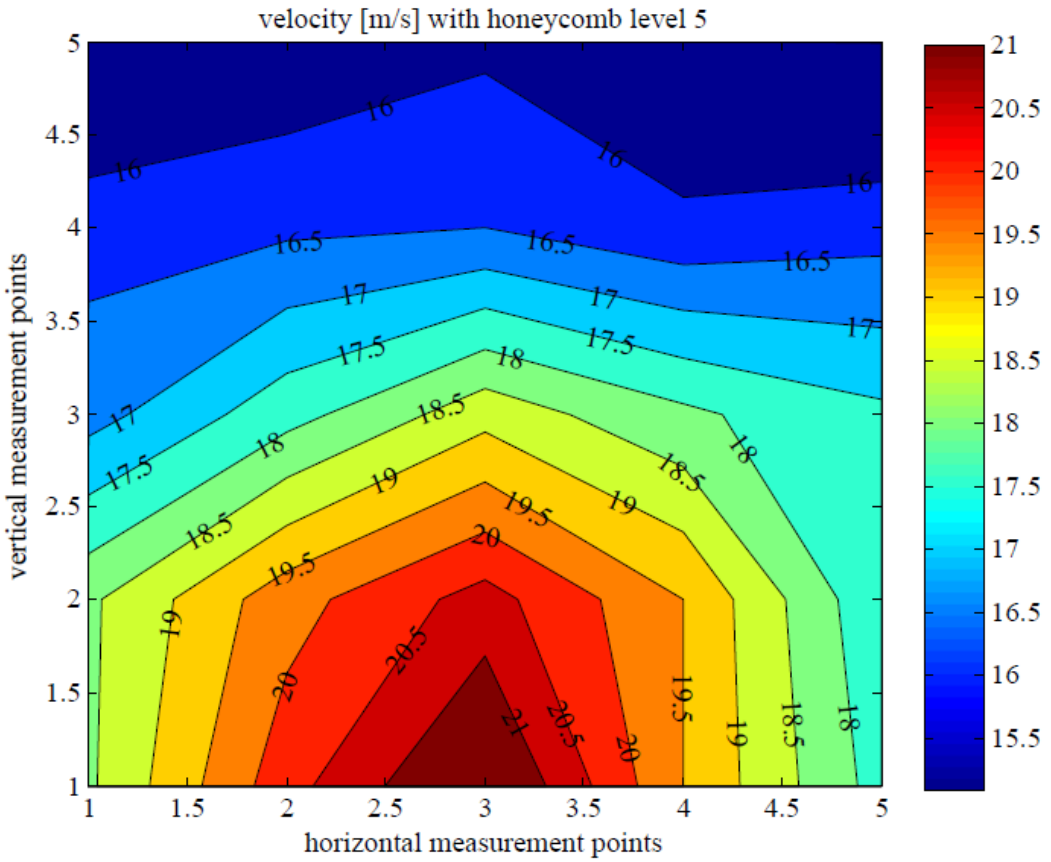

Figure 4.17. Velocity distribution with honeycomb, level 5.

At first sight, it is obvious that the airflow behavior changed completely. The main differences were:

- ✓ Highest speeds (red) were focused in the center of the exit section, but also in the lower area. This meant that the turbulence reduction had taken place, and the transverse component has been highly decreased leaving mainly the axial component of the airflow. The highest speeds were focused in the lower area because the fan exit is not the same size as the income section of the diffuser. The fan blows the air only in the lower area (*figure 4.18*). The next step should be to focus these speeds in the central region of the exit.

- ✓ The homogeneity was better (e.g. Figure 4.16 in the middle or Figure 4.17), although there were still remarkable differences between the lowest and the highest speeds. After installing the honeycomb the variation was progressive, there were not big jumps as it happened without it. Anyway, it was interesting to keep improving this factor.

upna Universidad Pública de Navarra Nafarroako Unibertsitate Publikoa
Todos los derechos reservados
Eskubide guztiak erresalbatu dira

Figure 4.18. Fan exit.

4.2.2. Flow redirection

Once the highest speeds were focused in the lower centre area, the only thing needed was to lift them to the geometrical centre of the exit section. Besides this, turbulence decrease was still interesting.

In order to mainly achieve the first goal, a new device was designed and tested. It might also improve homogeneity, but it was thought to redirect the air stream and set the highest speeds in the geometrical center. This device consists in two wooden sheets, installed horizontally in the transversal area of the wind tunnel. Both blades are able to rotate around their longitudinal axis, and are independent one form the other, so that they can interact in a different way with the air stream and cause the desired effect (*figure 4.19*).

Figure 4.19. Airflow redirecting device.

upna Universidad Pública de Navarra Nafarroako Unibertsitate Publikoa
Todos los derechos reservados
Eskubide guztiak erresalbatu dira

The idea was that once the air came out of the fan, it would hit into the sheets. They should be fixed with an angle that should be adequate to redirect the wind to the center of the wind tunnel section, so that higher speeds would be reached there. Therefore, they had to be installed next to the exit of the fan, between it and the diffuser. In order to make easier the attachment and detachment of this device, it is assembled in a wooden frame. This frame fits exactly the exit of the fan, so it does not need any fixation in that side. In the side that joins the diffuser, both are clamped together, just to be sure that there is not an air leak. For this purpose, the frame has also a rubber joint, and as soon as pressure is made between both pieces, the union is sealed (*figure 4.20* and *figure 4.21*).

Figure 4.20. Device installaed in the fan exit.

Figure 4.21. Device fixation.

In order to control the spin of each blade separately, both of them have independent wheels to rotate the axis. The divisions of the wheels allow fixing the sheets every 15 degrees. Both wheels can be linked by a wooden piece between, making both axes unable to turn. It has to be taken into account that the design of this device is not the purpose of this project; therefore the device is just a prototype. The blades may be improved (*figure 4.23*), and more accurate rotation may be interesting (although the results achieved were good) as well as improving the controller (*figure 4.22*).

upna Universidad Pública de Navarra Nafarroako Unibertsitate Publikoa
Todos los derechos reservados
Eskubide guztiak erresalbatu dira

Figure 4.22. Spin control system.

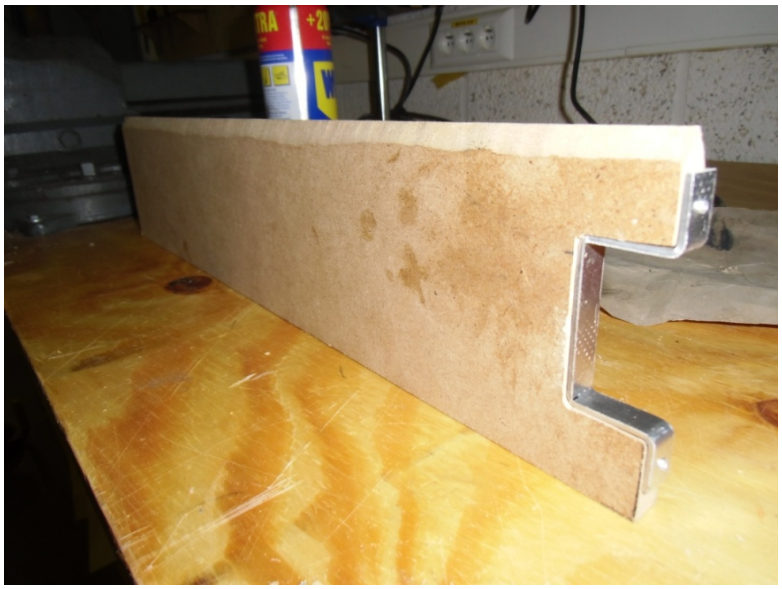

Figure 4.23. Airflow redirecting blade shape.

Several trials were made, fore levels 1, 3 and 5. First of all, the speed distribution was checked again without the device, and then with the device installed but angle 0 for both sheets, in order to see the influence of just assembling it. The results were:

upna Universidad Pública de Navarra Nafarroako Unibertsitate Publikoa
Todos los derechos reservados
Eskubide guztiak erresalbatu dira

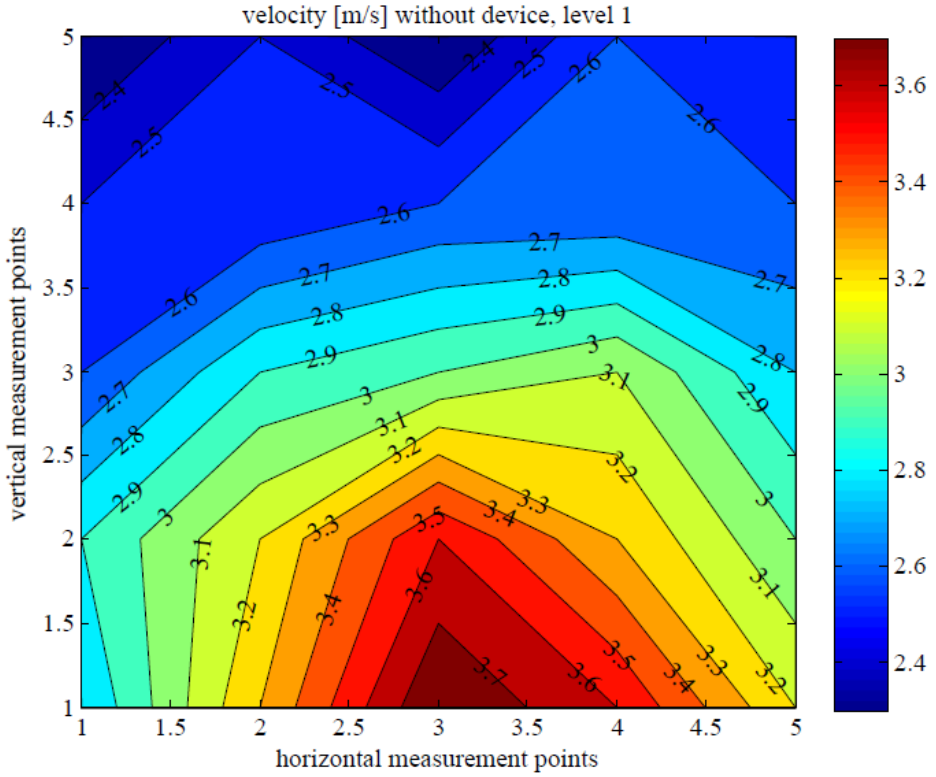

Figure 4.24. Velocity distribution without device. Level 1.

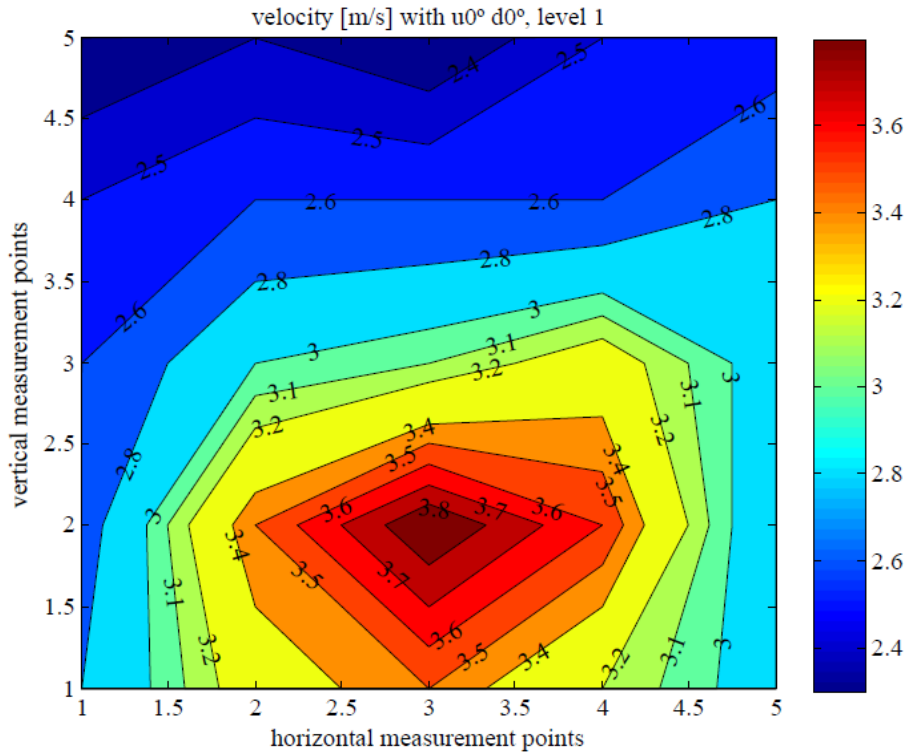

Figure 4.25. Velocity distribution with device (u0º d0º). Level 1.

upna Universidad Pública de Navarra Nafarroako Unibertsitate Publikoa
Todos los derechos reservados
Eskubide guztiak erresalbatu dira

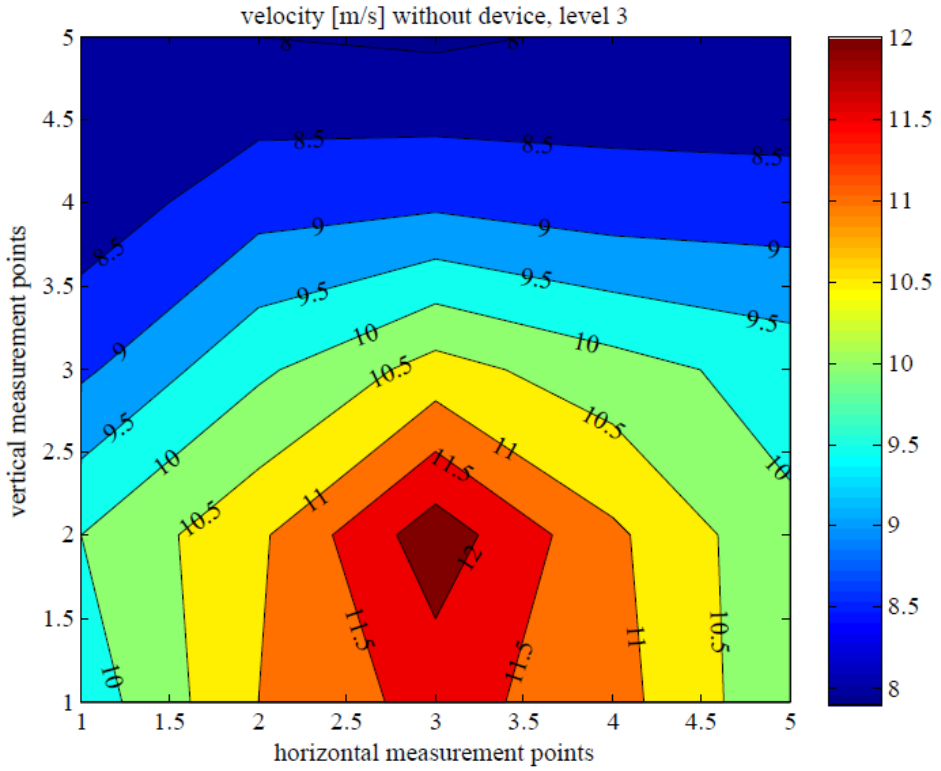

Figure 4.26. Velocity distribution without device. Level 3.

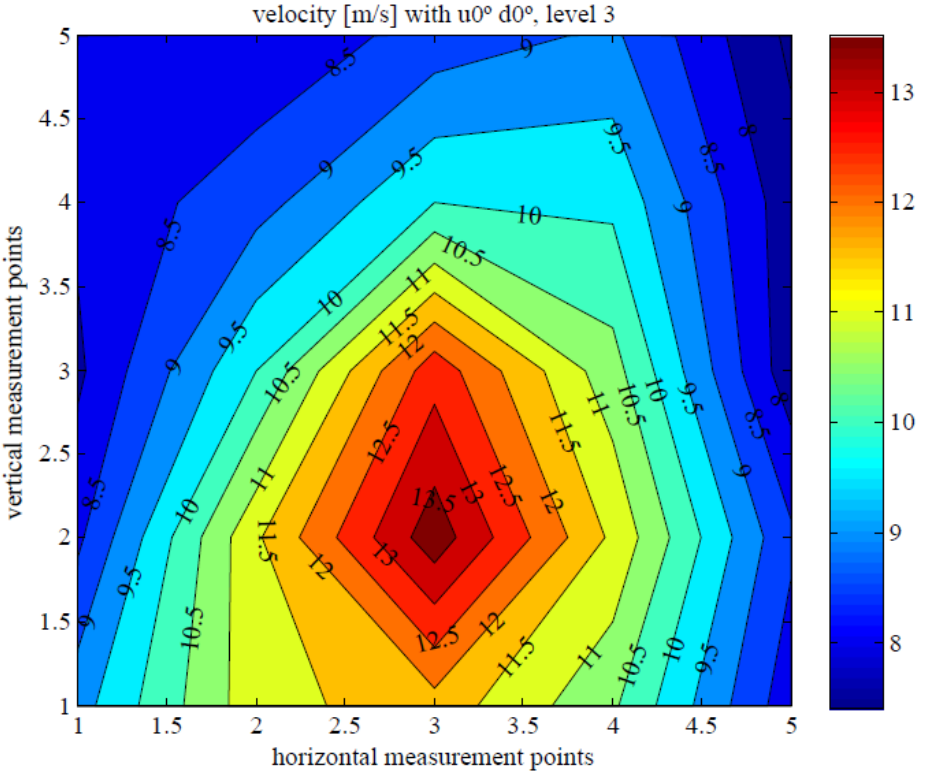

Figure 4.27. Velocity distribution with device (u0º d0º). Level 3.

upna Universidad Pública de Navarra Nafarroako Unibertsitate Publikoa
Todos los derechos reservados
Eskubide guztiak erresalbatu dira

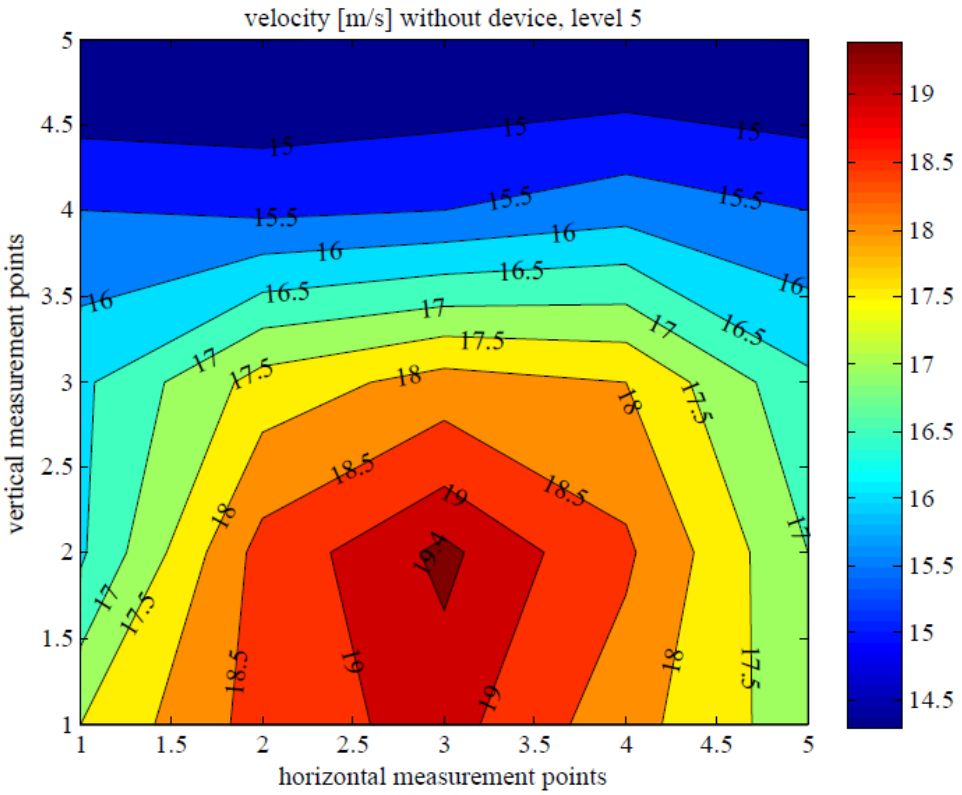

Figure 4.28. Velocity distribution without device. Level5.

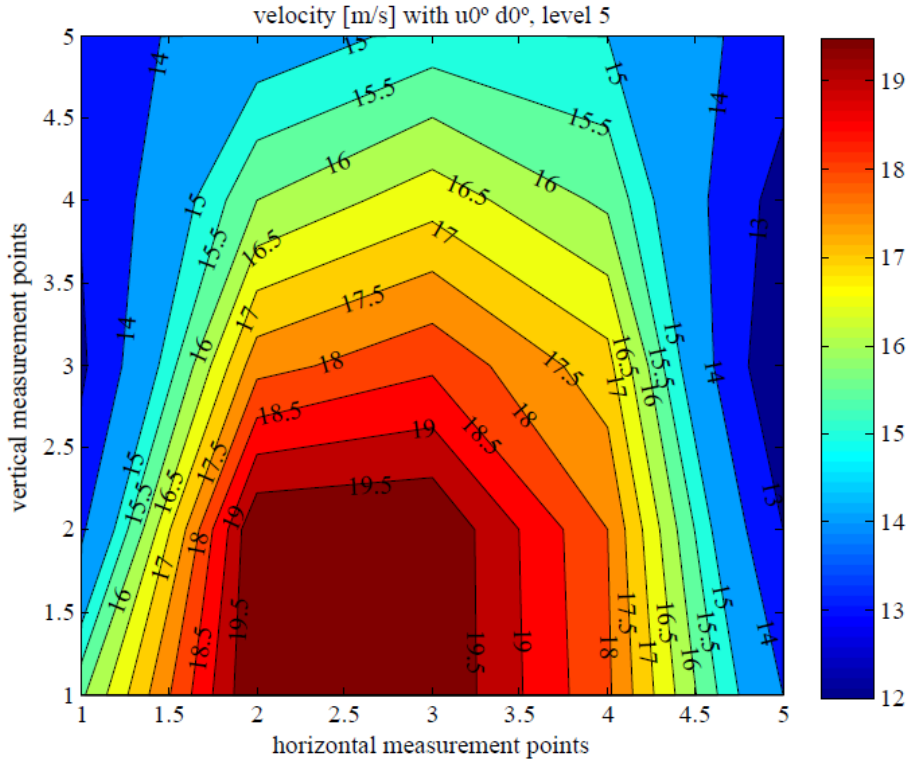

Figure 4.29. Velocity distribution with device (u0º d0º). Level 5.

upna Universidad Pública de Navarra Nafarroako Unibertsitate Publikoa
Todos los derechos reservados
Eskubide guztiak erresalbatu dira

It may need a detailed reading of the results, but it can be appreciated that just the fact of installing the device has three different effects:

- ✓ Regarding the range of speeds, it seems like in both sides (left and right) of the exit section the speeds are lower with the new part and higher in the center, comparing to the results obtained without the device (*figures 4.27 and 4.29*). The rise of speed is not very high, so it might be due to the device or due to differences in the conditions or the readings of the anemometer. But the drop is bigger, so it is likely to be related with the blades assembled.

- ✓ According to what it has just been explained, some homogeneity is lost, as once again, the jump from the sides to the center is bigger.

- ✓ It seems like the highest speeds are lifted a little bit, being closer to the geometrical center of the exit section.

After this test the next step was to try the different angle settings for each blade and repeat the tests. The setting of 15 degrees for both sheets was the one with best results. The obtained results were:

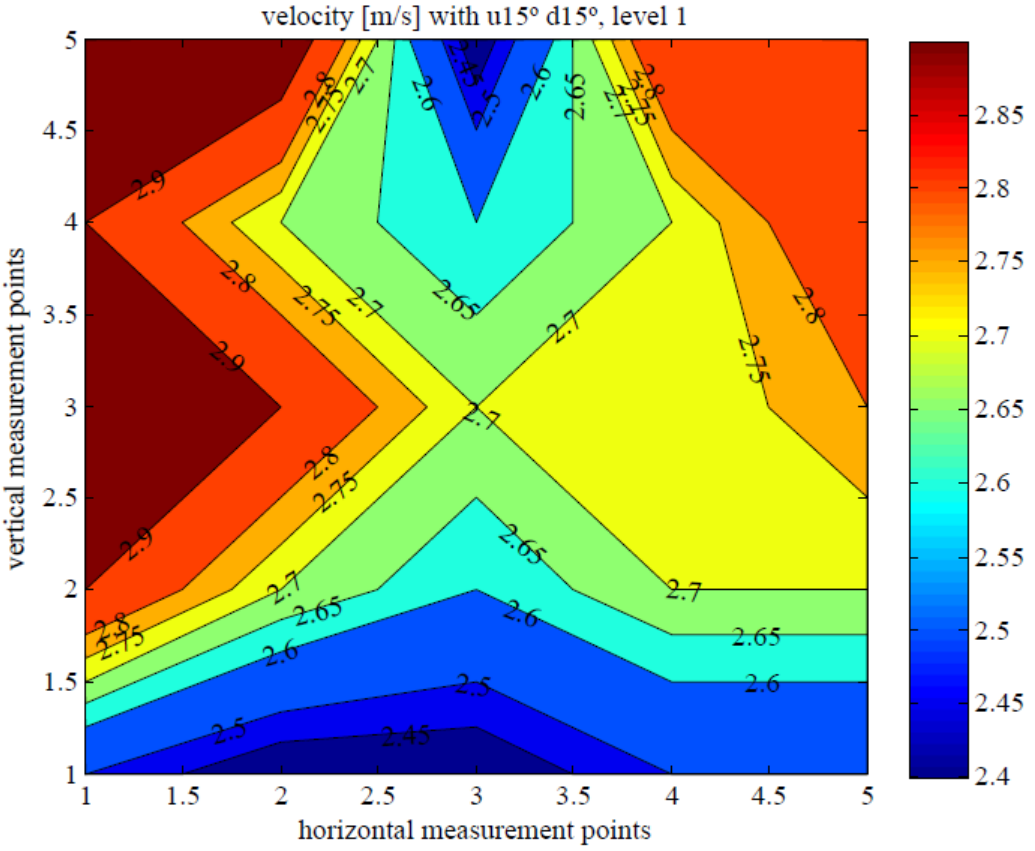

Figure 4.30. Velocity distribution with device (u15º d15º). Level 1.

upna Universidad Pública de Navarra Nafarroako Unibertsitate Publikoa
Todos los derechos reservados
Eskubide guztiak erresalbatu dira

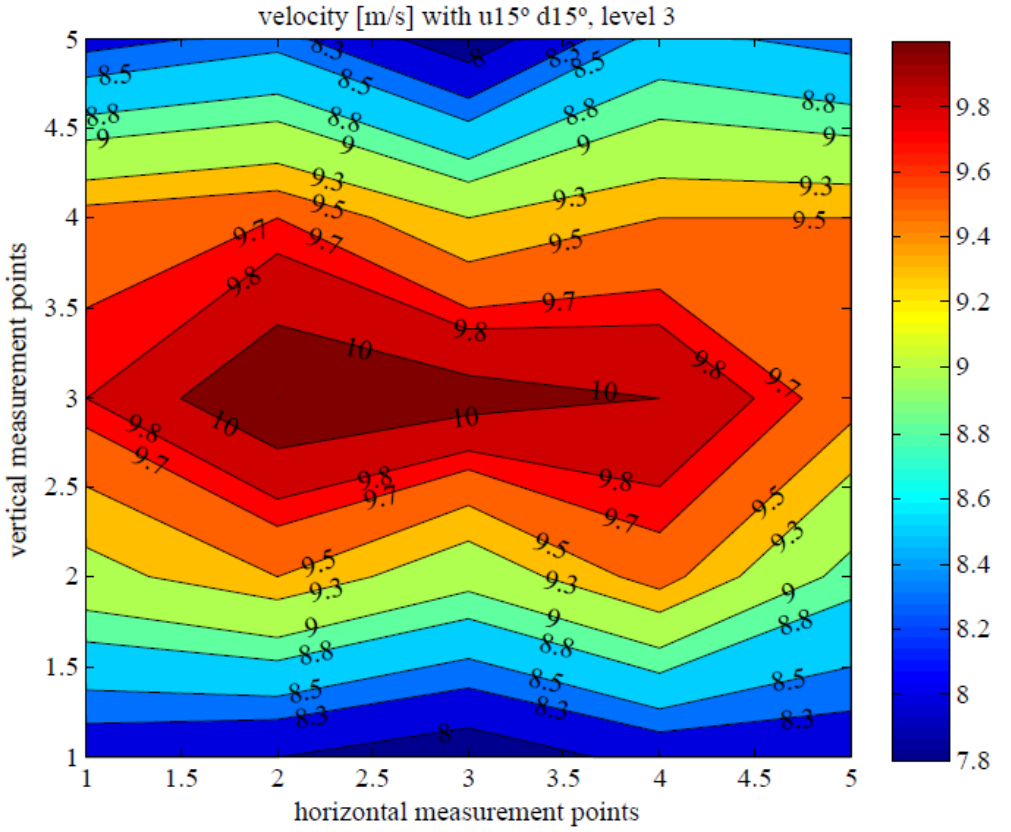

Figure 4.31. Velocity distribution with device (u15° d15°). Level 3.

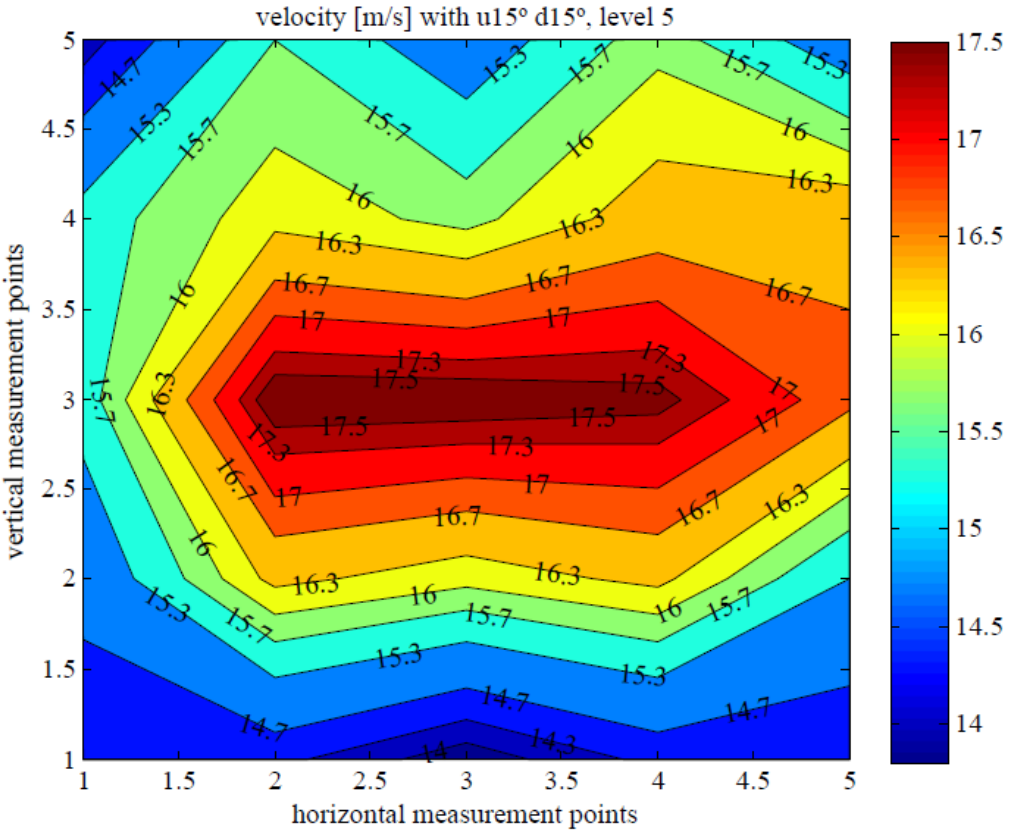

Figure 4.32. Velocity distribution with device (u15° d15°). Level 5.

upna Universidad Pública de Navarra Nafarroako Unibertsitate Publikoa
Todos los derechos reservados
Eskubide guztiak erresalbatu dira

And again the differences can be noticed:

- ✓ At level one the distribution looks like it has no order. But if the speed values are analyzed, it can be noticed that they are very close. The flow is highly homogeneous, and the differences between speeds are not important *(figure 4.30)*.

- ✓ Now the highest speeds (red) are focused in the centre area of the exit section. This was the main goal, so it is a great success, as it is the area where the profile with the smart blade is tested *(figure 4.32)*.

- ✓ On the other hand, there has been a speed fall, and the tests can be performed just up to 17.5m/s. In order to achieve higher speeds, a longer reduction cone could be tried.

Despite the good results obtained, other configurations were tried. For the test in which both sheets were fixed at 30 degrees, and before measuring the speeds, it could be felt just with the hands that the airflow was pushed very high, so the highest speeds were expected to be focused in the upper area. And these are the results achieved:

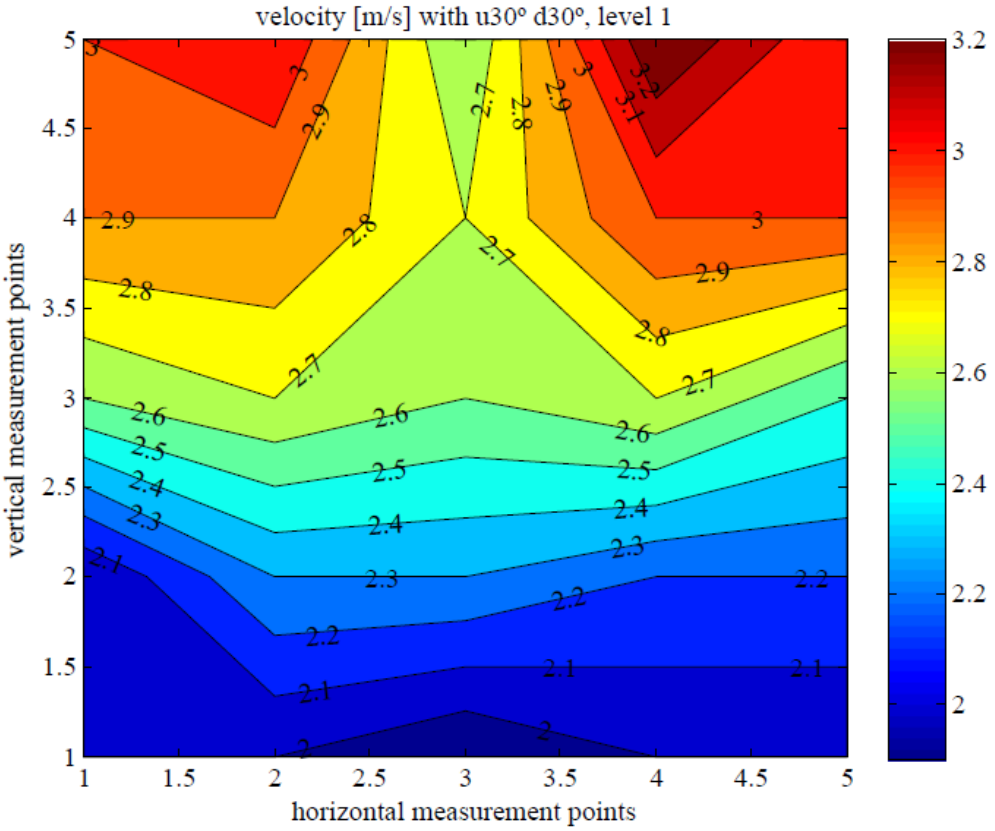

Figure 4.33. Velocity distribution with device (u30º d30º). Level 1.

upna Universidad Pública de Navarra Nafarroako Unibertsitate Publikoa
Todos los derechos reservados
Eskubide guztiak erresalbatu dira

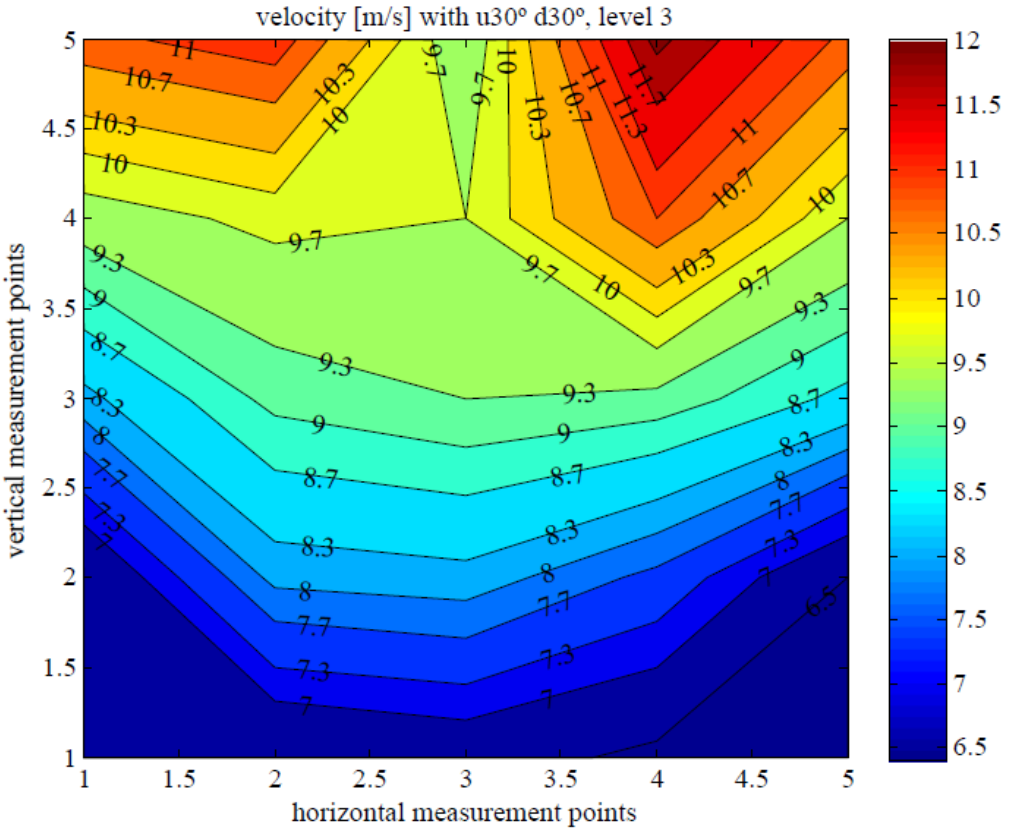

Figure 4.34. Velocity distribution with device (u30º d30º). Level 3.

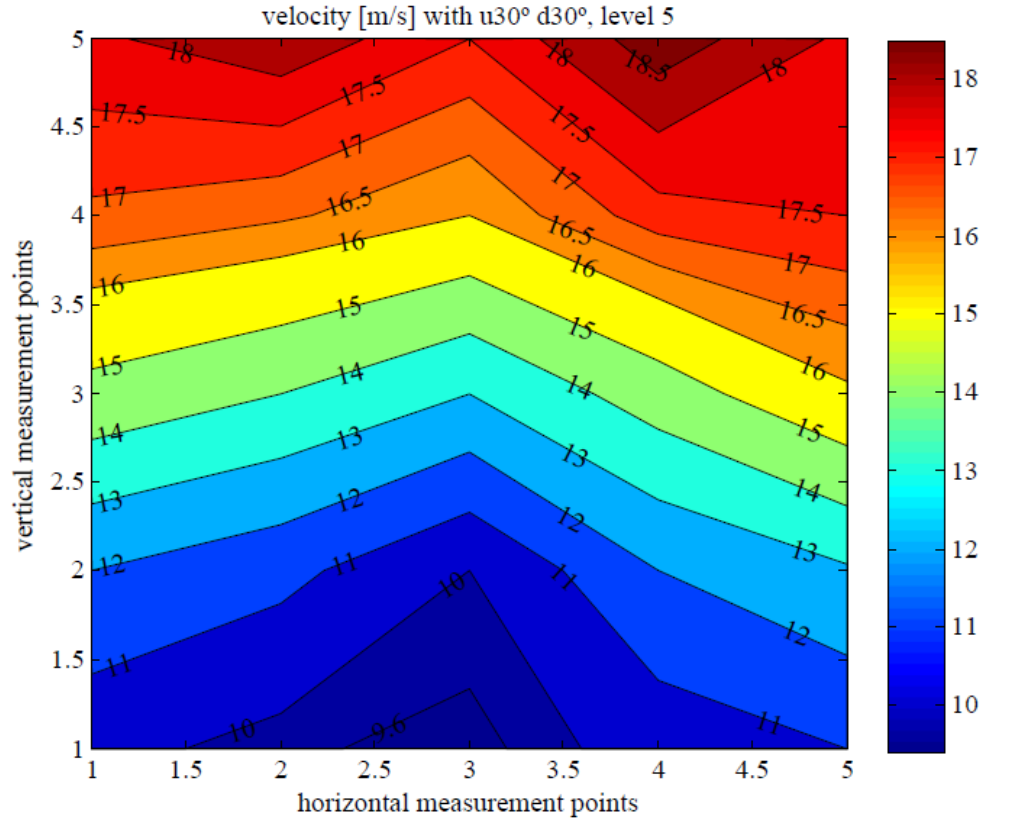

Figure 4.35. Velocity distribution with device (u30º d30º). Level 5.

upna Universidad Pública de Navarra Nafarroako Unibertsitate Publikoa
Todos los derechos reservados
Eskubide guztiak erresalbatu dira

At first sight, the effect was the expected:

- ✓ Highest speeds are now focused in the upper area *(figure 4.35)*. This might be interesting for some experiments, in case someone needs that distribution. But as far as this project is concerned is useless.

Some more trials were made setting different angles for each blade but the results were not good. In conclusion, the designed device with the 15 degrees configuration achieved the goal of pointing the flow toward the center of the section.

upna Universidad Pública de Navarra Nafarroako Unibertsitate Publikoa
Todos los derechos reservados
Eskubide guztiak erresalbatu dira

5. Theoretical calculations

In order to achieve the goal of this research it was necessary to predict some approximations of the data that would be obtained before doing the experiments, so that the procedures and tests could be properly designed, as well as the experimental setup. Also the equipment for the measurements and other needs could be chosen. In addition to this it is also important to compare the theoretical expected results with the experiments.

The pressure distribution created in an airfoil changes depending on the airfoil shape, wind conditions and the AoA. The shape is defined by the chosen profile and the microtab, installed or not, in its surface, so it was a known parameter. Likewise the wind conditions were known as they are set by the wind tunnel's limits and the atmospheric pressure and temperature which can be directly measured from the laboratory.

An approximation of the pressure distribution over a wing profile and the calculations of other parameters can be predicted or simulated using the vortex panel method.

5.1. Vortex panel method

The Vortex panel method is a technique for solving complex fluid flow problems over two dimension geometries (Anderson, 2008 [1]). This method allows starting to solve easy ideal fluid flow problems and after that getting the approach of the complex fluid problem. As ideal fluid flows are solutions to Laplace's equation and it is linear, the superposition of ideal problems can be organized to get the solution of complex flow patterns.

The vortex panel method turns the airfoil shape into linear panels. The pressure side and the suction side are divided into the same number of panels starting in the leading edge and ending in the trailing edge. The vortex phenomenon is studied for all the middle points of these panels, called control points, considering their boundary conditions and also the Kutta condition. The panel division of an arbitrary shape airfoil is shown in the *figure 5.1*.

upna Universidad Pública de Navarra Nafarroako Unibertsitate Publikoa
Todos los derechos reservados
Eskubide guztiak erresalbatu dira

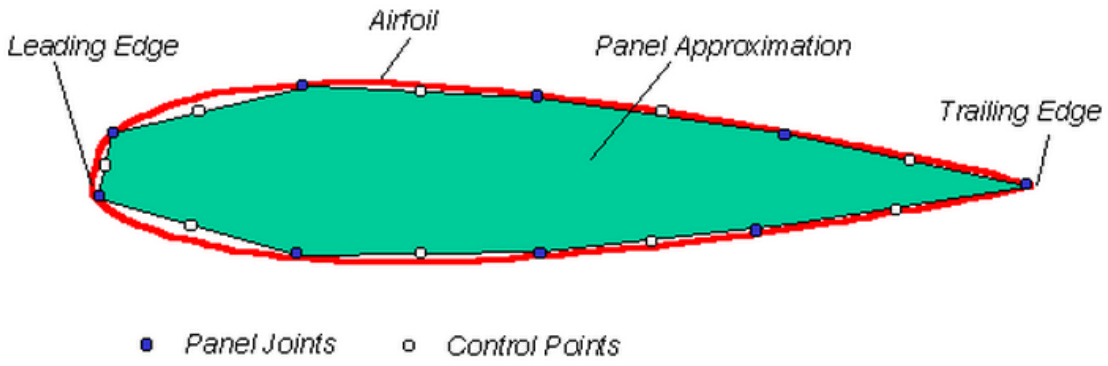

Figure 5.1. Panel division for an arbitrary shape airfoil [13].

It is possible to calculate the vortex sheets in every control point for an inviscid and incompressible flow. Furthermore, the Kutta condition says that the vortex sheet in the trailing edge is zero (the flow must smoothly leave the trailing edge in the upper and the lower edge) (Anderson, 2008 [1]). The integration of the stream function of all infinitesimal vortices at the profile surface while applying the Kutta condition would give the solution for the complex problem. Instead, the vortex panel method does the superposition of all vortices on all panels applying a numerical method. Once these vortices are solved, the velocity and pressure fields can be calculated and so the pressure coefficient for each point (C_p).

It is important to notice that the accuracy of the results is affected by the number of the panels. Due to the implementation of the numerical method, the more number of panels the more accurate the solution would be, since we are representing a continuous curve by series of broken straight lines. It is also important to increase the number of panels where the pressure gradient is big, for instance near to the leading edge, again to get a better numerical solution.

5.2. Simulation of the pressure values

Before doing the experiments, it was interesting to have some data to compare with. In order to obtain it, some theoretical calculations were done using the vortex panel method. Besides, the results could help to choose the appropriate device for the pressure measurements.

First of all, it was important to determinate the parameters of the experimental setup and the conditions surrounding the test.

The airfoil GU25(5)8-11 profile was chosen due to different reasons. To begin with the trailing edge of this airfoil is thicker than others, which may help to the installation of the microtab in the experimental setup. Besides, another research

upna Universidad Pública de Navarra Nafarroako Unibertsitate Publikoa
Todos los derechos reservados
Eskubide guztiak erresalbatu dira

involving smart devices and microtabs was being done in the aerodynamics department of the Erasmushogeschool with this profile, so the results in both researches could be compared if the same profile was used. The geometrical shape is defined by the numerical coordinates of its contour points. This data is given by the profile data base [14]. For the chosen airfoil the data points are shown in the *appendix 2* and the *figure 5.2* shows GU25(5)8-11 airfoil's shape:

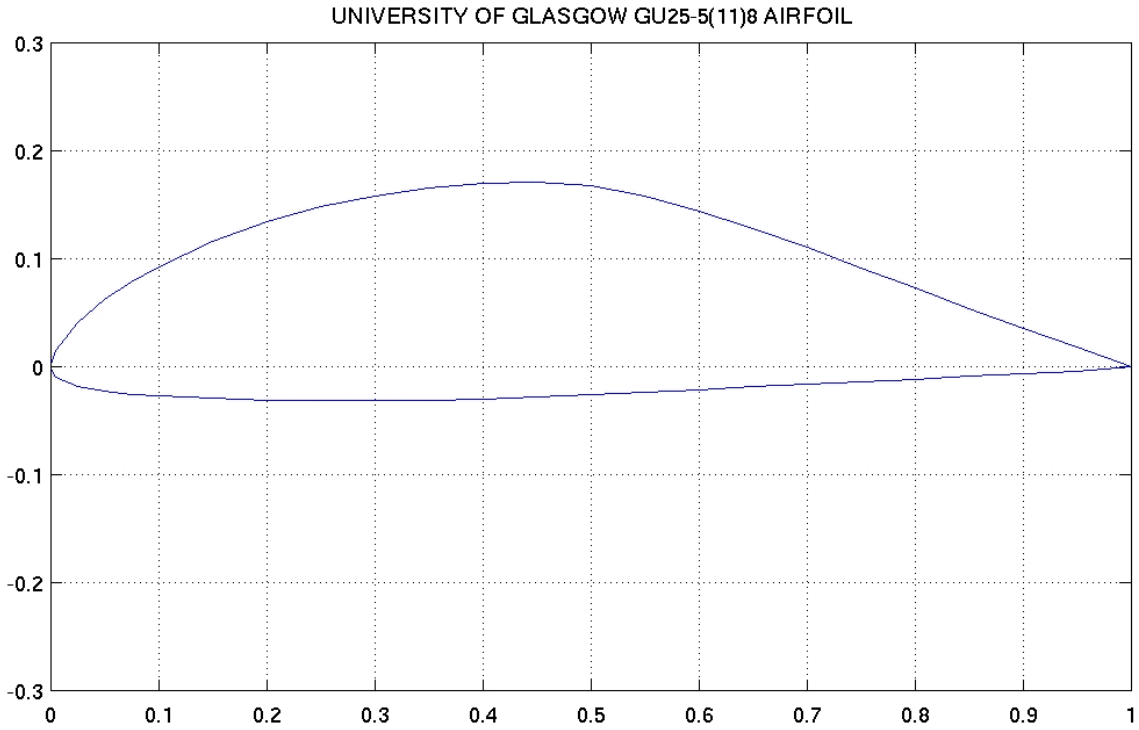

Figure 5.2. GU25(5)8-11 airfoil [14].

Secondly, the AoA modifies both, the pressure distribution and the lift coefficient. As one of the purposes of this simulation is to predict the limits of the pressure measured in the tests, different AoAs must be tested. The AoA for which the lift is maximum is called the maximum lift coefficient angle. This angle is one of the data given in the profile data base [15]. For the GU25(5)8-11 is:

$$C_{L,max} = 15°$$

upna Universidad Pública de Navarra Nafarroako Unibertsitate Publikoa
Todos los derechos reservados
Eskubide guztiak erresalbatu dira

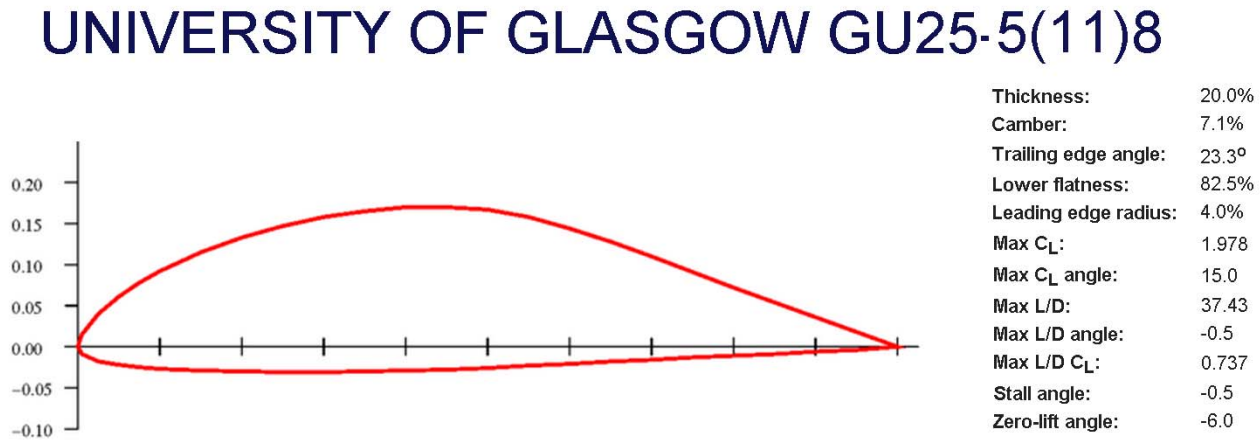

Figure 5.3. GU25(5)8-11 data [15].

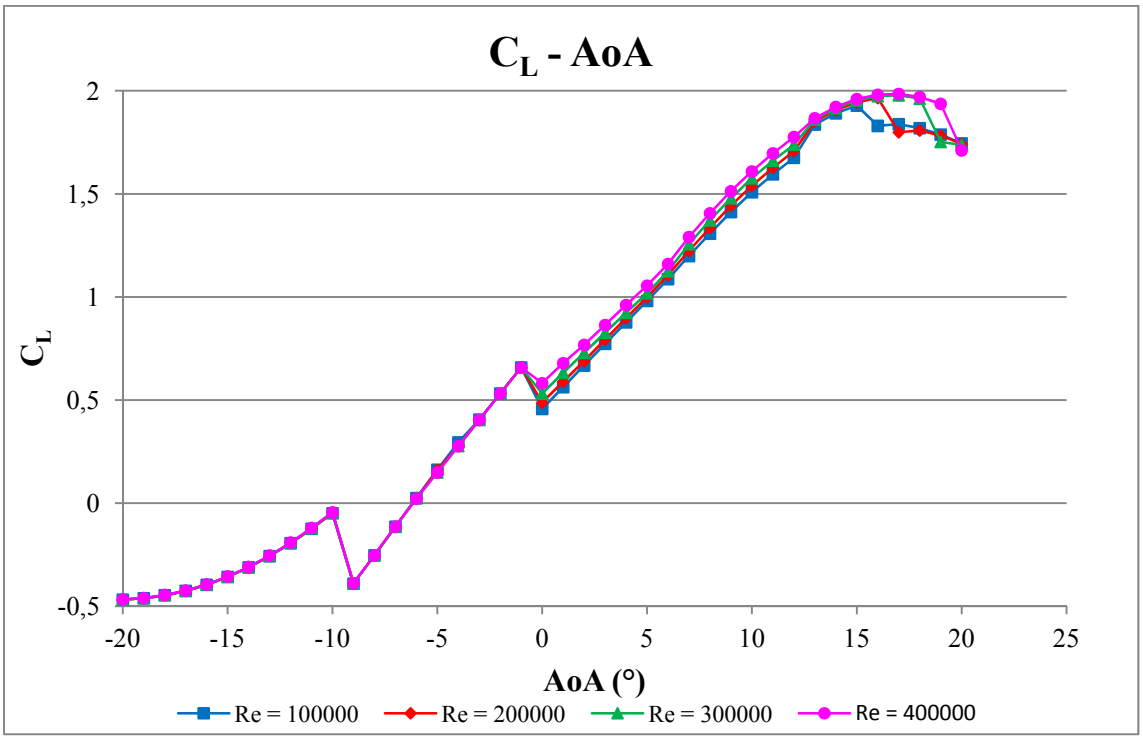

Figure 5.4. C_L and C_m versus AoA [16].

Figure 5.3 shows the characteristics of the GU25(5)8-11, and *figure 5.4* shows the C_L versus the AoA for different Reynolds numbers. It can be appreciated that the theoretical behavior of the profile for AoAs from -20˚ to -0.5˚ is almost the same for the Reynolds numbers that are simulated.

upna Universidad Pública de Navarra Nafarroako Unibertsitate Publikoa
Todos los derechos reservados
Eskubide guztiak erresalbatu dira

The simulation was done using a vortex panel method application [16], for different wind speeds up to 17 m/s, which was the highest reachable in the Erasmushogeschool's wind tunnel. Also different AoAs were simulated. In *figure 5.5* the output of the used applet is shown.

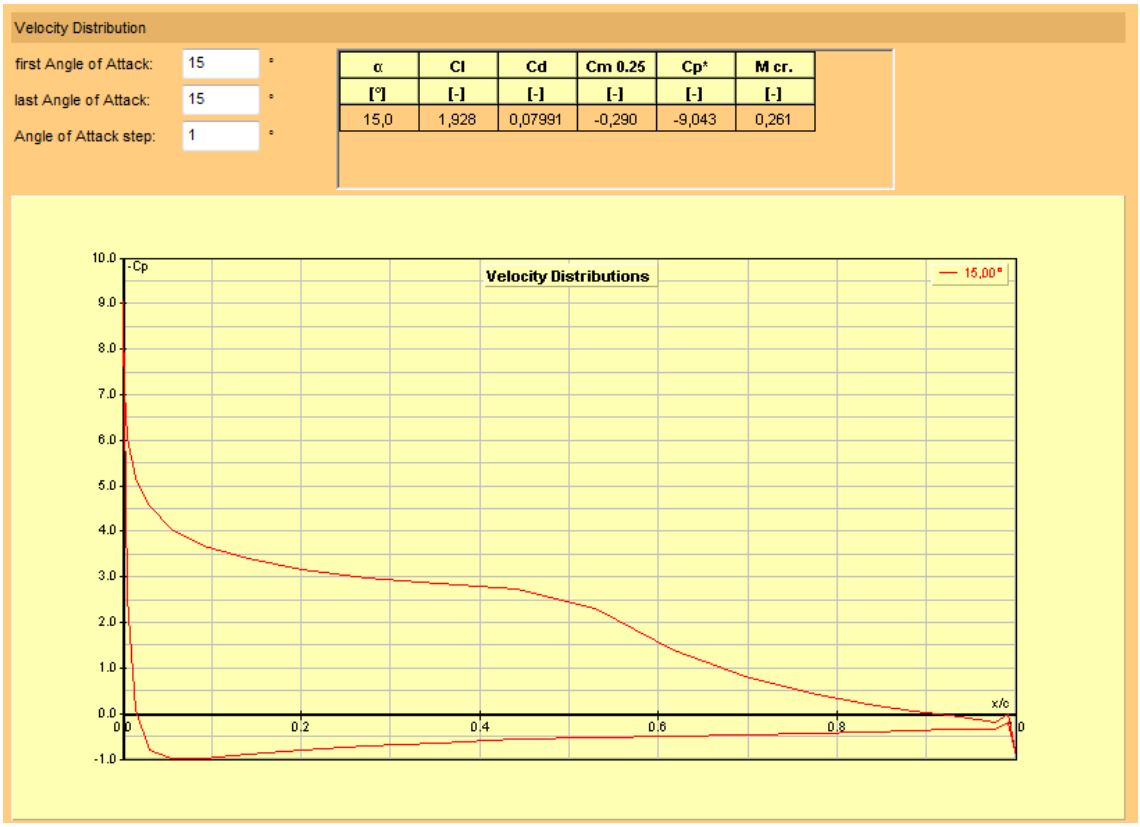

Figure 5.5. Output of the vortex panel method application for 15 degrees of AoA [16].

The software used showed the shape of the airfoil built with the points that were introduced, graphic representation of the pressure coefficient (C_p) for each point and a table with the values of the aerodynamic coefficients.

With this data dynamic pressure can be calculated in each point from the pressure coefficient equation (*equation 5.1*). It is important to notice that this is what will be measured, the pressure difference between the total pressure and the static pressure. The air density used is taken from tabulated dry air values for 20 ºC. This temperature was chosen because it was a close value to the different temperatures that could be given in the laboratory.

$$\rho_{20\,^{\circ}C} = 1.204\ \frac{kg}{m^3}$$

$$C_p = \frac{P - P_\infty}{\frac{1}{2}\rho_\infty V_\infty^2}$$

Equation 5.1. Pressure coefficient [1].

upna Universidad Pública de Navarra Nafarroako Unibertsitate Publikoa
Todos los derechos reservados
Eskubide guztiak erresalbatu dira

In order to achieve different aims several simulations were accomplished:

- ✓ *17 m/s and 15 degrees of AoA:* this simulation shows the maximum expected lift, in order to compare the data found with our calculations.

- ✓ *Different wind speeds*: these tests allowed knowing the range of pressures that could be expected. The conclusion was that for low speeds the dynamic pressures were really small, so it would be difficult to measure them accurately.

- ✓ *Different AoAs*. Several AoAs between -20º and 20º were studied in order to have data to compare with the experimental results and collect pressure values, so that the measuring device could be chosen.

The calculated pressure values for 17 m/s and 15 degrees of AoA are shown in the figure below (*figure 5.6*). Data of the calculations can be found in *appendix 3*:

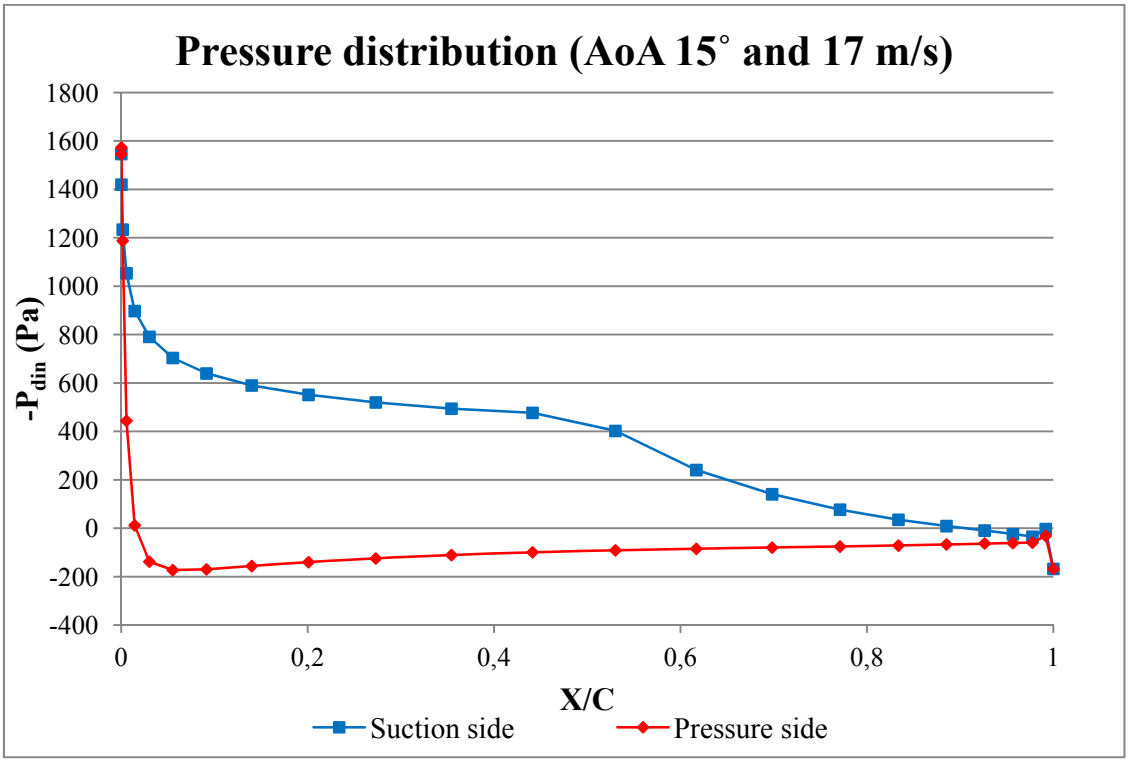

Figure 5.6. Theoretical pressure distribution for 15 degrees of AoA and 17 m/s.

The highest predicted pressure difference in the locations of the pressure taps was -1654 Pa, found for an AoA of -20˚ and a wind speed of 17 m/s. This data has to be taken into account in order to choose a measuring device. Anyway, most values are under 1250 Pa (which is the limit of the pressure transducer of the lab).

upna Universidad Pública de Navarra Nafarroako Unibertsitate Publikoa
Todos los derechos reservados
Eskubide guztiak erresalbatu dira

6. Setup

In order to reach good results in the experiments, the design of the set up has to be well thought and developed. As the authors of this project did not have any notion about building test set ups for wind turbine blades, some advice was taken. The invaluable help of the Von Karman Institute, especially from Professor M. Carbonaro, was crucial for the set up accomplishment.

6.1. General description

In the following sections all the procedures that led to the final set up are explained. This chapter could be especially interesting for those people that, as the authors did, have to build a set up with no previous experience in this field. Not only the different possibilities are explained, but also some techniques to choose the most appropriate one.

6.2. Blade

6.2.1. Core with ribs

The first idea was to build a blade made out of wooden or metal ribs and foam. There would be three ribs along the span of the wing. Two ribs, one in each side of the blade, and a third one in the middle. The tubes used for the pressure measurements (it will be explained later) would end in the middle rib, where holes should be made to allow the air income. Between ribs there would be foam, so that the whole assembly would be a solid blade with the shape of the profile chosen *(figure 6.1)*.

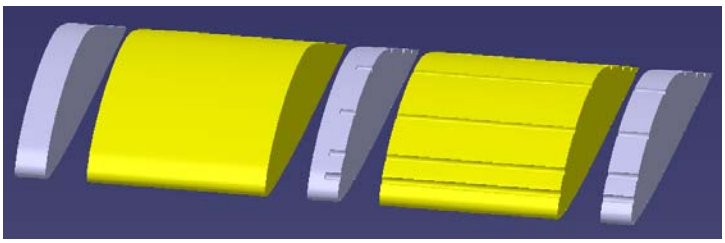

Figure 6.1. Sketch of the foam cores (yellow) with wooden or metal ribs (grey).

upna Universidad Pública de Navarra Nafarroako Unibertsitate Publikoa
Todos los derechos reservados
Eskubide guztiak erresalbatu dira

The main purpose of the ribs is to give stiffness to the blade, by making the foam pieces shorter. Besides, they would be useful for the construction. If a piece of foam is fixed between two wooden / metal ribs, then the foam can be easily cut and / or sanded just by following the shape of the ribs. This is a great advantage, as just a small milling machine to cut out the ribs is needed. So from small pieces we can end up in a big blade with the correct shape.

After assembling all the parts, the whole piece would be covered with fiberglass and epoxy, in order to give uniformity to the shape of the blade and some extra stiffness.

But there is a problem in this way of building the blade. Before sticking the ribs to the foam, they should to be perfectly aligned. This means that two or three axes would be necessary, attaching the ribs and going through the foam. This is a disadvantage, as extra error in the shape could be introduced, besides the existing deviation due to the good condition of the tools, and human error in the use of the milling machine. Also, making the holes from side to side of the foam pieces can be difficult, as long drill bits are usually too thick.

Besides, if fiberglass and epoxy are used, it might not be necessary to introduce the middle rib just for the stiffness. And this rib would not be especially beneficial for the pressure measuring system. So maybe it could be a good idea to build the whole piece in foam, but this means the necessity of a big milling machine if the ribs will not be used for the shaping.

6.2.2. Foam core

After analyzing the pros and cons of the first solution, a new concept was born. The idea was just to build the whole blade in foam, and covering it afterwards with fiberglass and epoxy *(Figure 6.2)*.

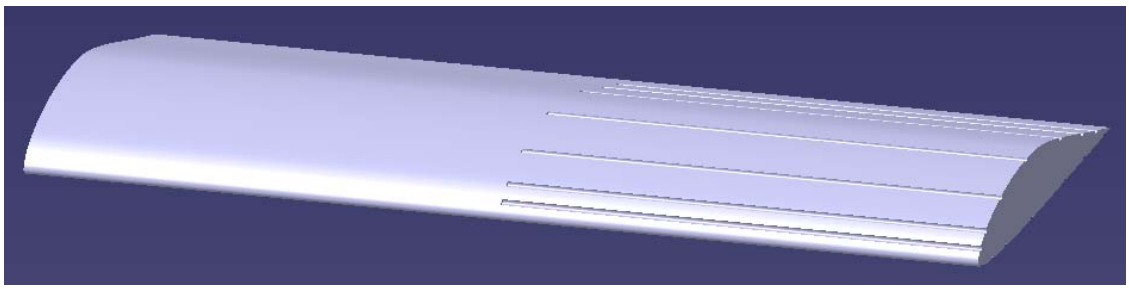

Figure 6.2. Foam core without ribs.

In order to do this, a big milling machine would be used. With the same machine the shape of the profile and the grooves for the tubes can be milled. The main problem is that the tool should be changed, and this change is done manually, so some error would be introduced. Another problem might be to do the holes in the epoxy accurately,

upna Universidad Pública de Navarra Nafarroako Unibertsitate Publikoa
Todos los derechos reservados
Eskubide guztiak erresalbatu dira

as it would be more difficult to find the position of the tubes. But the shape of the blade would be really uniform along the span. The lack of unions and pieces makes this design very interesting. Besides, the tool can be changed after milling the surface, so the error will affect only to the depth of the grooves, which can be fixed by making them deeper manually.

The real problem in this design could be the connection with the device for the control of the AoA. The connection could be made through a wheel connected with plugs to the blade (it will be explained later). If the plugs were connected directly to the foam, the blade would probably move due to the force of the wind, as the foam is not very stiff. Besides after some tests, the wing would be loose. To avoid this, a stiff rib should be added to the foam before covering with the epoxy and the fiberglass or a different union would be needed.

6.3. Angle measurement

All the solutions considered consist in attaching a digital angle gauge to a piece that would spin with the blade (called "controller" from now on). The main issues to think about are the connection between the blade and the controller, and the way the angle of the controller will be set and fixed.

6.3.1. Connection

6.3.1.1. Plugs

One option is to connect the blade with the controller by using plugs, screws or something similar. It is apparently an easy way but three matters have to be taken into account.

First of all, for this connection an additional rib should be added to the foam before adding the epoxy and the fiberglass, in order to avoid the deterioration of the foam as it has been explained before *(Figure 6.3)*.

upna Universidad Pública de Navarra Nafarroako Unibertsitate Publikoa
Todos los derechos reservados
Eskubide guztiak erresalbatu dira

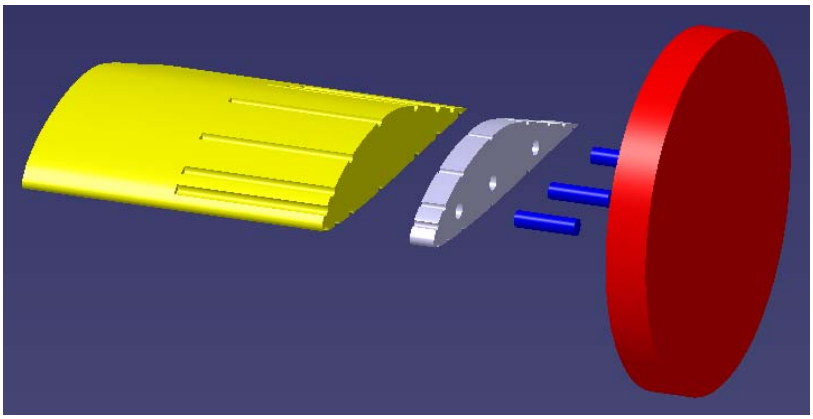

Figure 6.3. Sketch of the connection using plugs.

Secondly, the holes for the connection have to be made very accurately, as it is needed that when the blade has AoA of 0º the protractor measures an angle of 0º. As the accuracy of the gauge is 0.1 degrees, and we want to keep it or at least reach 0.5 degrees of accuracy, this operation can be complicated, as once that the controller is attached it may not be possible to know the error made.

Finally, the tubes of the pressure taps have to come out somehow. With this solution, holes for them may be necessary in the controller or the controller and the tube should be in opposite sides which is not very practical.

6.3.1.2. Blade profile shaped piercing

Another option would be to make the blade go through the controller. With this solution the problem of the tubes disappears. The piece and the shape of the profile for the hole can be made with a laser cut machine. The main problem would be that the dimensions of the profile designed in the computer do not consider the extra size due to the epoxy ant the fiberglass. So the hole would need some sanding, that has to be made very smoothly to guarantee the accuracy *(Figure 6.4)*.

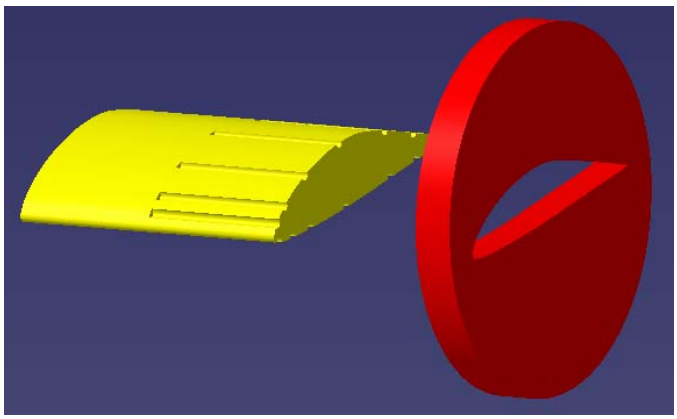

Figure 6.4. Sketch of the blade profile shaped piercing.

upna Universidad Pública de Navarra Nafarroako Unibertsitate Publikoa
Todos los derechos reservados
Eskubide guztiak erresalbatu dira

6.3.2. Angle control and fixation

6.3.2.1. Manual spinning and screw

The first idea is the most basic device. It would be a wheel and a screw in the center, or several screws around the wheel that would allow fixing it. The wheel would be spun manually.

The best characteristic of this design is its simplicity, but spinning manually and holding the wheel until the screws are tightened for the fixation could result into big inaccuracy.

6.3.2.2. Gear box

Another option would be to build a reduction gear box. If the accuracy searched is of 0.5 degrees, and in order to do it easy to handle, each turn of the main wheel (the one spun) should result in 1 or 0.5 degrees of spin in the controller.

The design implies two problems. The first is that it is very difficult to build the mechanism without play, and with play is difficult to assure the accuracy. The second is the complexity of the mechanism, which makes the construction worse and future modification or repairs harder.

6.3.2.3. Double screw system

This idea consists in two screws that touch the controller, one in each side of the controller's rotational axis. If the blade has to be rotated clockwise, the function of the left screw would be to push the blade in the desired direction, and the mission of the right one would be to avoid that the blade spins freely in that direction due to the air influence. If the blade has to be spun counterclockwise the missions of the screws are the opposite.

upna Universidad Pública de Navarra Nafarroako Unibertsitate Publikoa
Todos los derechos reservados
Eskubide guztiak erresalbatu dira

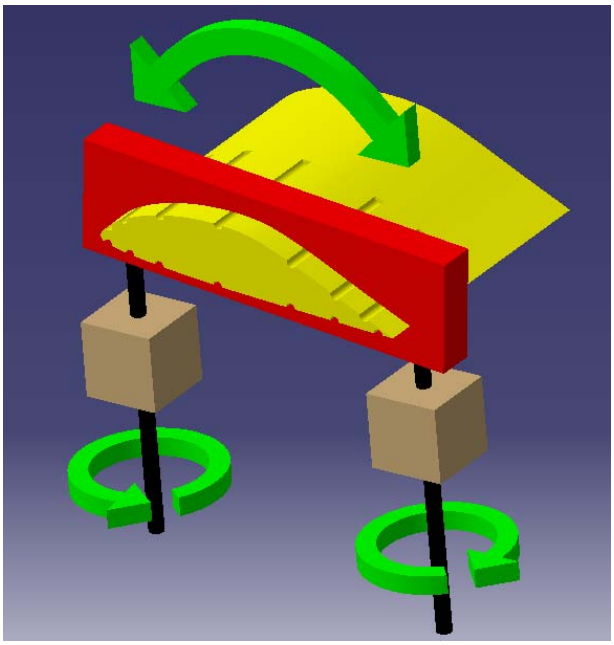

Figure 6.5. Sketch of the double screw system.

This system allows moving the controller very accurately with the turning of the screws. The main problem could be to synchronize both screws, but that is a matter of practice.

6.4. Pressure taps

For the installation of the pressure taps, the advice of Professor M. Carbonaro was extremely useful. The air will go into some holes drilled in the blade and directed through tubes to the pressure sensor. The solution consists in carving grooves in the surface of the blade to hide the tubes. The grooves should be made in the core of the blade, so that they will be covered with the fiberglass and the epoxy. After installing the tubes and covering everything, the holes would be made through the fiberglass and the epoxy, and end into the tubes.

The tubes used in the Von Karman Institute are extremely expensive for the budget of this project (no details about them are given to avoid compromising their know-how), so they had to be replaced by plastic tubes, which may not work the same way. There are 14 tubes inside the wing, distributed along the profile. The concentration of tubes is higher in the leading edge and the trailing edge, as variations in the pressure distribution are bigger in these areas. The tubes are located as shown in *Table 6.1*, where the tubes are numbered beginning in the trailing edge of the pressure side, and going all over the profile clockwise, to finish in the trailing edge of the suction side.

upna Universidad Pública de Navarra Nafarroako Unibertsitate Publikoa
Todos los derechos reservados
Eskubide guztiak erresalbatu dira

Tube	1	2	3	4	5	6	7	8	9	10	11	12	13	14
X/C (%)	90	80	65	40	20	10	2.5	2.5	7.5	20	40	65	80	90

Table 6.1. Tubes location along the wing chord.

Figure 6.6. Location of the tubes.

6.5. Pressure measuring device

Two different devices were thought to carry out the experiments: a water column manometer and a pressure transducer.

The water column manometer has 24 columns that can be filled with different liquids. The measurements are done by comparing the height of the liquid in the columns with the one (or many) taken as reference, so the maximum of comparisons is 23. The manometer can be tilted in order to achieve higher accuracy in the measurements.

The pressure transducer available in the wind tunnel lab was a Dwyer Magnesense MS-111, connected to a power source with and output of 12 V. This transducer has three different settings, to measure from 0 Pa up to 250 Pa, 500 Pa or 1250 Pa. The output current goes from 0.004 A up to 0.02 A. In order to calculate the pressure, a resistor can be connected between the transducer and the power source. Then the calculation can be done by using the Ohm's law.

$$V = I * R$$

Equation 6.1. Ohm's law.

V is the voltage in V; I the current in A and R the resistor in Ω. The value of the resistor is decided by the user, and the higher it is, the more accurate the measurements will be. The voltage can be measured with a multimeter, therefore, the current can be calculated. Then, knowing that 0.004 A correspond to 0 Pa, and 0.02 A to the maximum pressure settled, the pressure value can be obtained.

The circuit should be the following.

upna Universidad Pública de Navarra Nafarroako Unibertsitate Publikoa
Todos los derechos reservados
Eskubide guztiak erresalbatu dira

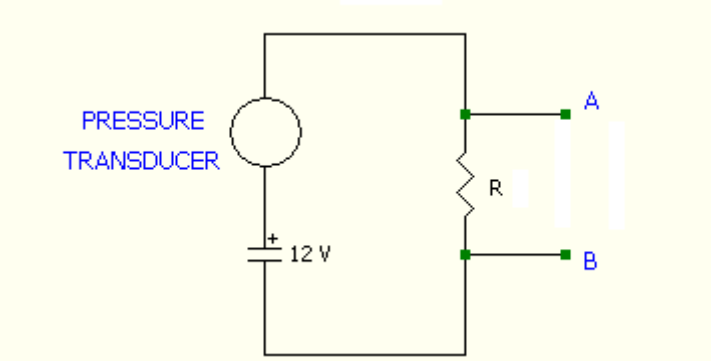

Figure 6.7. Circuit for the pressure transducer.

6.6. Microtab

The microtab could consist in a wire, a piece of wood or one of the tubes used for the pressure taps. Whatever it will be it has to be stiff, in order to keep the microtab straight along the span. As it should be possible to fix and remove the microtab so that different experiments can be done, it is important not to damage the airfoil surface with the fixation system. Regarding to the results in different studies, the height of the microtab should be around 1% of the chord in order to achieve good results.

The first solution would be clamps in the extremes of the blade. But the clamps will have to be screwed to the airfoil, which is an important fact to take into account in the manufacture of the blade, as the trailing edge is very thin and the screws would go from side to side.

Another option is to glue the microtab to the surface. In order to be able to remove the microtab without damaging the blade, the glue must not be aggressive to the epoxy, and it has to be easy to clean.

6.7. Fixation within the testing section

The whole set up has to be installed in a test section that is where the air stream of the wind tunnel goes through. The fixation to the test section has several requirements:

- ✓ Allowing the rotation of the blade to make possible changing the AoA with the controller.

- ✓ Blocking the movement of the setup along the longitudinal axis of the wind tunnel.

upna Universidad Pública de Navarra Nafarroako Unibertsitate Publikoa
Todos los derechos reservados
Eskubide guztiak erresalbatu dira

- ✓ Blocking the movement of the setup along the transverse axis of the wind tunnel.

- ✓ Assuring the absence of play to avoid vibrations in the blade that would affect the results.

- ✓ Allowing the measurements.

In the wind tunnel laboratory there was already a test section. Therefore, instead of building a new one from zero, the existing one was adapted for the requirements. The original section consisted in a rectangular prism, with open sides that allowed to the air passing through it. The upper side had a rectangular hole, which was used to introduce the hot wire anemometer during the tests. The lower side had also rectangular holes covered with plates. This side was covered with a single plate to eliminate the gaps.

In order to satisfy these requirements the fixation would need many independent parts. The solution developed was the following:

In the walls of the test section, there are two circular holes. The blade has two wheels assembled that fit exactly into those holes. With this configuration the rotation is allowed and the longitudinal movement blocked. If the wheels fit perfectly, then the absence of play is also guaranteed. In order to block the transverse movement, two plates are screwed just outside the holes. This plates have holes, big enough to let the wing go trough for the control and the pressure measurements, but smaller than the holes in the walls. These plates block the transverse movement.

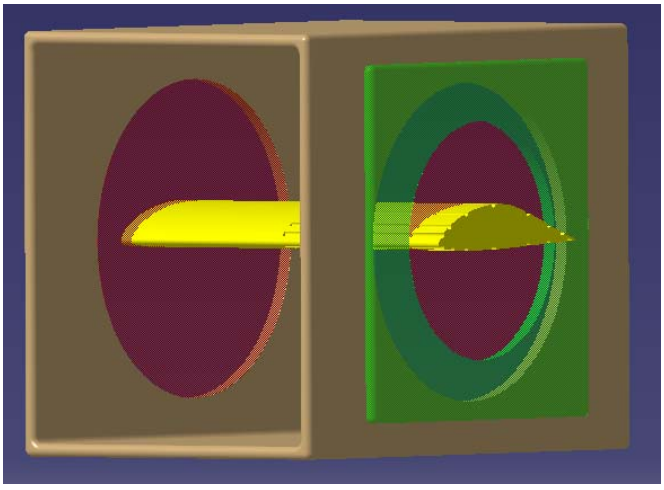

Figure 6.9. Sketch of the fixation within the test section.

The setup can be installed with the blade in vertical or horizontal position. At first sight it is the same, but the characteristics of the air flow in the wind tunnel have to

upna Universidad Pública de Navarra Nafarroako Unibertsitate Publikoa
Todos los derechos reservados
Eskubide guztiak erresalbatu dira

be taken into account as well as the influence of gravity regarding to the way the setup is installed, the access to the tubes and the controller, and the reading of the gauge. For the authors it was more comfortable to make a horizontal setup.

6.8. Decision making

Some of the components of the setup were less difficult to choose, due to the previous experience of the authors in building structures with similar characteristics (e.g. the fixation within the test section) or to the help obtained to find a good solution (e.g. the meeting in the VKI that led to the pressure measuring system). The pressure measuring device was chosen after testing their capacities. But the choice of the design for other components was more complex, especially due to the lack of previous experience in wind tunnel testing and wing building, and the amount of time and work that would take to try all the possible setups.

Therefore, in order to make the decisions for each component logically, and to develop the best solution, the Controlled Convergence Method (DATUM) was used (Tassinari, 1995 [8]). This method is used in product design along with others to achieve an optimal design. To use this method, first it is necessary to identify the requirements that the "product", or in this case the component of the setup, has to face. Once we know them, different designs can be thought.

The choice among these designs is made by a comparative grid. In the grid, the different designs versus the requirements are represented. One of the designs is taken as the reference or DATUM, and then, the other designs are compared in every requirement to the DATUM. If the compared design is better in a feature, then it is marked with a +, if it is worse with a -, and if it is equal with an =. Then the results are counted. The result would be conclusive if a design has more + than -, and more + than any other. If the result is no conclusive, another design can be chosen as DATUM, and if it does not work the designs should be reconsidered.

To make sure that the method works perfectly it is necessary a group of people with experience in the field, and to make several iterations until the group is satisfied and the design seems optimal. It is not possible in this case, but the method would help anyway to the decision.

As an example, the DATUM is applied to the choice of the controller, more exactly the device for the angle control and fixation, in the next pages. The data of other components can be found in *appendix 4*.

upna Universidad Pública de Navarra Nafarroako Unibertsitate Publikoa
Todos los derechos reservados
Eskubide guztiak erresalbatu dira

The requirements of this component are:

1) Allowing the user to control the AoA easily.
2) Accuracy of at least 0.5 degrees.
3) Helping the user to rotate the blade smoothly.
4) Allowing the fixation of the AoA in a specific value.
5) Minimum play in order to avoid vibrations or changes.
6) Simple manufacture, regarding to the tools available.
7) Low interference with the pressure measurement system so that both can be installed in the same side for better handling.

According to these requirements three different designs were developed (subsection 6.3.2):

- ✓ Manual spinning and screw
- ✓ Gear box
- ✓ Double screw system

Finally the grid is applied, taking the gear box as DATUM:

Requirements	Manual spinning and screw	Gear box	Double screw system
1 (Control)	-	DATUM	=
2 (Accuracy)	-		+
3 (Smooth rotation)	-		=
4 (Value fixation)	-		+
5 (Play)	+		+
6 (Manufacture)	+		+
7 (Interference)	=		=
Σ+	2		4
Σ-	4		0
Σ=	1		3

Table 6.2. Comparative grid of the "device for angle control and fixation" designs.

Taking a look to the results obtained, it is obvious in this case that the best of the three designs is the double screw system.

upna Universidad Pública de Navarra Nafarroako Unibertsitate Publikoa
Todos los derechos reservados
Eskubide guztiak erresalbatu dira

6.9. Final setup

After the whole design process a functional setup was built. The main description is:

- ✓ *Foam core:* it is made in a single piece, with grooves carved in order to lodge tubes for the pressure measurements. The foam is covered with a single layer of fiberglass and epoxy in order to make it stiff *(figure 6.10)*.

Figure 6.10. Foam core with the fiberglass and epoxy layer.

- ✓ *Blade profile shaped piercing:* the connection to the controller is made by piercing two plates with the shape of the profile. The two plates are used to give depth to the controller. This is useful in order to make easier to puss the controller and to fix the digital protractor to it *(figure 6.11)*.

- ✓ *Double screw system:* two screws, one in each side of the controller, push it. The screws are fixed within wooden blocks with a nut, which also transforms the rotation of the screws into linear movement. Therefore, the movement of the controller is very smooth and accurate *(figure 6.11)*.

upna Universidad Pública de Navarra Nafarroako Unibertsitate Publikoa
Todos los derechos reservados
Eskubide guztiak erresalbatu dira

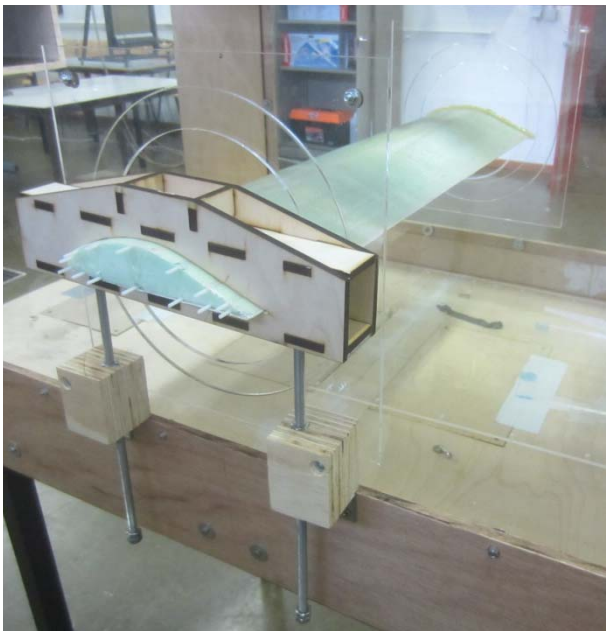

Figure 6.11. Blade profile shaped piercing and double screw spin system.

- ✓ Pressure Taps: 14 pressure taps are directly drilled in the wing surface. The drills go into Polyoxymethylene tubes lodged in the foam grooves. The Polyoxymethylene is a plastic material with high stiffness, low friction and excellent dimensional stability, some very good characteristics for this use. The tubes have 0.9 mm inner diameter and 2.5 mm outer diameter. The location of the taps was described in *subsection 6.4*. After covering the core with fiberglass and epoxy, some error is introduced in the coordinates. The chord of the final blade is 173 mm, which means 3 mm of difference from the original. Recalculating the positions with the new size, the biggest error doesn't reach the 1%. Therefore, the error will be neglected during the experiments.

- ✓ *Water column manometer:* the water column manometer is able to measure higher pressure differences than the transducer, and it is faster, as all the taps can be analyzed at the same time. The liquid used is water, and the tilt is 20˚ from the horizontal.

- ✓ *Glued microtab:* a metal cylinder of 2 mm of diameter, and a wooden rectangular prism with a section 2.5 mm wide and 4 mm high were used as tabs. 2 mm represent the 1.156% of the chord, a little bit thicker than in other similar experiments (Johnson *et al.*, 2008 [4] and Johnson *et al.*, 2010 [5]). The 4 mm height microtab is used to obtain more marked results, and represents the 2.312% of the chord. The main fixation is two drops of hot melt glue, which can be easily removed from the surface. Besides, to avoid air circulation under the microtab, adhesive is used (*figure 6.12.*).

upna Universidad Pública de Navarra Nafarroako Unibertsitate Publikoa
Todos los derechos reservados
Eskubide guztiak erresalbatu dira

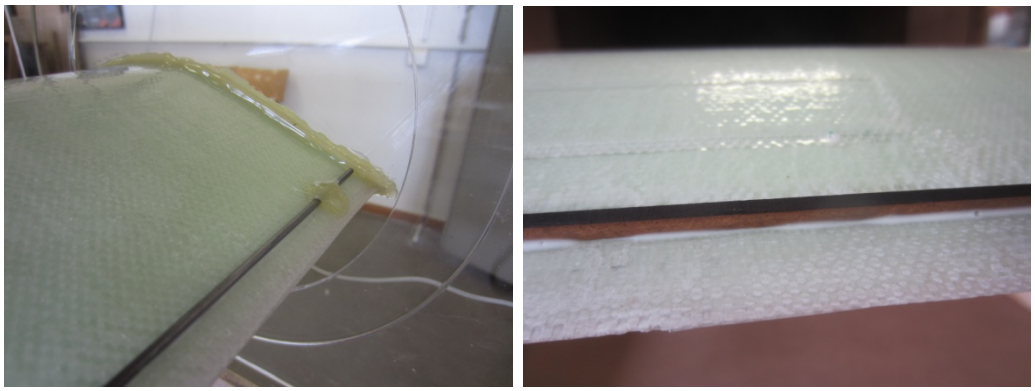

Figure 6.12. Details of the microtabs

6.10. Manufacturing issues

In order to build good setup, there are some relevant issues to take into account. The aim of this subsection is to gather the know-how obtained during the manufacturing process. This information can be very useful, as it can reduce considerably the number of trials before achieving a satisfying result.

6.10.1. Foam core

The foam core was milled in a single piece as there was a big milling machine available. The tools had to be changed manually, as well as the zero was set manually. The piece had to be done in two milling processes, upper and lower side. The main issue is the accuracy of the shape, especially to obtain a good leading edge and a good trailing edge. Anyway, the trailing edge deserves more attention, as errors in the leading edge and the grooves for the tubes can be acceptably solved with sanding, but errors in the trailing edge may end in a useless core *(figure 6.13)*.

Figure 6.13. Milling defect in the trailing edge.

upna Universidad Pública de Navarra Nafarroako Unibertsitate Publikoa
Todos los derechos reservados
Eskubide guztiak erresalbatu dira

In order to achieve a good shape, several factors have to be considered:

- ✓ *Constant XY zero:* to make sure that the XY zero is exactly the same throughout all the manufacturing, the material block shall be fixed to the table of the milling machine. To protect this table, first a board was fixed to the table. This board was big enough to put the foam block on it. The XY zero was settled in the board, and then two holes were made in the board. Then the foam block was fixed to the board, and two holes equal to the ones in the board were made on it. Thanks to this, when the foam is turned to change from the upper side to the lower or vice versa, it can be fixed to the board with plugs, and therefore the XY zero will remain unchanged in the foam *(figure 6.14)*. Holes should be made in both sides of the foam block or through the whole block, so that the foam can be flipped more than once.

Figure 6.14. Detail of the plug for XY zero.

- ✓ *Deformation of the material:* the foam block has to be well fixed to the board, avoiding long free stretches. By doing so, the deformations due to the forces of the fixing points or the forces of the milling machine can be avoided.

- ✓ *Order of the operations:* some operations need a tool change, which means to settle a new zero in the Z axis (height). Every time that the zero is fixed some error is introduced, as it is done manually. Besides, for some operations the height accuracy is more important than for others (core shape > grooves > holes for XY zero). The best result was obtained by following this order: holes in the board, holes in the upper side of the foam, upper surface, lower surface, holes in the lower side of the foam, lower grooves and upper grooves. This order gives the best balance between the number of tool changes and the number of times that the block had to be flipped and fixed.

upna Universidad Pública de Navarra Nafarroako Unibertsitate Publikoa
Todos los derechos reservados
Eskubide guztiak erresalbatu dira

- ✓ *Changes in the shape of the foam block:* even though the foam is well fixed, the shape of the foam might not be exactly the same when it is flipped over. Therefore, it is recommended to give the blade some extra length, so that when the lower side starts to be milled, the result can be analyzed, and the Z zero adjusted if necessary.

6.10.2. Tubes and grooves

The accuracy of the grooves remains in background during the milling. Therefore, once the tubes are installed, the grooves should be filled with several layers of epoxy in order to be sure that the shape will be correct when the core is covered with the fiberglass *(figure 6.15)*.

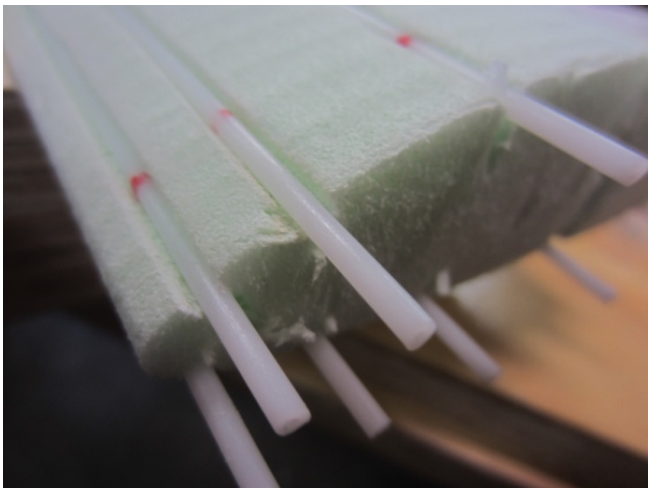

Figure 6.15. The grooves disturb the foam shape.

It is also a good idea to cover one of the tips of the tubes. By doing this, it is guaranteed that the air will have only one exit. Besides, the epoxy will not enter to the tube, so there is no chance of drilling into a section filled with epoxy *(figure 6.16)*.

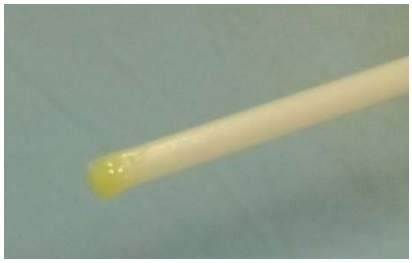

Figure 6.16. Detail of a covered tip.

upna Universidad Pública de Navarra Nafarroako Unibertsitate Publikoa
Todos los derechos reservados
Eskubide guztiak erresalbatu dira

6.10.3. Fiberglass and epoxy

Meticulous work is needed to achieve a good result when covering the wing core. The first step is to find mylar or plastic foil without creases. The size of the foil must be enough to cover the core and allow holding the plastic to keep it tight. Then a piece of fiberglass is put on the foil. It has to be big enough to cover the core too. Notice that the extra fiberglass will have to be cut away afterwards, so it is better if the piece is no too big.

When the foil and the fiberglass are ready, the epoxy is poured over them. Using a brush, the epoxy must be hit in order to impregnate the fiberglass *(figure 6.17)*. Then a roller should be used to eliminate the air bubbles trapped between the plastic and the fiberglass.

Figure 6.17. Impregnation of the fiberglass with epoxy.

After this, the core must be covered. The best way is to put the core on the fiberglass and fix one side to it, wrapping the other side afterwards. In order to be sure that the shape is correct, the wrap must be tight. As some air may be trapped, a piece of cardboard or wood can be used to release it. The wood must be pushed against the surface and moved towards where the air can go out.

It is also important to be careful with the tension of the wrap, as it might bend the trailing edge. But anyway it has to be tight or the leading edge will not have the right shape (*figure 6.18* shows defects of different trials). And also be careful when releasing the air, as using the wood too many times can result into lack of epoxy in some areas.

upna Universidad Pública de Navarra Nafarroako Unibertsitate Publikoa
Todos los derechos reservados
Eskubide guztiak erresalbatu dira

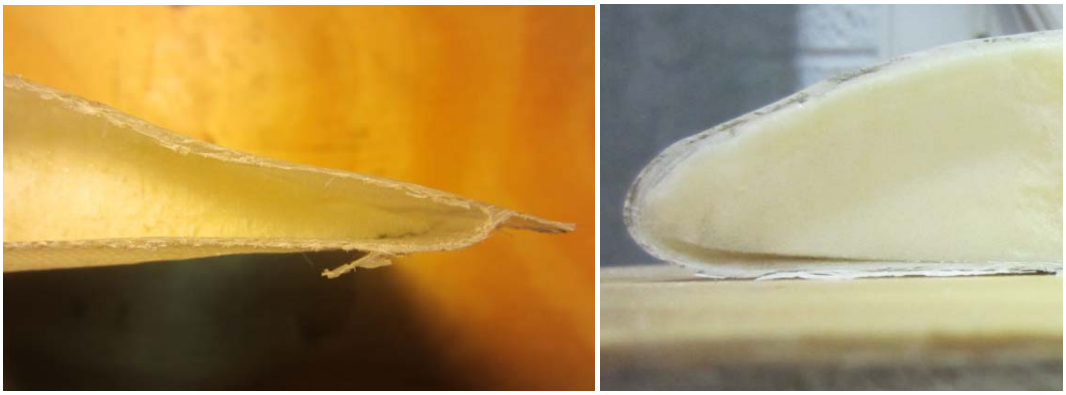

Figure 6.18. Defects in the airfoil shape due to tension issues.

Even though the fiberglass is perfectly attached to the core, some bubbles and creases may appear during the curing process. If the bubbles are filled with epoxy, they can be eliminated by sanding them, but if not, it will result in a gap in the epoxy *(figure 6.19)*. This issue may be avoided by using a vacuum pump, but it could not be tried during the manufacturing of the setup.

Figure 6.19. Detail of a bubble defect on the epoxy.

6.10.4. Trailing edge

The trailing edge is one of the most relevant parts of the profile, and the most difficult to perfect. In order to achieve a straight and smooth edge some tool must be used. It is useful to build moulds where the blade can rest. To prevent the blade from changing its position during the sanding, it must fit in the moulds perfectly. Two moulds were built for this setup. In the first one the wing lays on its pressure side, and next to the trailing edge the mould has the inclination of the upper side. The second one is the opposite. Both moulds had covers in order to fix the wing inside and prevent them from moving while sanding the trailing edge *(figure 6.20)*.

upna Universidad Pública de Navarra Nafarroako Unibertsitate Publikoa
Todos los derechos reservados
Eskubide guztiak erresalbatu dira

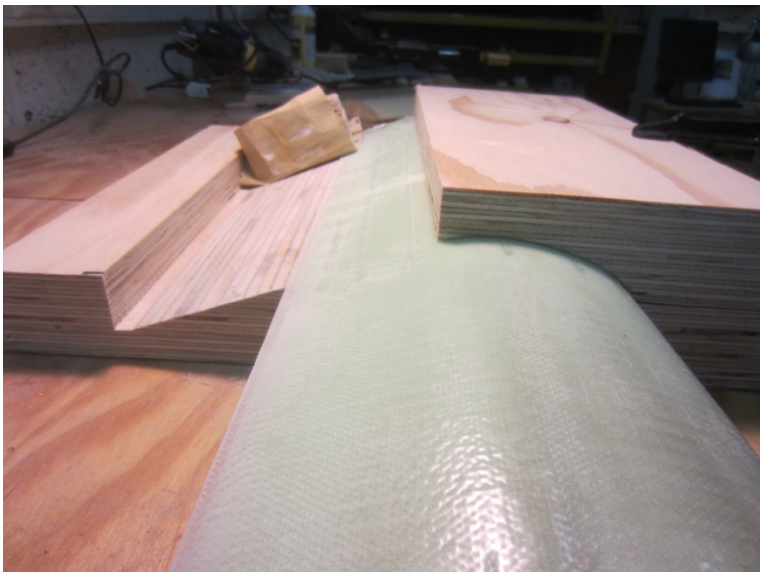

Figure 6.20. Trailing edge sanding device.

When sanding the trailing edge, be careful when it gets close to the expected shape. Too much sanding and air trapped in the epoxy may result into an open trailing edge *(figure 6.21)*.

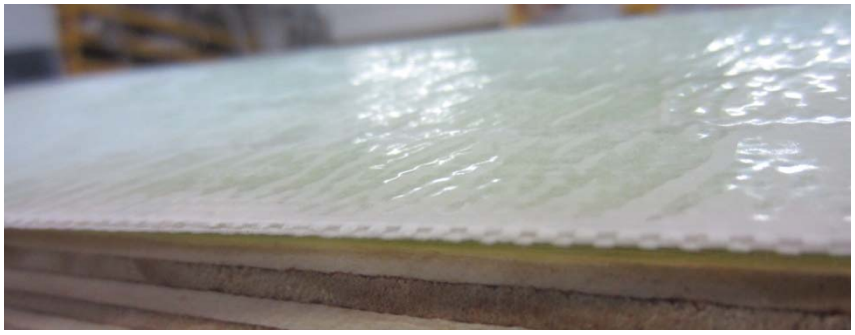

Figure 6.21. Defect in the trailing edge due to too much sanding.

6.11. Final setup performance

During the experiments the final setup showed its strong and weak points.

- ✓ *Blade:* the foam core with a layer of fiberglass and epoxy was perfectly stiff. No deformation was observed visually or in the results. Besides the shape was homogeneous, without cracks that could interfere with the measurements. Anyway, it is also true that once the core is built, until it is

upna Universidad Pública de Navarra Nafarroako Unibertsitate Publikoa
Todos los derechos reservados
Eskubide guztiak erresalbatu dira

covered with epoxy is very fragile, so it is necessary to be extremely careful. The blade had some manufacture defects, such as lack of epoxy in some areas of its surface, small bubbles and slight separations between the epoxy layers in some points of the trailing edge. Despite all this, the finish was as good as expected after sanding the protuberances.

- ✓ *Angle control:* the connection performed with the blade profile shaped piercing was perfect. There was no play between the controller and the wing, and the angle reference for both was the same, as the blade fit perfectly. Besides the double screw system allowed spinning the blade with the same accuracy of the protractor (0.1º). But sometimes it was not easy to set the angle at the desired value, as the readings from the digital gauge oscillated, and the controller was moved when trying to fix it.

- ✓ *Pressure measuring:* the POM tubes worked without any problems. None of them was stuck with the dust of the drilling, and they were perfectly visible during this task thanks to the transparency of the cover of the wing. The water column manometer made possible to measure the pressure in all the tubes at the same time, although adaptors were needed to connect the tubes and the manometer. The main issue was the accuracy of the manometer, which did not allow analyzing the blade at low wind speeds.

- ✓ *Microtab:* both microtabs functioned as expected. They were not completely stiff, but after gluing them to the blade, and adding some adhesive to avoid air leaks, the stiffness was higher. Unfortunately gluing and removing the microtabs, and cleaning the wing after each experiment resulted in damaging the surface. For the number of tests accomplished it was a good solution, simple and efficient, but for a longer term the blade would not resist.

- ✓ *Fixation within the test section:* the design of the fixation was simple and achieved all its requirements. Thanks to the lack of play between the wheels and the walls of the test section, all the movements except the spin around the rotational axis were perfectly restricted. The only disadvantage of this design was that the assembly of the blade into the test section required some time, due to the necessity of taking to pieces some of the plastic covers as well as the double screw system. Besides this operation may be difficult for only one person.

upna Universidad Pública de Navarra Nafarroako Unibertsitate Publikoa
Todos los derechos reservados
Eskubide guztiak erresalbatu dira

7. Experiments

The goal of this master thesis is to study the pressure distribution in a wing and its variation when a microtab is installed on its suction side, in order to alleviate loads. In this chapter the data of the experiments carried out will be shown.

In order to compare the results and the influence of the microtab in the aerodynamic performance of the airfoil, some pressure measurements had been taken with pressure taps for different configurations of the setup. First of all, the GU25(5)8-11 profile was installed in the test section, and the dynamic pressure was measured in the 14 pressure taps for several angles of attack, between -20° and 20° and different speeds. The angles were chosen regarding to their importance in the lift curve of the profile, taking readings for closer angles of attack when the lift coefficient changed its performance. Then, different microtabs were installed in the suction side of the airfoil at different positions, and the measurements were repeated. Also a trial in the pressure side was made.

Before every experiment, the wind speed was measured in the test section with a hot wire anemometer as well as the atmospheric temperature. Also the atmospheric pressure was measured in the wind tunnel lab using an aneroid barometer.

7.1. Measurements without the microtab

The first step was to measure the pressure distribution of the blade built. It was important to study its behavior in order to compare the results with further experiments, and to compare the performance of the wing with the theoretical results. The theoretical data used to compare the results of both speeds was the results obtained with Javafoil [16].

To do so, the blade was tested without microtab, and for different speeds which were 8.2 m/s and 17 m/s. The first speed is the lowest with which the pressure distribution could be read clearly enough from the manometer. The decision of testing this speed came from another experimental study that yielded the following graph (*figure 7.1)*.

upna Universidad Pública de Navarra Nafarroako Unibertsitate Publikoa
Todos los derechos reservados
Eskubide guztiak erresalbatu dira

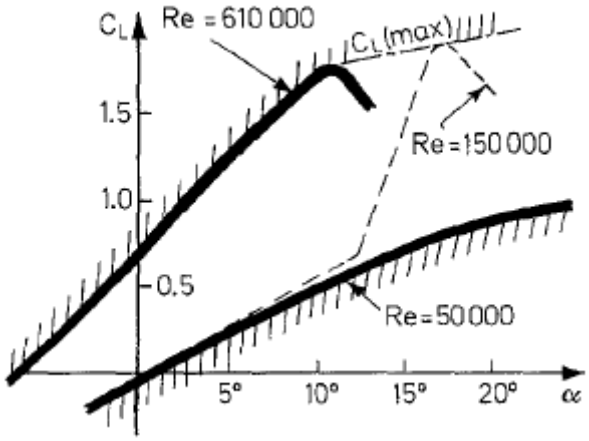

Figure 7.1. General behavior of the GU25-5(8)11 [12].

The graph shows that for really low Reynolds numbers (Re ≤ 50000) the relationship between the C_L and the AoA is quite linear and without a clear stall angle, at least until an AoA of 20˚. Then at Re = 150000 some different behavior was detected, and then, as the Reynolds number grows, the graph is more typical. As the maximum speed of the tests (17 m/s) meant a Reynolds number of 205000, which is close to the area of special functioning, another speed closer to Re = 50000 seemed interesting, in order to see if there were different behaviors. Unfortunately, 8.2 m/s yields a Reynolds number of 100000, which is still close, but it could result useful.

The results of both tests were:

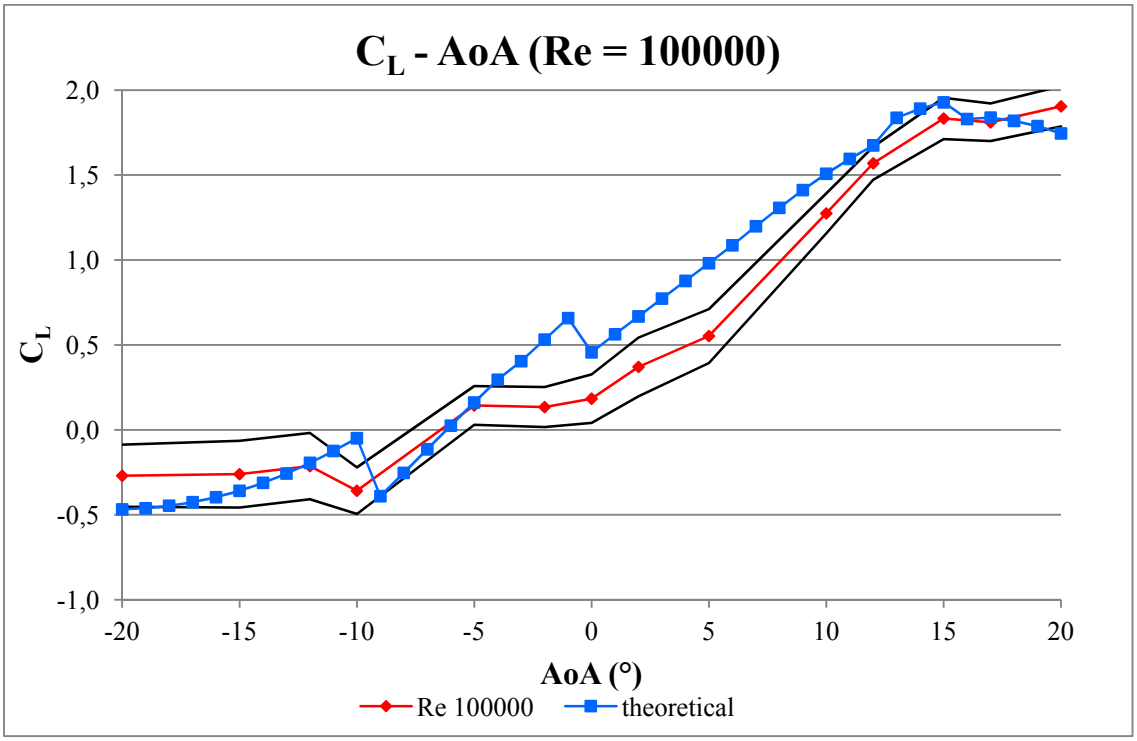

Figure 7.2. C_L vs AoA for Re = 100000.

upna Universidad Pública de Navarra Nafarroako Unibertsitate Publikoa
Todos los derechos reservados
Eskubide guztiak erresalbatu dira

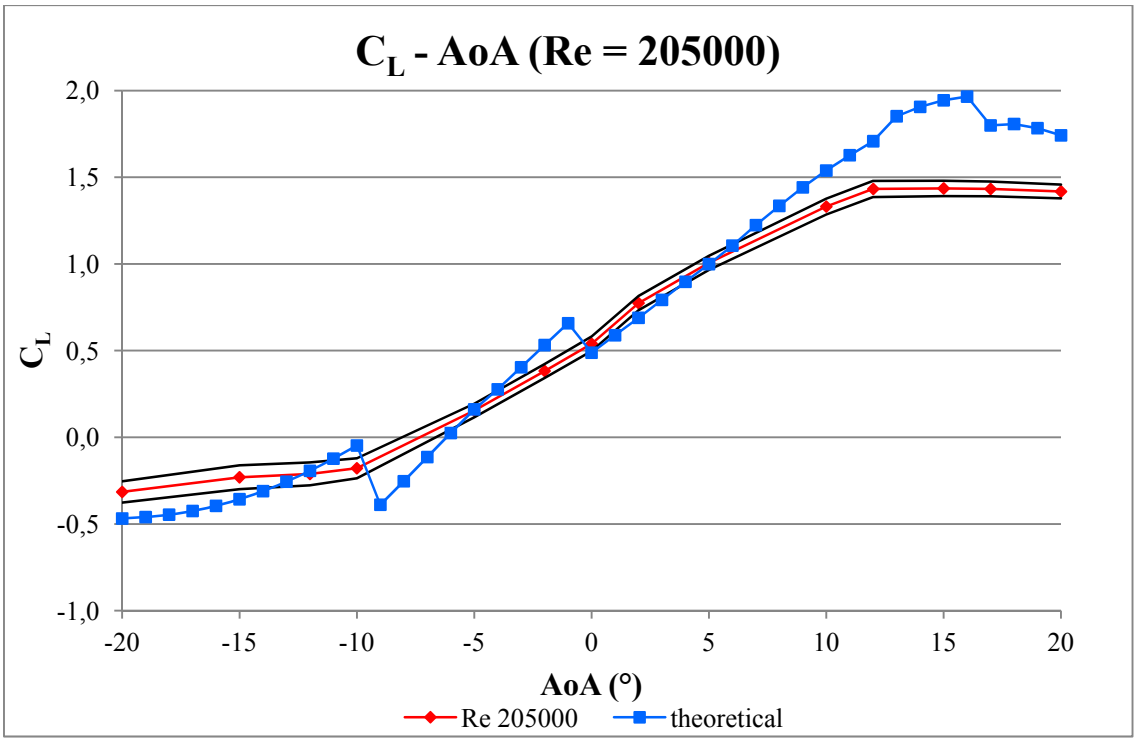

Figure 7.3. C_L vs AoA for Re = 205000.

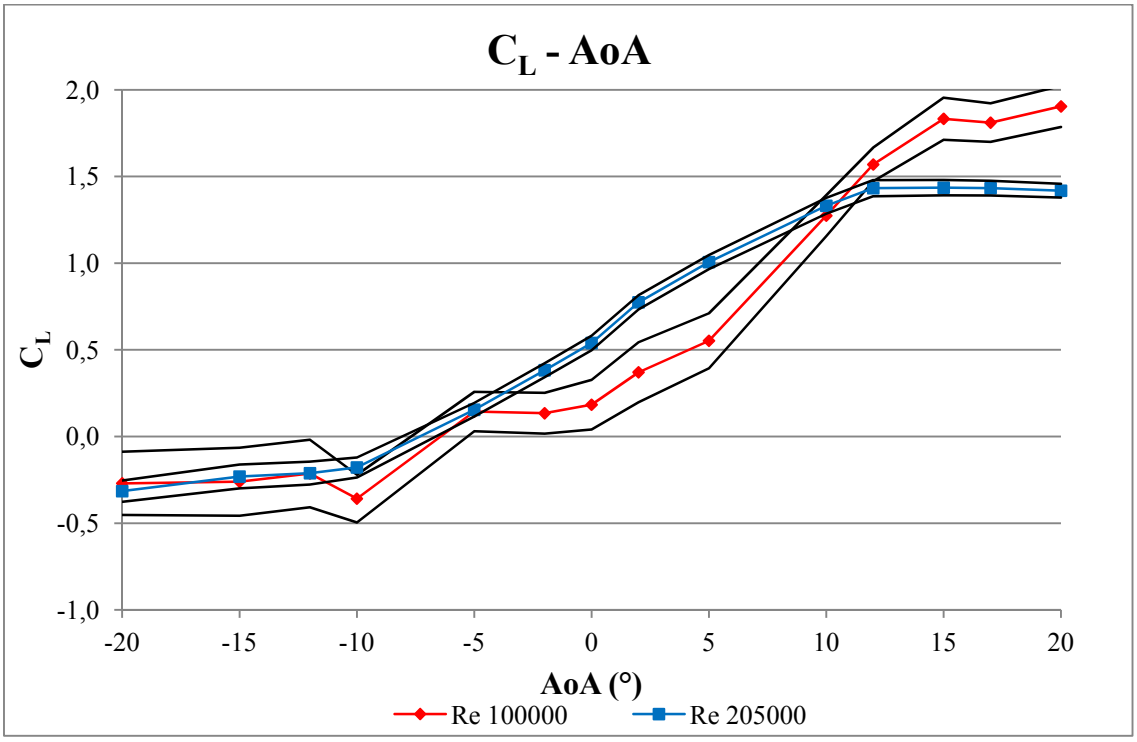

Figure 7.4. C_L vs AoA for both Reynolds numbers.

The black lines represent the relative error, and their calculations can be found in *appendix 5*.

upna Universidad Pública de Navarra Nafarroako Unibertsitate Publikoa
Todos los derechos reservados
Eskubide guztiak erresalbatu dira

At first sight it can be appreciated that the measured values differ from the theoretical. This is something that could be expected, due to variations in the shape of the wing and/or in the environmental conditions of the tests. It is not alarming and it usually happens, as it can be seen if comparing the results from a different experimental study (R.A. McD. Galbraith, 1985 [12]).

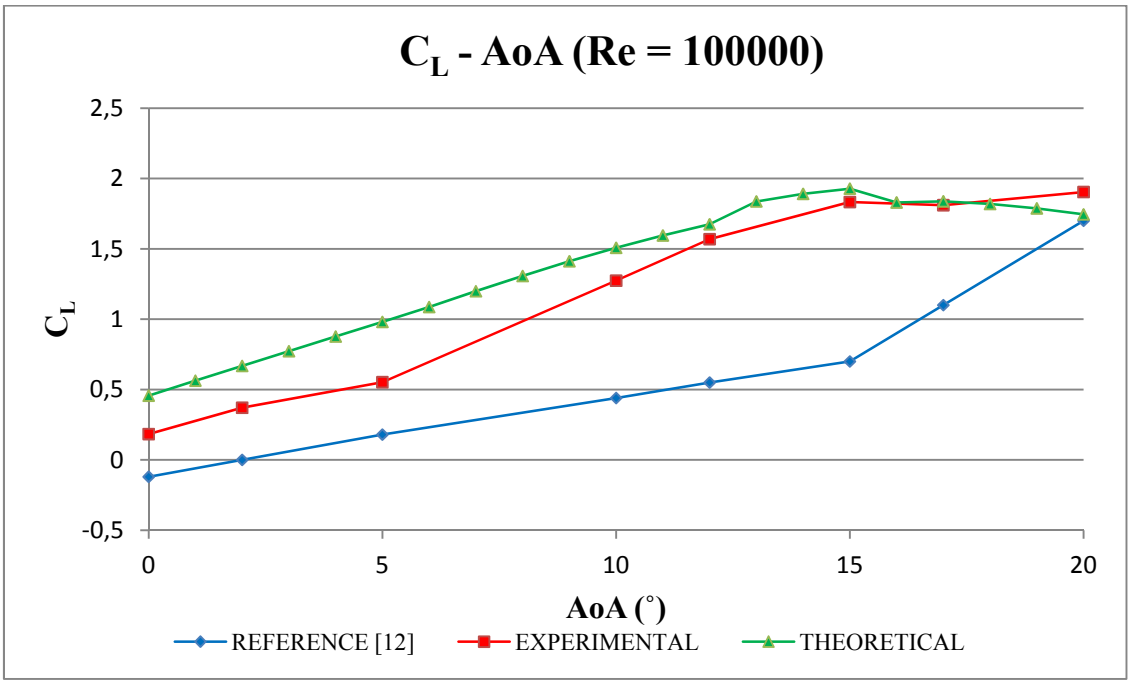

Figure 7.5. Comparison with a different study for Re = 100000.

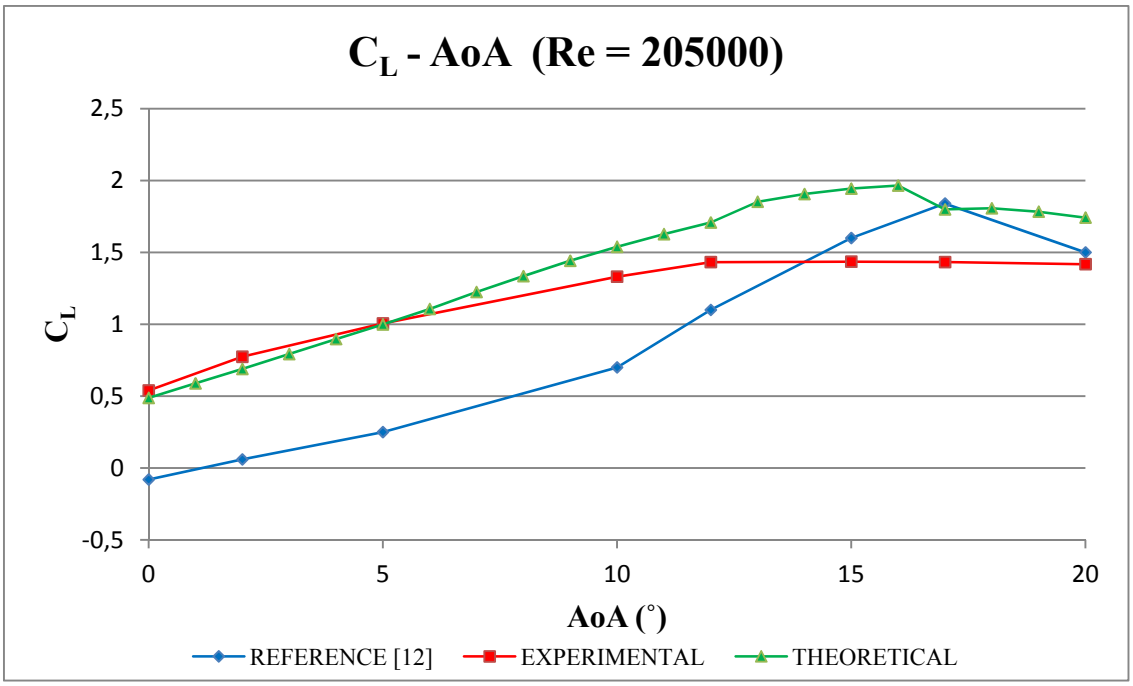

Figure 7.6. Comparison with a different study for Re = 205000.

upna Universidad Pública de Navarra Nafarroako Unibertsitate Publikoa
Todos los derechos reservados
Eskubide guztiak erresalbatu dira

The readings of both experimental studies are different from the theoretical result. Anyway, the measurements of the tests carried out in this thesis have certain approach to the theoretical values. For Re = 100000 values become closer for AoAs bigger than 12˚ and for Re = 205000 the approach is clear for AoAs between 0˚ and 5˚.

Despite the values, the behavior observed for both Reynolds numbers is interesting. In *figure 7.2* lift drops due to stall happen for the same AoAs as in the calculations. Some degrees after the last stall (around an AoA of 5˚) the slope of the C_L grows, reporting a behavior similar to the one expressed in *figure 7.1* for Re = 150000. Although both, the calculations and the other study (R.A. McD. Galbraith, 1985 [12]) say that the C_L should decrease for 20˚, the tests show a different performance in our wing.

In *figure 7.3*, where the Reynolds number is higher than 150000, the areas of stall and the increase of C_L disappear. The lift becomes more linear between -10˚ and 10˚, and then at 12˚ the C_L drops although not very sharply, giving the graph the typical shape. In this case it seems like the maximum C_L is reached at 12˚ as reported in the other study (R.A. McD. Galbraith, 1985 [12]) and not at 15˚ as the calculations predict.

7.2. Measurements with the microtab located at 90% of the chord in the suction side

Once the performance of the wing was tested, it was time to study the effect of the microtab. The first location chosen was at the 90% of the chord, as there are studies [4] that report that this is the best location in order to obtain bigger lift reductions.

The first step was to try the metal cylinder as microtab. Its diameter is equal to the 1.156% of the chord, close to the 1%, which is approximately the thickness of the boundary layer. This size has been reported to have the optimum compromise between size and the effect produced (Johnson *et al.*, 2008 [4]). This microtab was tested for 8.2 m/s (Re = 100000) and 17 m/s (Re = 205000), in order to compare the effect of the microtab with the results of the bare blade. The results obtained were the following:

upna Universidad Pública de Navarra Nafarroako Unibertsitate Publikoa
Todos los derechos reservados
Eskubide guztiak erresalbatu dira

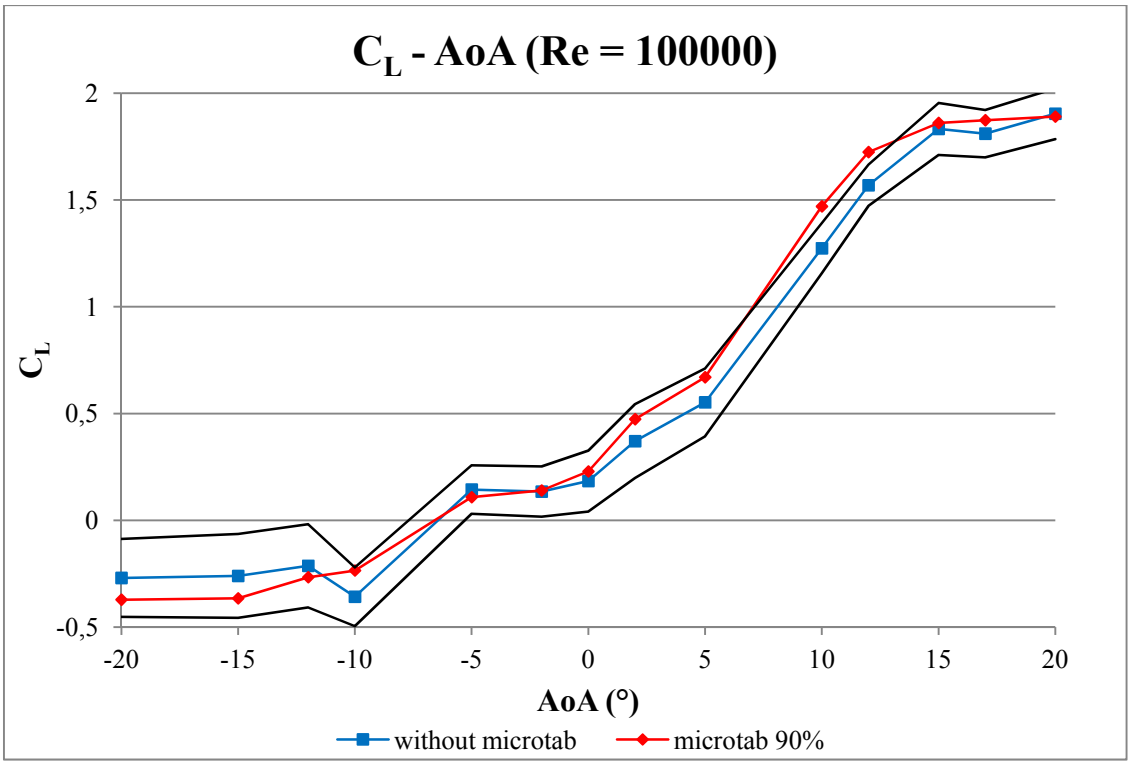

Figure 7.7. Metal cylinder 2 mm diameter at 90% of the chord. Re = 100000.

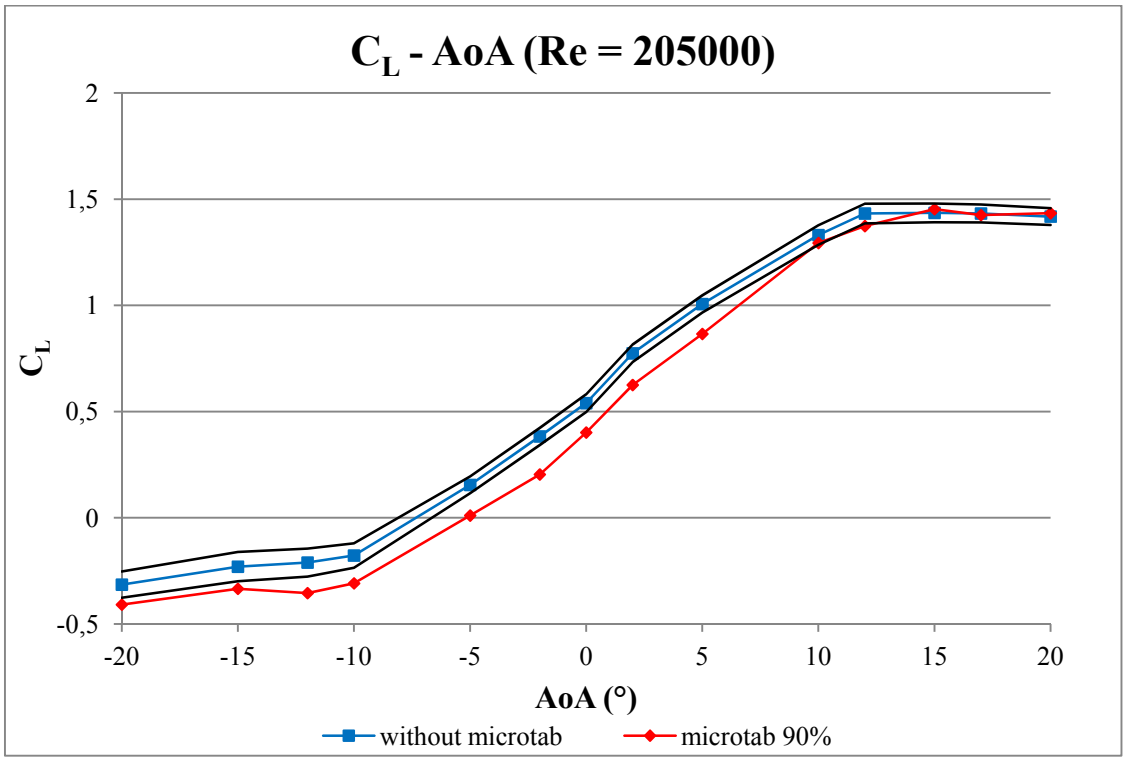

Figure 7.8. Metal cylinder 2 mm diameter at 90% of the chord. Re = 205000.

upna Universidad Pública de Navarra Nafarroako Unibertsitate Publikoa
Todos los derechos reservados
Eskubide guztiak erresalbatu dira

The effect that the microtab produced in the performance of the wing was completely different for both speeds. For 8.2 m/s (*figure 7.7*) the expected effect took place only between -20˚ and -12˚. Then, from -12˚ to -2˚ it seemed to have no repercussion, and after -2˚ the microtab produced lift enhancement until 12º, which is the opposite of what was expected. It could be attributed to a lack of repeatability, but comparing results from different days with similar conditions, we can state that that is not the problem (*appendix 6*). But the error lines show that there can be big variations in the measurements taken at 8.2 m/s. Therefore the results may not be representative of what really happens although it seems to be a trend to the described behavior.

For 17 m/s the effect is what expected until an AoA of 10˚. The installation of the microtab resulted in the displacement of the lift graph downward. After 10˚ the effect of the microtab became smaller until being unnoticeable. C_L values from both tests are in *tables 7.1 and 7.2*.

C_L with metal cylinder in the suction side (Re = 100000)					
AoA	Without	90%	AoA	Without	90%
-20	-0,27	-0,37	2	0,37	0,47
-15	-0,26	-0,37	5	0,55	0,67
-12	-0,21	-0,27	10	1,27	1,47
-10	-0,36	-0,24	12	1,57	1,72
-5	0,14	0,11	15	1,83	1,86
-2	0,13	0,14	17	1,81	1,87
0	0,18	0,23	20	1,90	1,89

Table 7.1. C_L values with and without microtab. Re = 100000.

C_L with metal cylinder in the suction side (Re = 205000)					
AoA	Without	90%	AoA	Without	90%
-20	-0,31	-0,41	2	0,77	0,63
-15	-0,23	-0,33	5	1,01	0,87
-12	-0,21	-0,35	10	1,33	1,29
-10	-0,18	-0,31	12	1,43	1,37
-5	0,15	0,01	15	1,44	1,45
-2	0,38	0,20	17	1,43	1,43
0	0,54	0,40	20	1,42	1,43

Table 7.2. C_L values with and without microtab. Re = 205000.

After these tests the wooden prism was tested as microtab for 17 m/s. Its bigger size was supposed to sharpen the effect, and therefore to help to analyze the results of the cylinder better (*figure 7.9*).

upna Universidad Pública de Navarra Nafarroako Unibertsitate Publikoa
Todos los derechos reservados
Eskubide guztiak erresalbatu dira

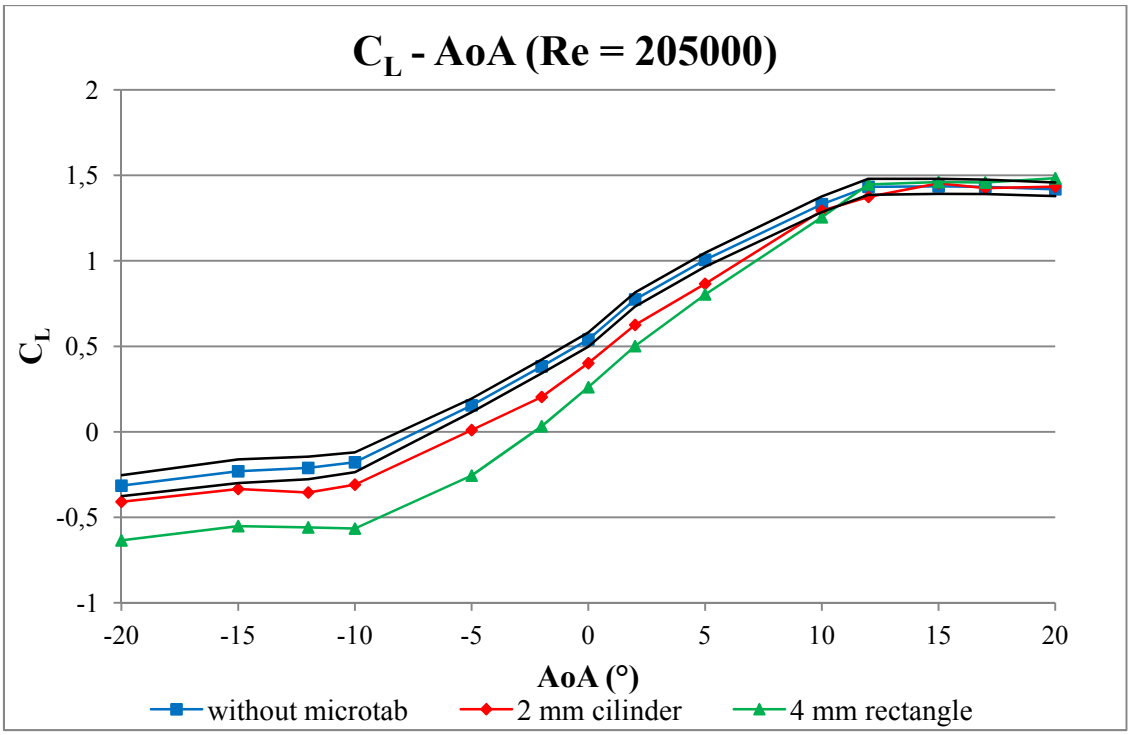

Figure 7.9. Wooden prism 4 mm height vs cylinder at 90% of the chord. Re = 205000.

With the bigger microtab the lift drop was sharper, as expected. But what resulted more interesting was that the behavior was the same for both sizes. The drop takes place clearly until 10˚, but then the lift curve attaches to the curve without microtab.

In order to quantify the effect, C_L values are represented in *table 7.3*.

C_L comparison of different microtabs (Re = 205000)							
AoA	Without	2 mm	4 mm	AoA	Without	2 mm	4 mm
-20	-0,31	-0,41	-0,64	2	0,77	0,63	0,50
-15	-0,23	-0,33	-0,55	5	1,01	0,87	0,80
-12	-0,21	-0,35	-0,56	10	1,33	1,29	1,25
-10	-0,18	-0,31	-0,57	12	1,43	1,37	1,45
-5	0,15	0,01	-0,26	15	1,44	1,45	1,46
-2	0,38	0,20	0,03	17	1,43	1,43	1,46
0	0,54	0,40	0,26	20	1,42	1,43	1,48

Table 7.3. C_L values with different microtabs. Re = 205000.

upna Universidad Pública de Navarra Nafarroako Unibertsitate Publikoa
Todos los derechos reservados
Eskubide guztiak erresalbatu dira

7.3. Measurements with the microtab located at 95% of the chord in the suction side

Once the effect of the microtab in the suction side was tested, as well as the influence of the wind speed and the size of the microtab, another parameter of study was the location. The microtab was placed in the suction side of the profile again, but at 95% of the chord. This way the effect of the microtab could be analized comparing it with the results achieved when located at 90% of the chord. The microtab used was the metal cylinder, as its diameter is closer to the 1% of the chord. The results for this experiment were:

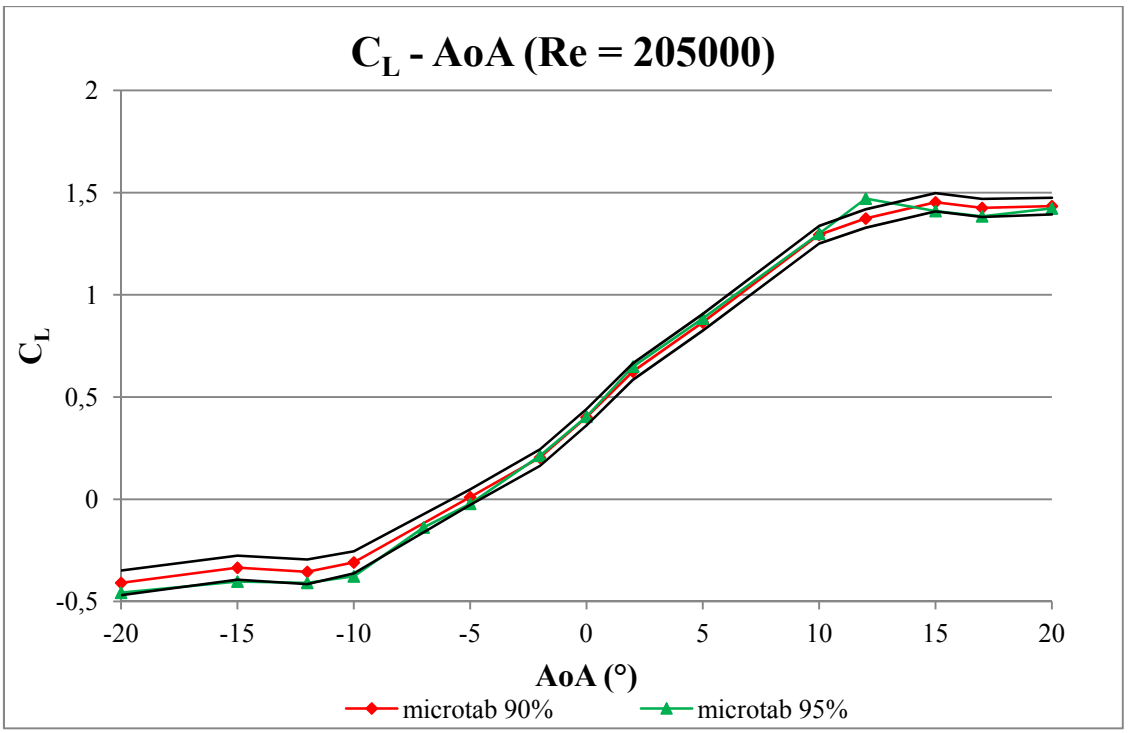

Figure 7.10. Microtab at 90 % vs 95%. Re = 205000.

Analyzing the performance of the wing regarding to the location of the microtab, it is remarkable that there are not significant differences in lift coefficient for the studied locations. For lower AoAs than -10 degrees, the lift coefficient is slightly higher when the microtab is installed at 90% of the chord. For others angles the lift coefficients are almost equal. If we take a look at the values (*table 7.4*) small differences can be appreciated. Anyway both C_L curves are between the error lines, which means that the differences are not meaningful.

upna Universidad Pública de Navarra Nafarroako Unibertsitate Publikoa
Todos los derechos reservados
Eskubide guztiak erresalbatu dira

C_L with metal cylinder in the suction side (Re = 205000)					
AoA	90%	95%	AoA	90%	95%
-20	-0,41	-0,46	2	0,63	0,65
-15	-0,33	-0,40	5	0,87	0,88
-12	-0,35	-0,41	10	1,29	1,30
-10	-0,31	-0,38	12	1,37	1,47
-5	0,01	-0,02	15	1,45	1,41
-2	0,20	0,21	17	1,43	1,38
0	0,40	0,40	20	1,43	1,42

Table 7.4. C_L for locations at 90% and 95% of the chord. Re = 205000.

Therefore it can be concluded that there were no substantial differences in the performance due to the location in the chord.

7.4. Measurements with the microtab located at 95% of the chord in the pressure side

In previous experiments the effect of the microtab as a lift reducer was studied. In order to extend the research and although it is not the main aim of this study, another effect was tested. As it has been already explained there are several ways to improve the performance of wind turbines. One possibility would involve decreasing the cut-in speed of the turbine by increasing the lift in its blades. It could be achieved deploying a microtab in the pressure side of the wing and, hence, increasing the lift coefficient.

In order to study the performance of the microtab as a lift enhancer, the wing with a microtab installed in its pressure side was tested. According to the literature (Johnson *et al.*, 2008 [4]), the microtab was located at 95% of the chord and it was the metal cylinder, which is 1.156% of the chord in height.

The obtained results were:

upna Universidad Pública de Navarra Nafarroako Unibertsitate Publikoa
Todos los derechos reservados
Eskubide guztiak erresalbatu dira

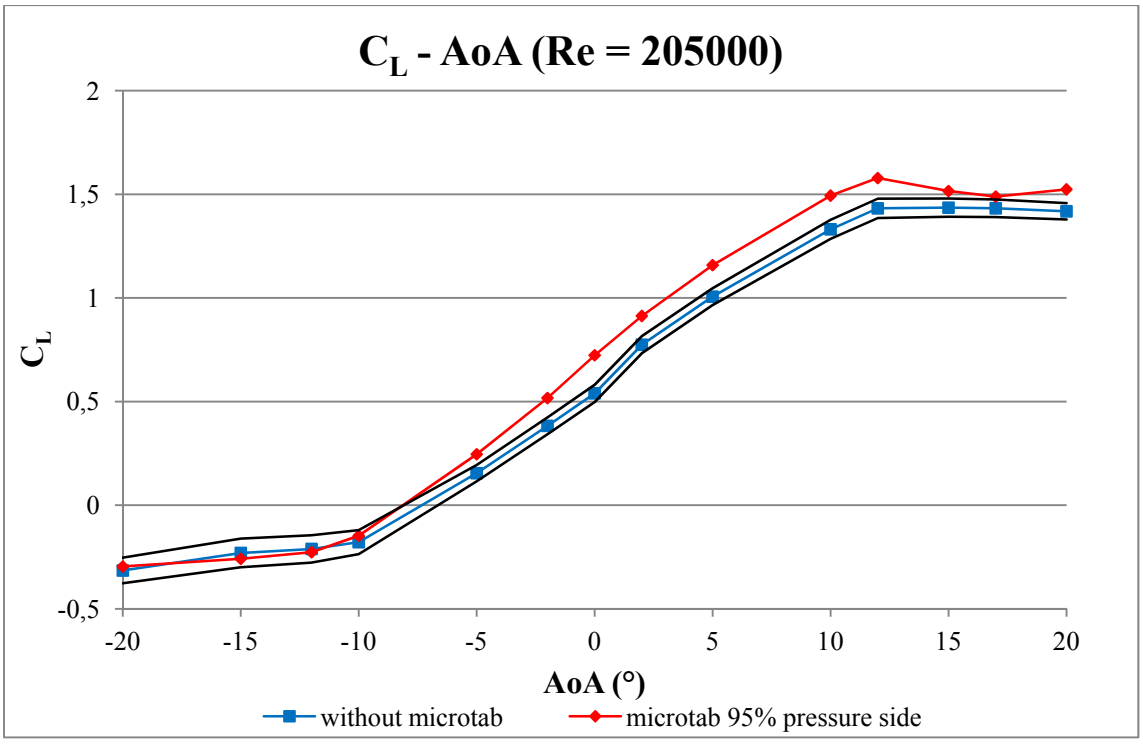

Figure 7.11. Metal cylinder at 90% of the chord in the pressure side. Re = 205000.

In this case a substantial effect of the microtab in the lift coefficient is visible. The lift curve has increased for all the AoAs except for those between -20˚ and -10˚, in which the variation is irrelevant. The variation for the data in the "constant slope" area is significant, since it is bigger than the calculated relative error. C_L values can be checked in *table 7.5*.

C_L with metal cylinder in the pressure side (Re = 205000)					
AoA	Without	95%	AoA	Without	95%
-20	-0,31	-0,30	2	0,77	0,91
-15	-0,23	-0,26	5	1,01	1,16
-12	-0,21	-0,23	10	1,33	1,49
-10	-0,18	-0,15	12	1,43	1,58
-5	0,15	0,25	15	1,44	1,52
-2	0,38	0,52	17	1,43	1,49
0	0,54	0,72	20	1,42	1,52

Table 7.5. C_L with microtab at 95% of the chord in the pressure side. Re = 205000.

The increase of the lift coefficient is widespread for values of AoA higher than -10º, so it is possible to conclude that the installation of a microtab in the pressure side allows increasing the lift in a wing.

upna Universidad Pública de Navarra Nafarroako Unibertsitate Publikoa
Todos los derechos reservados
Eskubide guztiak erresalbatu dira

7.5. Performance of the built GU 25(5)8-11 profile

The overall performance of the profile built was very close to the expected one. An indicator of this could be the similarities between the theoretical pressure distributions and the ones measured for every AoA. The behavior of the wing follows the same pattern than the data obtained with the Javafoil application.

It is true that decrease of the lift expected for AoA close to -10 and also around 0 degrees due to the stall, could only be noticed when testing the wing at low Reynolds numbers (Re = 100000). For high Reynolds (Re = 205000) this behavior did not take place and also lower values for the maximum lift coefficient were achieved, when comparing with the calculations. The theoretical simulation said that values close to 1.9 in the C_L could be achieved for AoA around 15 degrees. Instead, the built airfoil achieved a maximum value of the C_L of 1.44 for an AoA of 15º.

These variations may happen due to differences between the original shape of the wing, and the one built. Anyway, the results obtained were satisfying.

upna Universidad Pública de Navarra Nafarroako Unibertsitate Publikoa
Todos los derechos reservados
Eskubide guztiak erresalbatu dira

8. Conclusions

After concluding the tests and comparing the results some conclusions were developed. It may be recalled that the main aim of this thesis was to study the behavior of the microtabs in order to alleviate loads.

8.1. Influence of the microtab

Analyzing the results of the tests accomplished, there is no doubt about the influence of a microtab in a wing. The deployment of this device means a small change in the shape of the profile, but the effects are remarkable. Just with a tab of 1% of the chord, the same order of magnitude as the thickness of the boundary layer, the C_L curve can be decreased considerably (*table 8.1*).

C_L drop with metal cylinder in the suction side (Re = 205000)			
AoA	Original C_L range	C_L drop	Variation (%)
[-20°, -15°]	[-0.31, -0.23]	~ 0.10	[32.3, 50]
[-15°, 10°]	[-0.23, 1.33]	~ 0.15	[11.3, 50]

Table 8.1. C_L drop with microtab at 90% of the chord in the suction side. Re = 205000.

Thanks to the small size, it is a device that will require low quantities of energy and small actuators to function, and whose output will be highly beneficial to reduce loads. The effect of the microtab can be used for different aims:

- ✓ Mitigation of cyclic loads, such as the ones produced by the shadow effect. The impact of these loads could be reduced by smoothing the transition from normal conditions to the conditions in front of the tower. This could be done by deploying the device progressively in the suction side of the blades.

- ✓ Reduction of the lift in high wind speed conditions to avoid extreme loads. This effect could also be used to keep the wind turbine working in a wider range of wind speeds.

- ✓ Brake of the windmill, in both normal and extreme conditions.

upna Universidad Pública de Navarra Nafarroako Unibertsitate Publikoa
Todos los derechos reservados
Eskubide guztiak erresalbatu dira

To sum up, the microtab offers remarkable benefits without the necessity of installing big mechanisms in the blades of the wind turbine, and without requiring complicated technology or a big amount of electrical power. Its impact in the COE should be studied.

8.2. Wind speed as a crucial parameter

During the experiments it was observed that the influence of the microtab changed completely depending on the Reynolds number.

Although the possible error in the measurement is big for Re = 100000, the behavior of the C_L curve resembles to both, the theoretical results calculated with Javafoil [16] and the results that were achieved in another experimental study (R.A. McD. Galbraith, 1985 [12]). To the theoretical because of the two stall areas at -10º and -0.5º. And to the experimental study because of the sharp change of the slope, which results in reaching C_{Lmax}. The main difference between the experiments and the results in that paperwork is the values. The C_L values measured in the experiments are higher as seen in *figure 7.5*, and the change of slope takes place at an AoA of 5º, while the paperwork results report it at 12º. It could be due to the errors mentioned, plus differences between the blade tested and the one from the aforementioned study. Anyway is clear that for this Reynolds number, and probably until Re = 150000 the blade has a special behavior.

For Re = 205000 the stall areas are not visible and the C_L curve follows the Javafoil [16] results most of the time. So once the Re = 150000 exceeded the performance is closer to what theoretically expected.

Before installing the device in a wind turbine it must be tested at different Reynolds numbers in order to understand its behavior and avoid unexpected consequences. Knowing the performance of the chosen profile before testing the device can help to choose the best range of numbers, where different effects can be found.

8.3. Optimization between size and effect

It has been proved that the bigger the tab is the more pronounced the effect is. When the height of the microtab was twice as big, the effect the device was doubled (*table 8.2*).

upna Universidad Pública de Navarra Nafarroako Unibertsitate Publikoa
Todos los derechos reservados
Eskubide guztiak erresalbatu dira

C_L drop with metal cylinder in the suction side (Re = 205000)					
AoA	Original C_L range	2 mm		4mm	
		C_L drop	%	C_L drop	%
[-20, -15]	[-0.31, -0.23]	~ 0.10	[32.3, 50]	~ 0.3	[100, 130]
[-15, 5]	[-0.23, 1.01]	~ 0.15	[11.3, 50]	~ 0.3	[29.7, 130]
[5, 10]	[1.01, 1.33]	~ 0.15	[11.3, 50]	~ 0.2	[15, 19.8]

Table 8.2. Comparison of C_L drop with different microtab sizes. Re = 205000.

But to deploy bigger tabs the mechanisms would have to be stronger and the required amount of energy would be higher to make it function. Besides, at some point we would change from microtabs to the regular devices that already used in aviation, and the effect will not be proportional to the increase of size in the same way as happens with small ones (Johnson *et al.*, 2008 [4]). It is the responsibility of the engineer to study the impact of different sizes in the COE, and to find the most balanced solution between cost and effect. This study should be carried out for the specific profile that would be installed in the wind turbine.

8.4. Location of the microtab

Although some of the literature reported different effects depending on the percentage of the chord at which the microtab was installed (Johnson *et al.*, 2008 [4]), there is no evidence of this in the results of the tests performed. Both locations tried (90% and 95%) yielded almost the same data.

Deeper studies about this parameter should be accomplished to determine if the location is really significant. There might have been factors, such as the characteristics of the flow in the wind tunnel, or the shape of the tab, that could have cancelled the effect of changing the location. It could also happen that the chosen locations do not differ in the way they affect the performance of the profile tested. It could be also that the differences between both locations could not be notice due to the resolution level of the setup, limited by the number of pressure taps installed and their location. It was not feasible to lodge tubes further than the 90% of the chord.

8.5. Possible influence of the shape

The two microtabs tested were different not only in size but also in shape. The small microtab was a cylinder of 2 mm of diameter, and the big one was a wooden

upna Universidad Pública de Navarra Nafarroako Unibertsitate Publikoa
Todos los derechos reservados
Eskubide guztiak erresalbatu dira

rectangular prism. It could not be tested whether the shape had influence in the performance of the device or not. It may be interesting to develop a study about this issue, in order to prove if the shape matters, and in that case what the best shape is.

8.6. Alternatives to produce more electricity

The tests of the microtab in the pressure side showed that it can enhance the lift. Although this may not be very useful for load alleviation, it can be used to improve the productivity of the wind turbine in different ways:

- ✓ The cut-in speed could be set at lower wind speeds due to the lift increase. This would mean more working time and working order for a wider range of wind speeds.

- ✓ More energy could be produced at certain wind speeds, as the lift would be higher. The nominal power could be reached before.

Anyway, the performance of the tab in the pressure side should be better studied in different conditions. It has to be taken into account that the tab installed in the suction side seemed to produce the opposite effect than expected at a Reynolds number of 100000 (although the results were not conclusive).

8.7. Airflow improvement

Last but not least, the airflow performance was improved before starting the tests. Thanks to the installation of the honeycomb the turbulence level of the airstream was reduced. Also the flow homogeneity was improved, since the speed variations were reduced from 5 m/s to 3.5 m/s for the maximum fan power, from 6 m/s to 2 m/s for the third level of the fan and from 1.4 m/s to 0.45 m/s for the lowest level (*table 8.3*). Therefore, a bigger area with similar values of wind speeds focused in the centre of the test section was available, allowing to measure the pressure over a wing that had almost equal flow conditions along its spanwise.

However, the maximum velocity in the test section decreased once the honeycomb and the redirectioning device were installed. In the beginning speeds up to 22 m/s were the highest while velocities of 17.5 m/s could only be achieved afterwards. Despite it reduces the range of Reynolds numbers for the experiments, the flow

upna Universidad Pública de Navarra Nafarroako Unibertsitate Publikoa
Todos los derechos reservados
Eskubide guztiak erresalbatu dira

conditions were more appropriate as a consequence of the turbulence reduction and the increase of homogeneity.

In *table 8.3*, the values of the maximum speed in the tunnel for each fan power level and the flow homogeneity variation are shown.

Fan power level	Maximum speed (m/s)		Flow homogeneity variation (m/s)	
	Before modifications	After modifications	Before modifications	After modifications
1	4.2	2.9	1.4	0.45
3	15	10	6	2
5	22	17.5	5	3.5

Table 8.3. Flow characteristics variation in the wind tunnel.

8.8. Further research

In this study the influence of microtabs for load alleviation has been tested and their benefits proved. Further research would be necessary to study the application of this technology for wind turbines in depth.

Further experimental research involving some topics that came out during the accomplishment of the experiments would be very interesting in order to continue with the investigation, and some of these recommendations could be taken into account:

- ✓ The experiments could be carried out in a wind tunnel with better characteristics. Better flow homogeneity and the wind speed stability would have an important impact in the accuracy of the experiments. There are already projects working to improve this situation, and their results will help in further experiments.

- ✓ The influence of the smart device regarding to different Reynolds numbers could be more deeply studied. To do so, more accurate pressure measuring devices can be tried, and high stability in the wind speed will help to reduce the error.

- ✓ Deeper investigation about the influence of the location of the tab would be necessary, as there is controversy between the results obtained and other studies (Johnson *et al.*, 2008 [4]). Also some development in the way of attaching the microtab to the wing would be interesting, to improve the method used. It is a difficult issue, as the locations of the microtabs are always really close to the trailing edge (up to 95% of the chord).

upna Universidad Pública de Navarra Nafarroako Unibertsitate Publikoa
Todos los derechos reservados
Eskubide guztiak erresalbatu dira

- ✓ Further research about the influence of the shape could be also interesting, in order to optimize the effect of the tab.

- ✓ Studying the variation on the aerodynamic performance change while deploying the microtab progressively would yield more data about the functioning of the device.

- ✓ In order to verify the viability of the use of microtabs, their impact in the COE should be studied.

upna Universidad Pública de Navarra Nafarroako Unibertsitate Publikoa
Todos los derechos reservados
Eskubide guztiak erresalbatu dira

Appendix

Appendix 1: Betz limit

This mathematical deduction is based on J. Ripa (2009) [7].

- **Continuity equation**

Applying conservation of mass to the control volume, the mass of fluid flowing per unit time is given by:

$$\dot{m} = \rho A_1 v_1 = \rho S v = \rho A_2 v_2$$

Equation Appendix 1.1

v_1 is the speed in front of the rotor, v_2 is the speed downstream of the rotor and v is the speed at the rotor section. ρ is the fluid density, and S is the area of the turbine rotor.

The force exerted on the wind by the rotor may be written as:

$$F = m \cdot a = m\frac{dv}{dt} = \dot{m}\Delta v = \rho S v(v_1 - v_2)$$

Equation Appendix 1.2

- **Power and work**

The work done by the force may be written incrementally as:

$$dE = Fdx$$

$$P = \frac{dE}{dt} = F\frac{dx}{dt} = Fv = \rho S v^2(v_1 - v_2)$$

Equation Appendix 1.3

However, power can be computed another way, by using the kinetic energy. Applying the conservation of energy equation to the control volume yields:

upna Universidad Pública de Navarra Nafarroako Unibertsitate Publikoa
Todos los derechos reservados
Eskubide guztiak erresalbatu dira

$$P = \frac{\Delta E}{\Delta t} = \frac{1}{2}\dot{m}(v_1^2 - v_2^2)$$

Equation Appendix 1.4

Looking back at the continuity equation, a substitution for the mass flow rate yields the following:

$$P = \frac{1}{2}\rho S v(v_1^2 - v_2^2)$$

Equation Appendix 1.5

Both of these expressions for power are valid. Equating these two expressions yields:

$$P = \frac{1}{2}\rho S v(v_1^2 - v_2^2) = \rho S v^2(v_1 - v_2)$$

$$\frac{1}{2}(v_1^2 - v_2^2) = \frac{1}{2}(v_1 + v_2)(v_1 - v_2) = v(v_1 - v_2)$$

Equation Appendix 1.6

$$v = \frac{1}{2}(v_1 + v_2)$$

Equation Appendix 1.7

Therefore, the wind velocity at the rotor may be taken as the average of the upstream and downstream velocities. Returning to the previous expression for power based on kinetic energy:

$$\dot{E} = \frac{1}{2}\dot{m}(v_1^2 - v_2^2)$$
$$\dot{E} = \frac{1}{2}\rho S v(v_1^2 - v_2^2)$$
$$\dot{E} = \frac{1}{4}\rho S(v_1 + v_2)(v_1^2 - v_2^2)$$

Equation Appendix 1.8

$$\dot{E} = \frac{1}{4}\rho S v_1^3\left(1 - \left(\frac{v_2}{v_1}\right)^2 + \left(\frac{v_2}{v_1}\right) - \left(\frac{v_2}{v_1}\right)^3\right)$$

Equation Appendix 1.9

upna Universidad Pública de Navarra Nafarroako Unibertsitate Publikoa
Todos los derechos reservados
Eskubide guztiak erresalbatu dira

Appendix 2: Profile coordinates

The geometrical shape of GU25(5)8-11 airfoil is defined by the numerical coordinates of its contour points. This data is given by the profile data base and the points are shown in the *table appendix 2* and the *figure Appendix 2* shows GU25(5)8-11 airfoil's shape:

Pressure side		Suction side	
1.000,0.00000	0.400,-0.02985	0.000,0.00000	0.450,0.17084
0.950,-0.00410	0.350,-0.03081	0.005,0.01552	0.500,0.16750
0.900,-0.00694	0.300,-0.03131	0.025,0.04082	0.550,0.15800
0.850,-0.00913	0.250,-0.03133	0.050,0.06199	0.600,0.14434
0.800,-0.01137	0.200,-0.03080	0.075,0.07876	0.650,0.12815
0.750,-0.01374	0.150,-0.02956	0.100,0.09291	0.700,0.11037
0.700,-0.01621	0.100,-0.02720	0.150,0.11593	0.750,0.09173
0.650,-0.01875	0.075,-0.02532	0.200,0.13388	0.800,0.07282
0.600,-0.02131	0.050,-0.02262	0.250,0.14787	0.850,0.05413
0.550,-0.02381	0.025,-0.01819	0.300,0.15844	0.900,0.03602
0.500,-0.02616	0.005,-0.00964	0.350,0.16582	0.950,0.01815
0.450,-0.02826	0.000,0.00000	0.400,0.17003	1.000,0.00000

Table Appendix 2. Coordinates of the GU25-5(11)8 airfoil

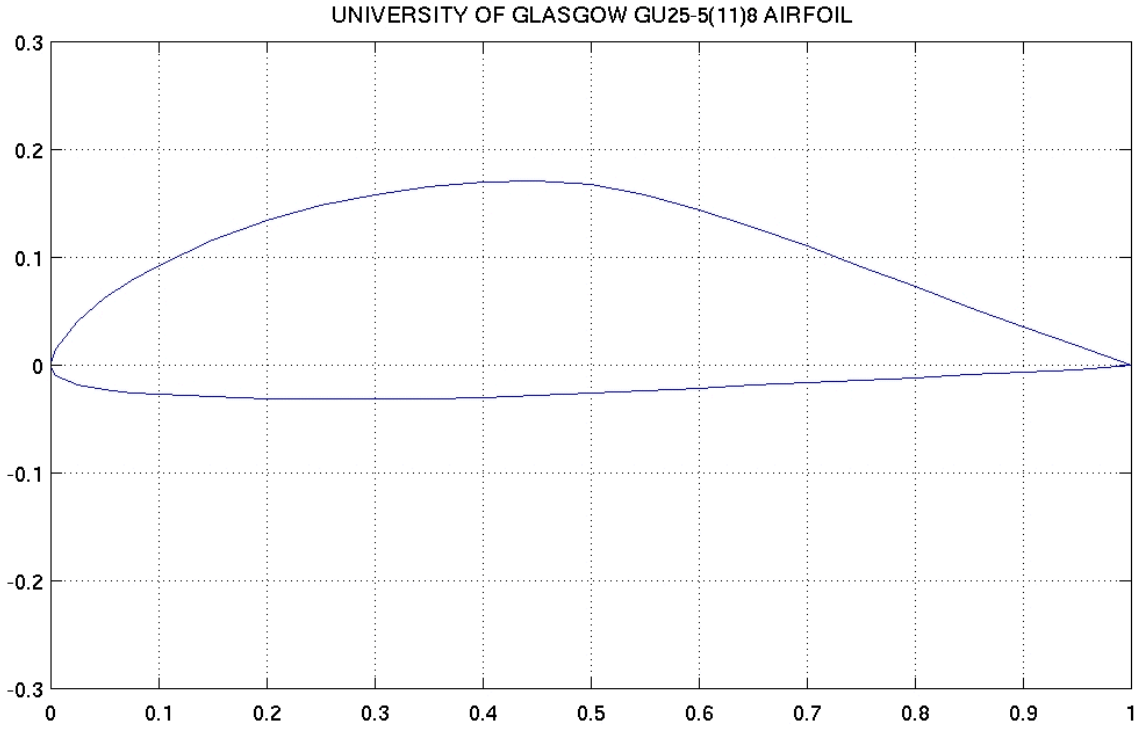

Figure Appendix 2. GU25-5(11)8 plot

upna Universidad Pública de Navarra Nafarroako Unibertsitate Publikoa
Todos los derechos reservados
Eskubide guztiak erresalbatu dira

Appendix 3: Vortex panel method simulation data

3.1. Output from the vortex panel method software

		Cp				
x	y	α = -20	α = -15	α = -10	α = -5	α = 0
1	0	0,95696	0,95606	0,95583	0,95627	0,95737
0,99175	0,003	0,32975	0,25299	0,18398	0,12485	0,07737
0,97742	0,00822	0,3502	0,2965	0,25176	0,21733	0,19425
0,95646	0,01582	0,30742	0,24918	0,20043	0,16264	0,13697
0,92621	0,02666	0,2767	0,20931	0,15143	0,10482	0,0709
0,88529	0,0413	0,2537	0,17379	0,10296	0,04337	-0,00317
0,83374	0,06016	0,22239	0,1252	0,03631	-0,04158	-0,10609
0,77109	0,08376	0,16554	0,0421	-0,07436	-0,1803	-0,2725
0,69822	0,11102	0,08468	-0,07822	-0,23681	-0,38628	-0,52208
0,61693	0,13909	-0,01995	-0,24312	-0,46771	-0,68691	-0,89405
0,53005	0,16243	-0,13936	-0,45701	-0,789	-1,12526	-1,45556
0,44116	0,17095	0,03043	-0,32775	-0,71904	-1,13156	-1,55278
0,35421	0,1663	0,30836	-0,046	-0,45456	-0,9049	-1,38334
0,27304	0,15314	0,564	0,22726	-0,19053	-0,67668	-1,21643
0,20086	0,13415	0,79065	0,49715	0,08742	-0,42609	-1,02779
0,13997	0,11177	0,95517	0,74703	0,37532	-0,14866	-0,809
0,09145	0,08831	0,99145	0,93848	0,65585	0,15216	-0,55731
0,05521	0,06576	0,77376	0,99463	0,89136	0,4671	-0,26526
0,03013	0,0457	0,06959	0,76671	0,99999	0,76235	0,06099
0,01436	0,02912	-1,49436	0,00076	0,83003	0,96824	0,4112
0,00557	0,01653	-4,52748	-1,70875	0,13868	0,95869	0,72635
0,00156	0,0079	-9,39738	-4,65783	-1,29413	0,59151	0,9418
0,00021	0,00262	-15,6551	-8,5955	-3,37095	-0,14017	0,99865
0	0	-20,97836	-12,02434	-5,26138	-0,89498	0,9422
0,00021	-0,00233	-26,17752	-15,50732	-7,30428	-1,81762	0,78594
0,00156	-0,00586	-28,66142	-17,68347	-9,02196	-2,94009	0,37736
0,00557	-0,01008	-21,09397	-13,52466	-7,3684	-2,81225	0,00536
0,01436	-0,01478	-12,93089	-8,58835	-4,93914	-2,09414	-0,13979
0,03013	-0,01937	-7,84769	-5,36999	-3,21913	-1,46047	-0,14744
0,05521	-0,02327	-4,85186	-3,39344	-2,08737	-0,97335	-0,08521
0,09145	-0,02663	-3,29562	-2,3503	-1,47825	-0,70597	-0,05693
0,13997	-0,0292	-2,35129	-1,7051	-1,0917	-0,52971	-0,03621
0,20086	-0,03081	-1,73856	-1,27935	-0,83102	-0,4072	-0,02077
0,27304	-0,03138	-1,32037	-0,98484	-0,64786	-0,31966	-0,01022
0,35421	-0,03075	-1,01964	-0,7704	-0,51256	-0,25396	-0,00244
0,44116	-0,02858	-0,77749	-0,5928	-0,39545	-0,19145	0,01302
0,53005	-0,02477	-0,55046	-0,41707	-0,26918	-0,11129	0,05181

upna Universidad Pública de Navarra Nafarroako Unibertsitate Publikoa
Todos los derechos reservados
Eskubide guztiak erresalbatu dira

0,61693	-0,02045	-0,37486	-0,279	-0,16793	-0,04503	0,08599
0,69822	-0,0163	-0,23611	-0,16852	-0,08562	0,01007	0,11565
0,77109	-0,01273	-0,12639	-0,08065	-0,01981	0,05427	0,13934
0,83374	-0,00984	-0,03765	-0,00939	0,03356	0,08992	0,15796
0,88529	-0,00761	0,02803	0,0419	0,0701	0,11176	0,16562
0,92621	-0,00559	0,09449	0,09545	0,11011	0,13804	0,17838
0,95646	-0,00363	0,17667	0,16563	0,16726	0,1815	0,20792
0,97742	-0,00192	0,27211	0,24809	0,23527	0,23404	0,24442
0,99175	-0,00069	0,32508	0,27124	0,22681	0,19313	0,17122
1	0	0,95696	0,95606	0,95583	0,95627	0,95737

Table Appendix 3.1.1. Output from the vortex panel method software for several AoA (α) [16].

		Cp			
x	y	α = 5	α = 10	α = 15	α = 20
1	0	0,95909	0,96139	0,96419	0,9674
0,99175	0,003	0,04299	0,02276	0,01729	0,02675
0,97742	0,00822	0,18324	0,18462	0,19835	0,22402
0,95646	0,01582	0,1242	0,12471	0,13848	0,16511
0,92621	0,02666	0,05069	0,04482	0,05345	0,07634
0,88529	0,0413	-0,03525	-0,05188	-0,05257	-0,0373
0,83374	0,06016	-0,15527	-0,18762	-0,20216	-0,19845
0,77109	0,08376	-0,34815	-0,40496	-0,4412	-0,45578
0,69822	0,11102	-0,64009	-0,73672	-0,80903	-0,85483
0,61693	0,13909	-1,08284	-1,24754	-1,38316	-1,48556
0,53005	0,16243	-1,76987	-2,05864	-2,3131	-2,5255
0,44116	0,17095	-1,96988	-2,3702	-2,74159	-3,07274
0,35421	0,1663	-1,87534	-2,36595	-2,84027	-3,28388
0,27304	0,15314	-1,79337	-2,38997	-2,9881	-3,5696
0,20086	0,13415	-1,69939	-2,42048	-3,16916	-3,92267
0,13997	0,11177	-1,58563	-2,45495	-3,39055	-4,364
0,09145	0,08831	-1,45098	-2,50171	-3,67757	-4,94282
0,05521	0,06576	-1,28348	-2,55661	-4,04598	-5,70632
0,03013	0,0457	-1,08276	-2,63416	-4,54606	-6,76037
0,01436	0,02912	-0,82417	-2,70034	-5,16029	-8,12928
0,00557	0,01653	-0,55126	-2,83534	-6,05648	-10,11681
0,00156	0,0079	-0,2539	-2,95927	-7,09211	-12,52683
0,00021	0,00262	0,01092	-3,07336	-8,16046	-15,09581
0	0	0,19434	-3,11585	-8,88777	-16,94607
0,00021	-0,00233	0,4273	-2,88266	-9,04335	-17,86759
0,00156	-0,00586	0,82958	-1,59716	-6,82912	-14,70735
0,00557	-0,01008	0,99881	0,13791	-2,55116	-6,98672
0,01436	-0,01478	0,86452	0,88828	-0,06924	-1,97894

upna Universidad Pública de Navarra Nafarroako Unibertsitate Publikoa
Todos los derechos reservados
Eskubide guztiak erresalbatu dira

0,03013	-0,01937	0,68006	0,99689	0,79342	0,07583
0,05521	-0,02327	0,55005	0,91314	0,99301	0,78726
0,09145	-0,02663	0,44916	0,79691	0,97576	0,98027
0,13997	-0,0292	0,3738	0,68787	0,89645	0,9932
0,20086	-0,03081	0,31654	0,59447	0,80458	0,94049
0,27304	-0,03138	0,27106	0,51563	0,71607	0,86627
0,35421	-0,03075	0,23435	0,44921	0,63562	0,7879
0,44116	-0,02858	0,21173	0,39866	0,56812	0,71496
0,53005	-0,02477	0,21516	0,37379	0,52289	0,65792
0,61693	-0,02045	0,22113	0,35628	0,48735	0,61035
0,69822	-0,0163	0,22791	0,34343	0,4587	0,57023
0,77109	-0,01273	0,23282	0,33187	0,43348	0,53457
0,83374	-0,00984	0,23562	0,32053	0,41012	0,50167
0,88529	-0,00761	0,23005	0,30308	0,3825	0,4659
0,92621	-0,00559	0,22991	0,29107	0,35998	0,43457
0,95646	-0,00363	0,24572	0,29375	0,35055	0,41439
0,97742	-0,00192	0,26612	0,29846	0,34046	0,39086
0,99175	-0,00069	0,16176	0,16502	0,18092	0,20896
1	0	0,95909	0,96139	0,96419	0,9674

Table Appendix 3.1.2. Output from the vortex panel method software for several AoA (α) [16].

upna Universidad Pública de Navarra Nafarroako Unibertsitate Publikoa
Todos los derechos reservados
Eskubide guztiak erresalbatu dira

3.2. Theoretical Cp distributions for different AoAs

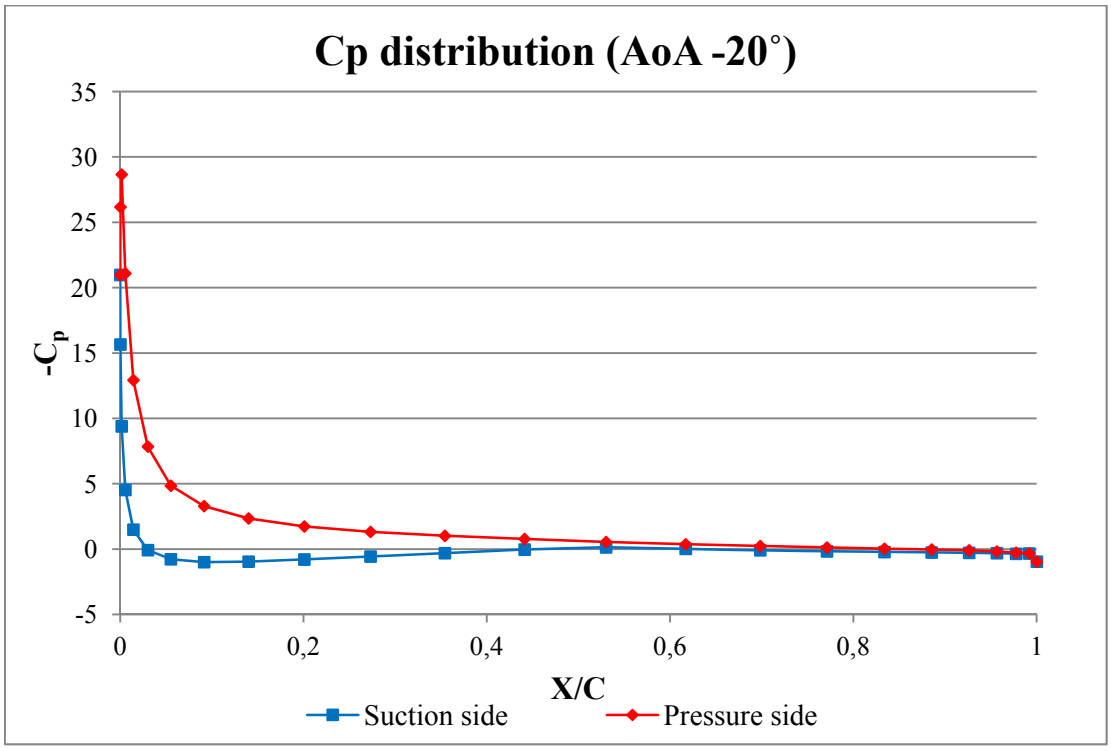

Figure Appendix 3.2.1. Theoretical Cp distribution, AoA -20°

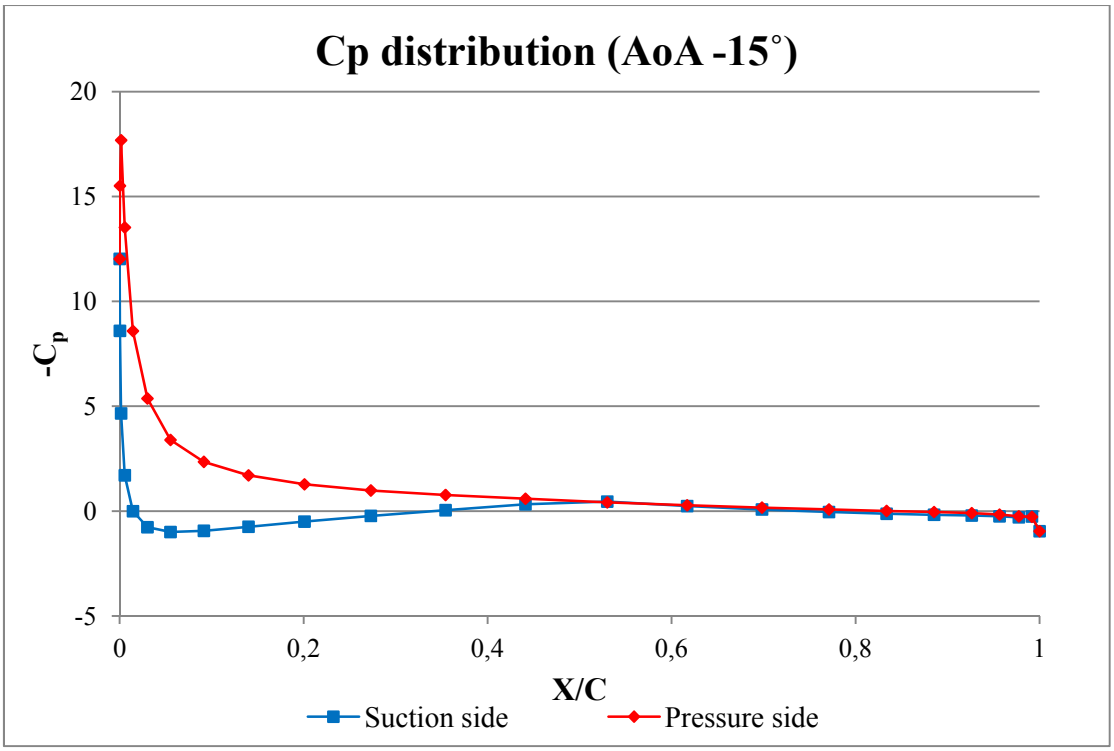

Figure Appendix 3.2.2. Theoretical Cp distribution, AoA -15°

upna Universidad Pública de Navarra Nafarroako Unibertsitate Publikoa
Todos los derechos reservados
Eskubide guztiak erresalbatu dira

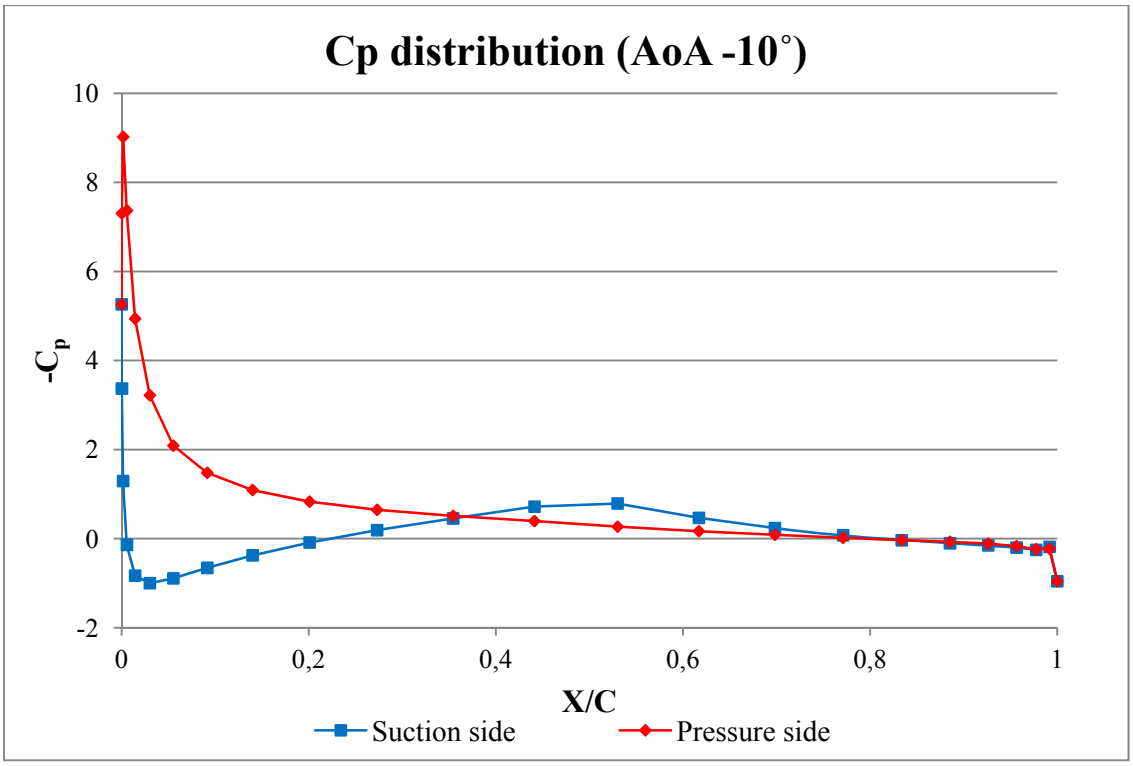

Figure Appendix 3.2.3. Theoretical Cp distribution, AoA -10˚

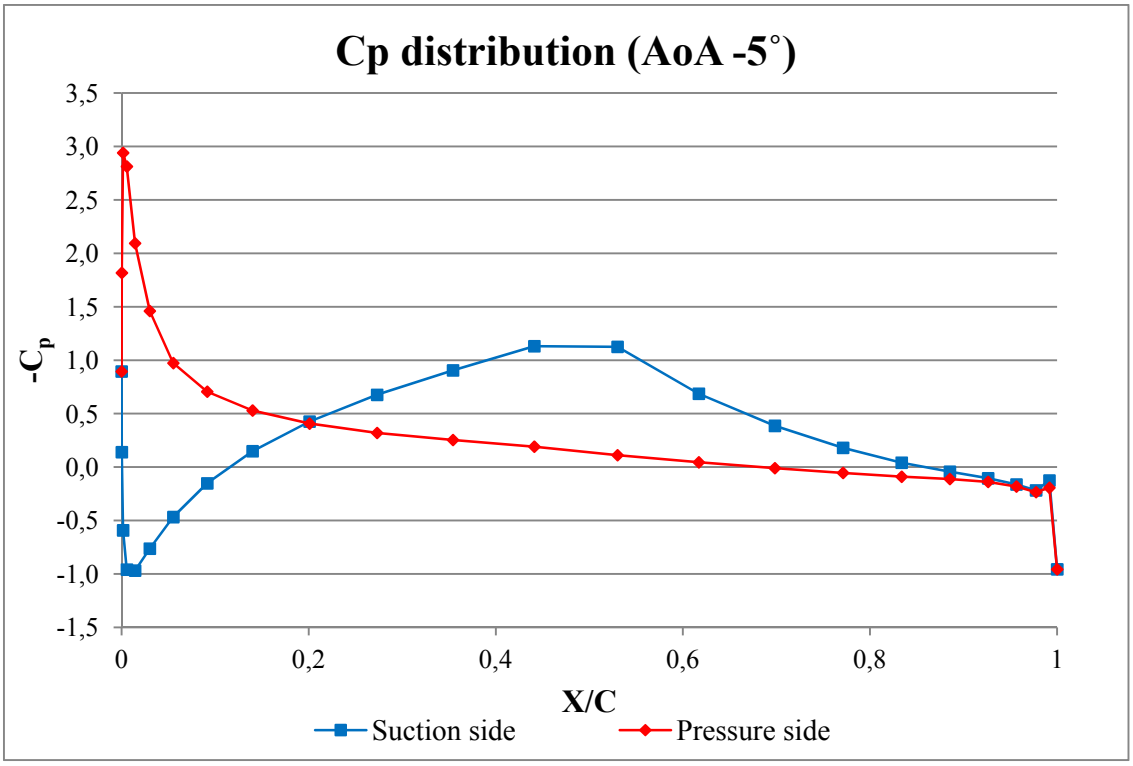

Figure Appendix 3.2.4. Theoretical Cp distribution, AoA -5˚

upna Universidad Pública de Navarra Nafarroako Unibertsitate Publikoa
Todos los derechos reservados
Eskubide guztiak erresalbatu dira

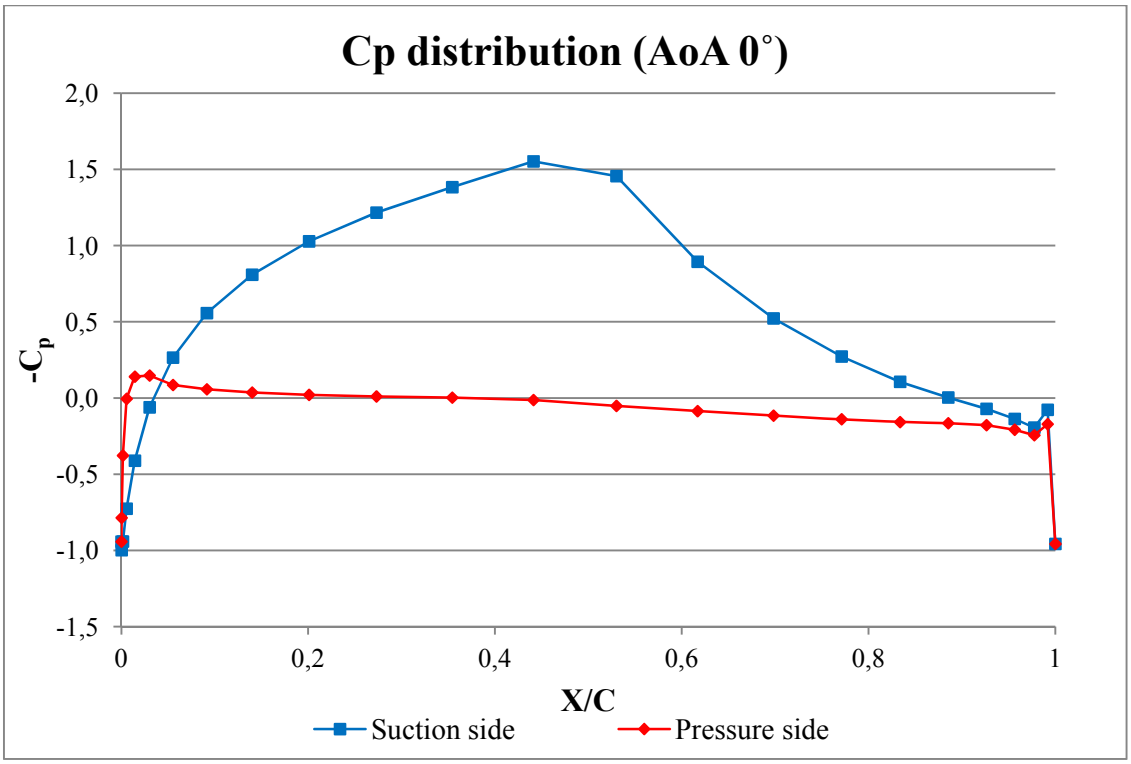

Figure Appendix 3.2.5. Theoretical Cp distribution, AoA 0˚

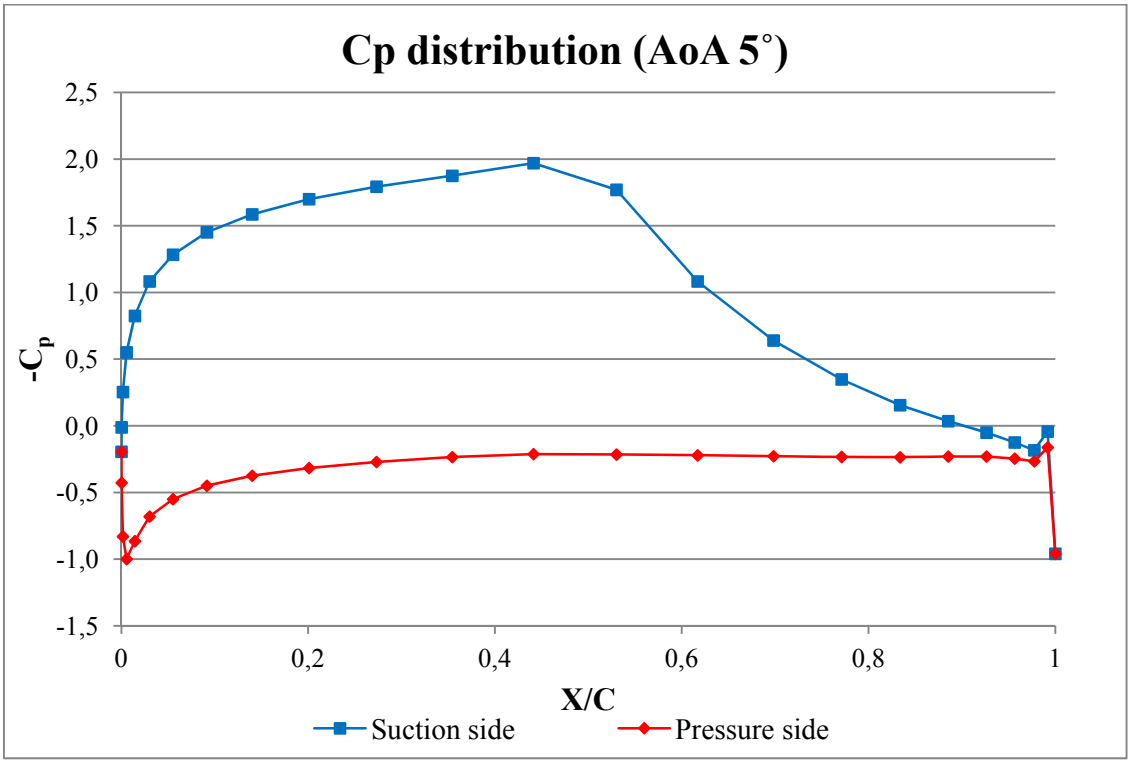

Figure Appendix 3.2.6. Theoretical Cp distribution, AoA 5˚

upna Universidad Pública de Navarra Nafarroako Unibertsitate Publikoa
Todos los derechos reservados
Eskubide guztiak erresalbatu dira

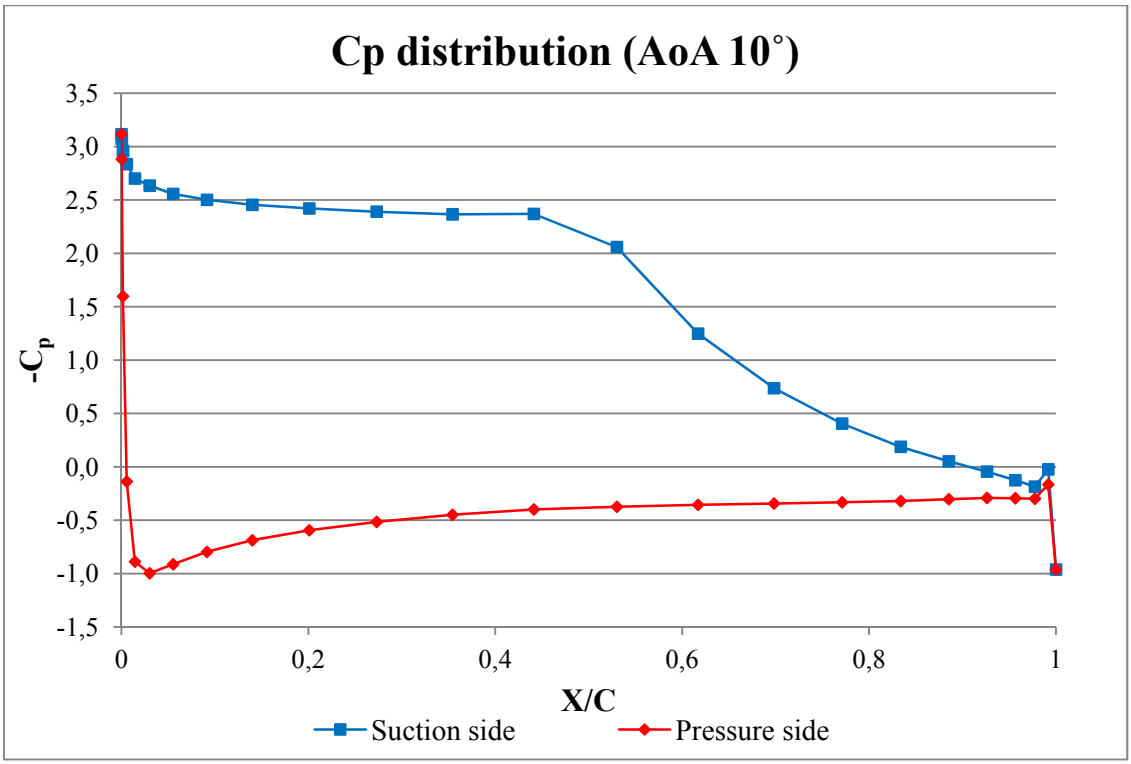

Figure Appendix 3.2.7. Theoretical Cp distribution, AoA 10˚

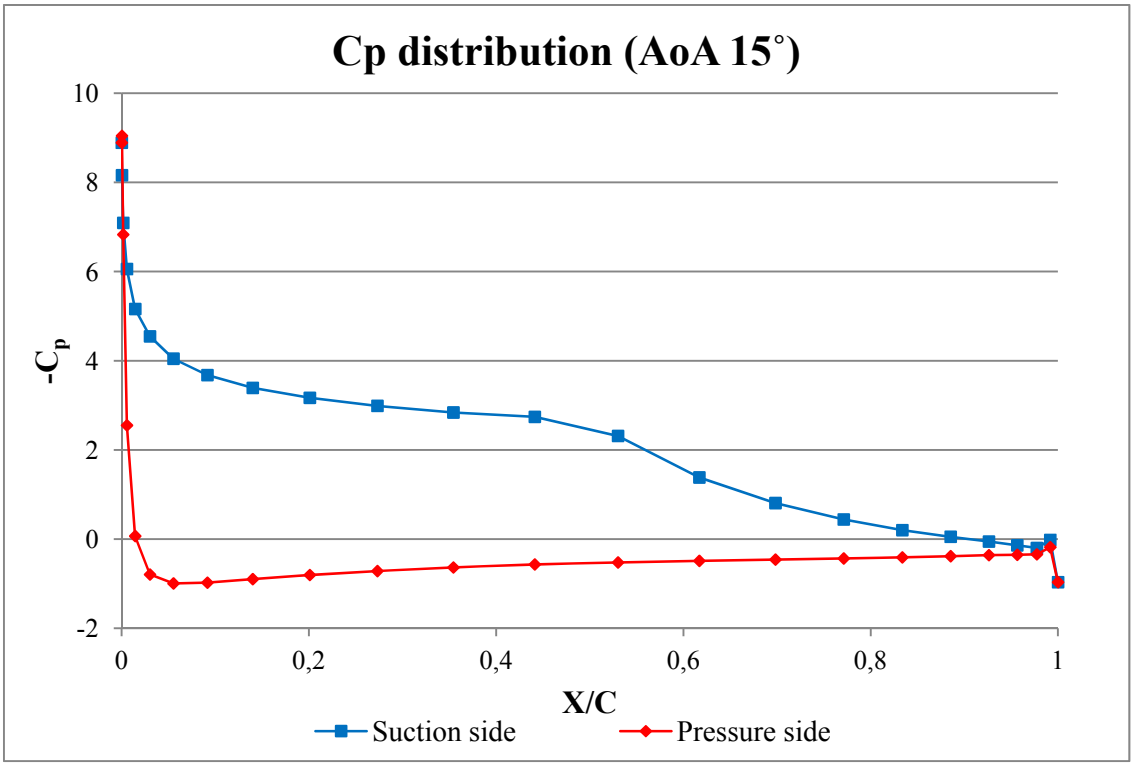

Figure Appendix 3.2.8. Theoretical Cp distribution, AoA 15˚

upna Universidad Pública de Navarra Nafarroako Unibertsitate Publikoa
Todos los derechos reservados
Eskubide guztiak erresalbatu dira

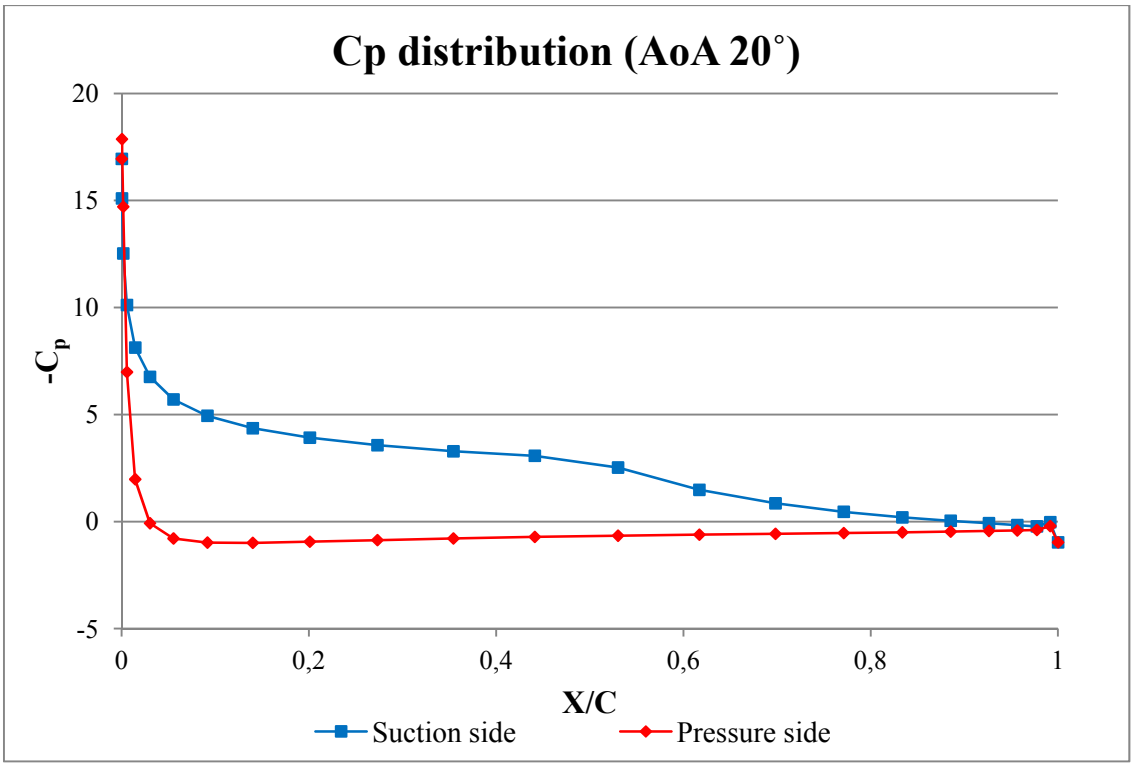

Figure Appendix 3.2.9. Theoretical Cp distribution, AoA 20˚

upna Universidad Pública de Navarra Nafarroako Unibertsitate Publikoa
Todos los derechos reservados
Eskubide guztiak erresalbatu dira

3.3. Theoretical pressure distributions for an AoA of 15°

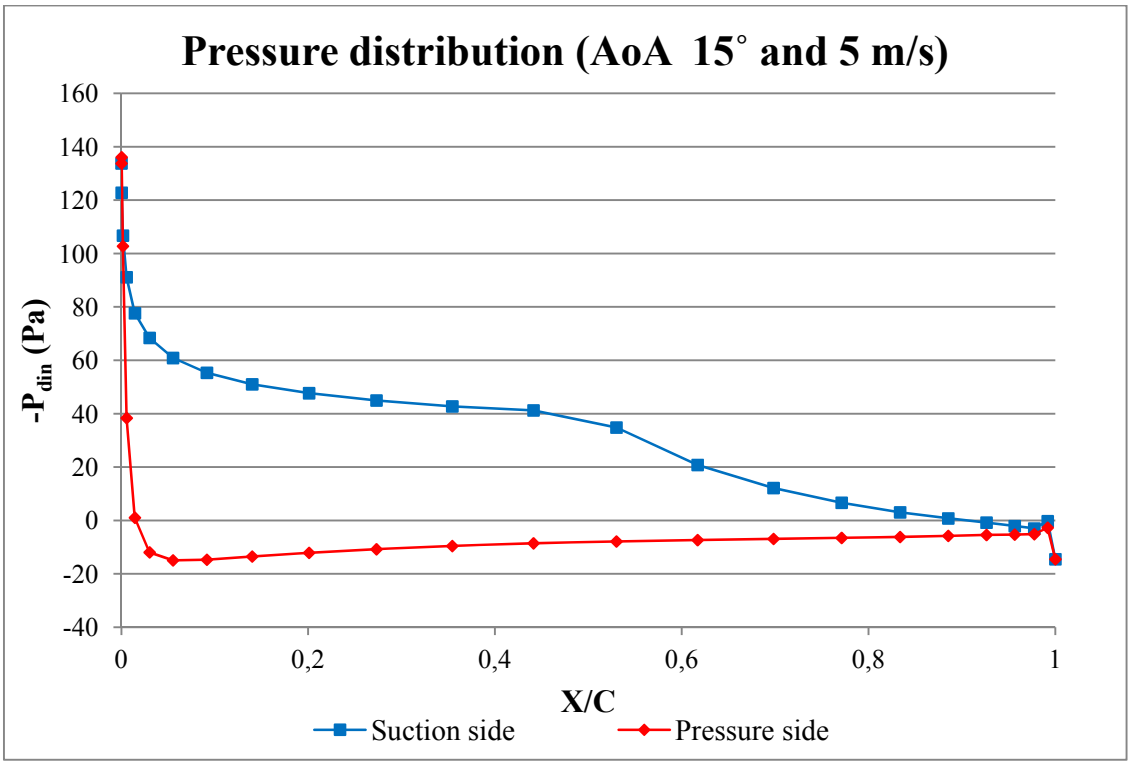

Figure Appendix 3.3.1. Theoretical pressure distribution, AoA 15°, wind speed 5 m/s

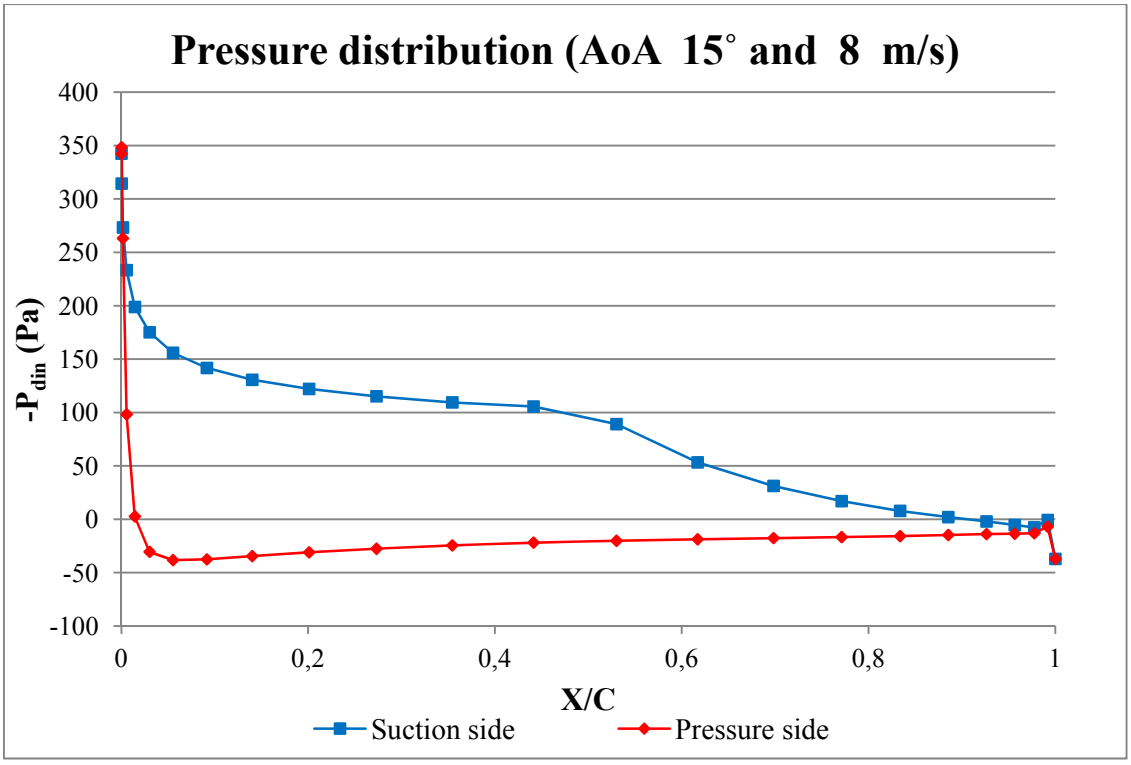

Figure Appendix 3.3.2. Theoretical pressure distribution, AoA 15°, wind speed 8 m/s

upna Universidad Pública de Navarra Nafarroako Unibertsitate Publikoa
Todos los derechos reservados
Eskubide guztiak erresalbatu dira

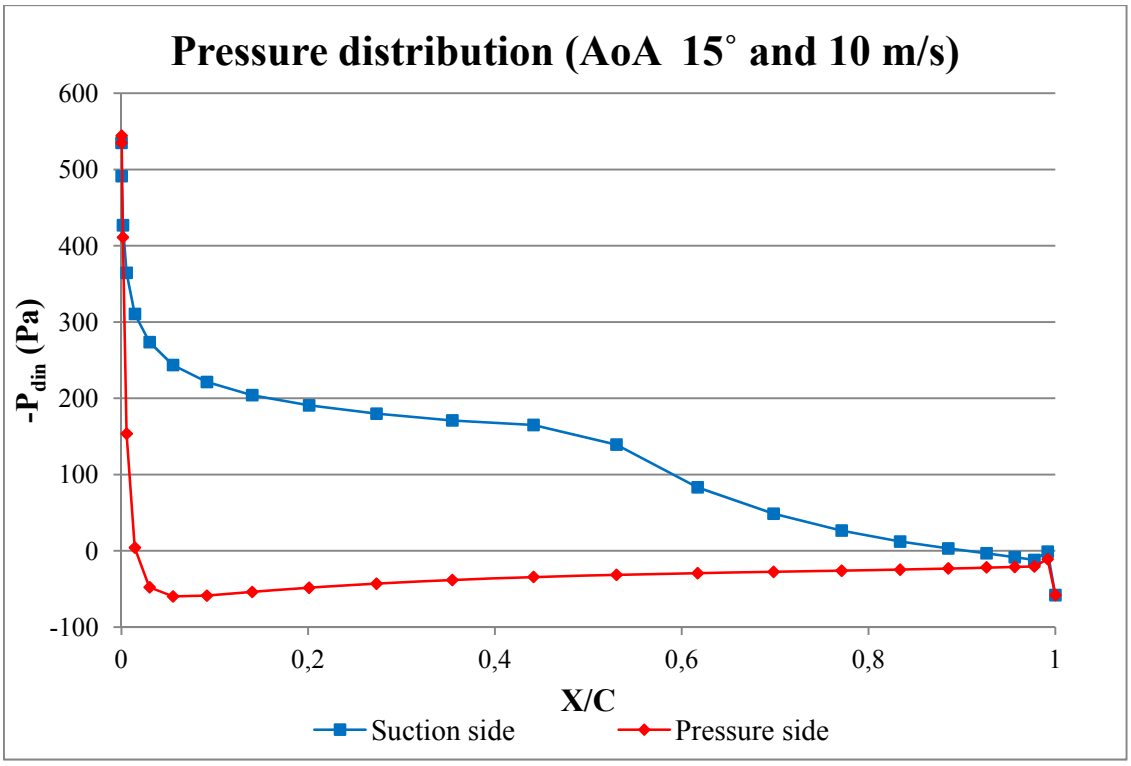

Figure Appendix 3.3.3. Theoretical pressure distribution, AoA 15°, wind speed 10 m/s

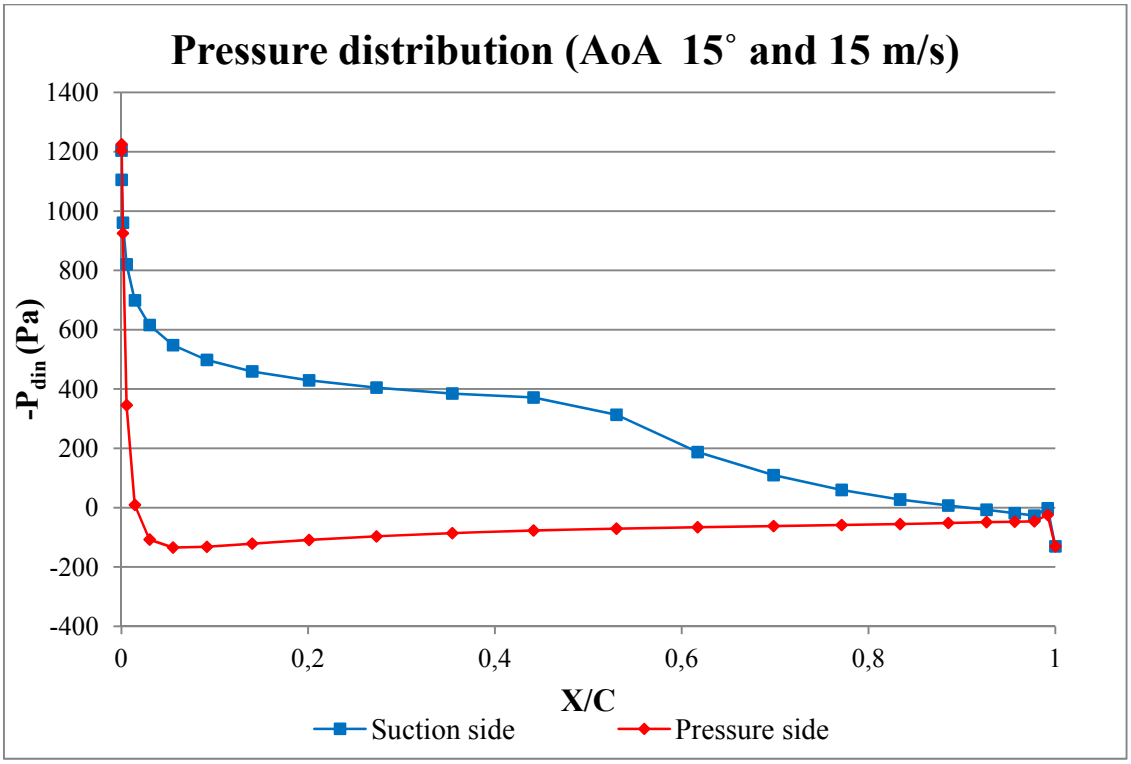

Figure Appendix 3.3.4. Theoretical pressure distribution, AoA 15°, wind speed 15 m/s

upna Universidad Pública de Navarra Nafarroako Unibertsitate Publikoa
Todos los derechos reservados
Eskubide guztiak erresalbatu dira

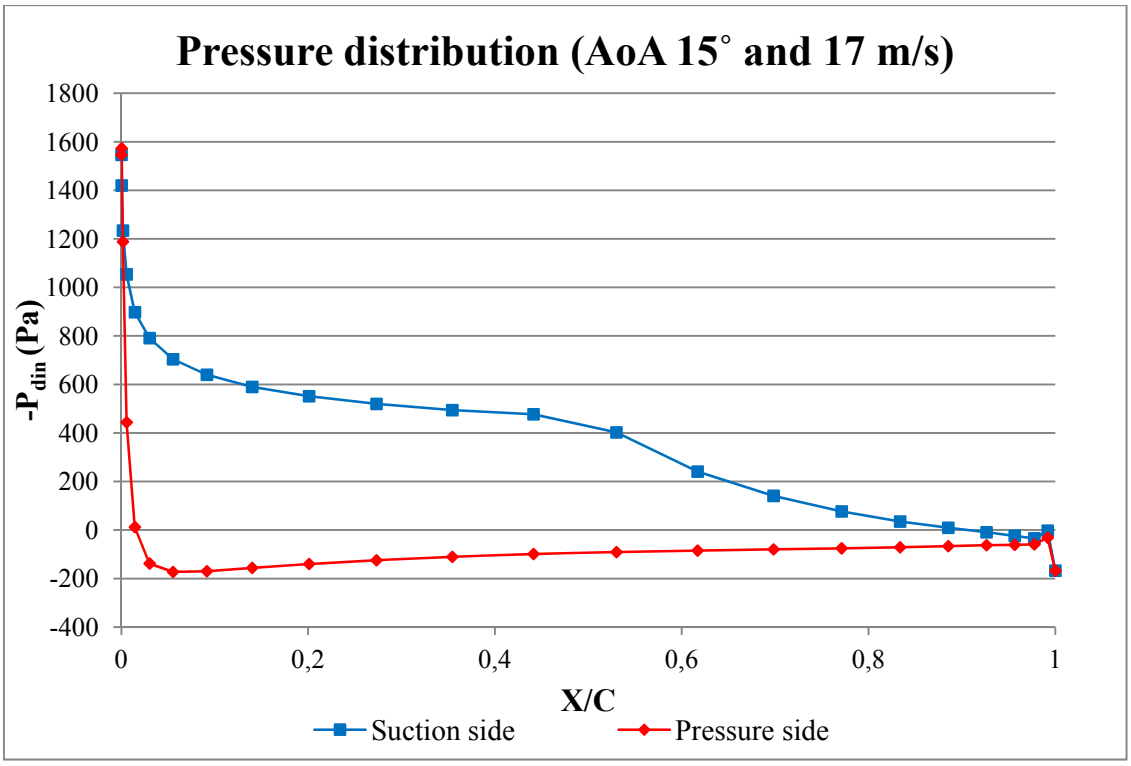

Figure Appendix 3.3.5. Theoretical pressure distribution, AoA 15°, wind speed 17 m/s

upna Universidad Pública de Navarra Nafarroako Unibertsitate Publikoa
Todos los derechos reservados
Eskubide guztiak erresalbatu dira

Appendix 4: DATUM

4.1. DATUM → Blade

- Requirements:
    1) Control of the shape of the core
    2) Assembling accuracy
    3) Weight
    4) Stiffness
    5) Manufacture
    6) Installation of the tubes for the pressure measurement

- Designs

    ✓ Core with ribs
    ✓ Foam core

Requirements	Core with ribs	Foam core
1 (Core)	DATUM	+
2 (Assembling))		+
3 (Weight)		+
4 (Stiffness)		-
5 (Manufacture)		+
6 (Tubes)		+
Σ+		5
Σ-		1
Σ=		0

Table Appendix 4.1. Comparative grid of the blade designs.

upna Universidad Pública de Navarra Nafarroako Unibertsitate Publikoa
Todos los derechos reservados
Eskubide guztiak erresalbatu dira

4.2. DATUM → Connection

- Requirements:
    1) Adaptability to different constructions of the blade
    2) Assembling accuracy
    3) Weight
    4) Stiffness
    5) Manufacture
    6) Installation of the tubes for the pressure measurement

- Designs

    ✓ Plugs
    ✓ Blade profile shaped piercing

Requirements	Plugs	Blade profile shaped piercing
1 (Core)	DATUM	+
2 (Assembling))		+
3 (Weight)		+
4 (Stiffness)		-
5 (Manufacture)		+
6 (Tubes)		+
Σ+		5
Σ-		1
Σ=		0

Table 4.2. Comparative grid of the "connection" designs.

upna Universidad Pública de Navarra Nafarroako Unibertsitate Publikoa
Todos los derechos reservados
Eskubide guztiak erresalbatu dira

Appendix 5: Relative error estimation

The relative error in pressure coefficient has been estimated from the *equation 5.1* applying the error propagation theory. This theory says that for multiplication and division of variables, both relative errors has to be added. If $Z = X \cdot Y$ or $Z = \frac{X}{Y}$ then:

$$\frac{\Delta Z}{Z} = \frac{\Delta X}{X} + \frac{\Delta Y}{Y}$$

Equation Appendix 5.1.

For the C_P, the relative error would be:

$$\frac{\Delta C_P}{C_P} = \frac{\Delta(P - P_\infty)}{(P - P_\infty)} + \frac{\Delta\rho}{\rho} + 2\frac{\Delta V}{V}$$

Equation Appendix 5.2.

As this is a very rough estimation, next equation is applied:

$$\left(\frac{\Delta C_P}{C_P}\right)^2 = \left(\frac{\Delta(P - P_\infty)}{(P - P_\infty)}\right)^2 + \left(\frac{\Delta\rho}{\rho}\right)^2 + \left(2\frac{\Delta V}{V}\right)^2$$

Equation Appendix 5.3.

Finally, the relative error of the pressure coefficient is:

$$\frac{\Delta C_P}{C_P} = \sqrt{\left(\frac{\Delta(P - P_\infty)}{(P - P_\infty)}\right)^2 + \left(\frac{\Delta\rho}{\rho}\right)^2 + \left(2\frac{\Delta V}{V}\right)^2}$$

Equation Appendix 5.4.

Where:

- $\Delta(P - P_\infty)$: for this value the accuracy of the manometer was taken.
- $(P - P_\infty)$ is the maximum measured pressure difference for each AoA.
- $\Delta\rho$ is the estimated variation of the air density during the experiment.
- ΔV is the expected variation of the free stream velocity (0.5 m/s).

The relative error of the air density is calculated applying the *equation Appendix 5.1* to the ideal gas equation:

$$P_{atm} = \rho R T$$

Equation Appendix 5.5.

$$\frac{\Delta\rho}{\rho} = \frac{\Delta P_{atm}}{P} + \frac{\Delta T}{T}$$

Equation Appendix 5.6.

upna Universidad Pública de Navarra Nafarroako Unibertsitate Publikoa
Todos los derechos reservados
Eskubide guztiak erresalbatu dira

The atmospheric pressure variation is the biggest difference between measured atmospheric pressures. In the same way, the temperature variation is also the biggest difference between the measured temperatures. From a conservative point, these two parameters had been multiplied by an uncertainty factor of 1.5. Since these parameters are valid for all the experiments the relative error of the air density can be calculated as a number.

$$\frac{\Delta\rho}{\rho} = \frac{\Delta P_{atm}}{P} + \frac{\Delta T}{T} = \frac{11 \cdot 1.5}{1013} + \frac{4 \cdot 1.5}{293.15} = 0.0367$$

Equation Appendix 5.7.

Once the relative error of the C_P is known, the maximum and the minimum C_L are calculated for each AoA using the trapezoid rule with maximum and minimum values of C_P. It is important to distinguish between the C_P in the pressure side (C_{Pp}) and the C_P in the suction side (C_{Ps}) of the airfoil.

- C_{Lmax} is calculated using the values of $C_{Pp} + \Delta C_P$ and $C_{Ps} - \Delta C_P$.
- C_{Lmin} is calculated using the values of $C_{Pp} - \Delta C_P$ and $C_{Ps} + \Delta C_P$.

Finally, the lift coefficient error would be:

$$\Delta C_L = C_{Lmax} - C_{Lmin}$$

Equation Appendix 5.8.

upna Universidad Pública de Navarra Nafarroako Unibertsitate Publikoa
Todos los derechos reservados
Eskubide guztiak erresalbatu dira

Appendix 6: Repeatability of the experiments.

Tests that took place in different days and with similar conditions yielded similar results. This fact points out good repeatability in the experiments.

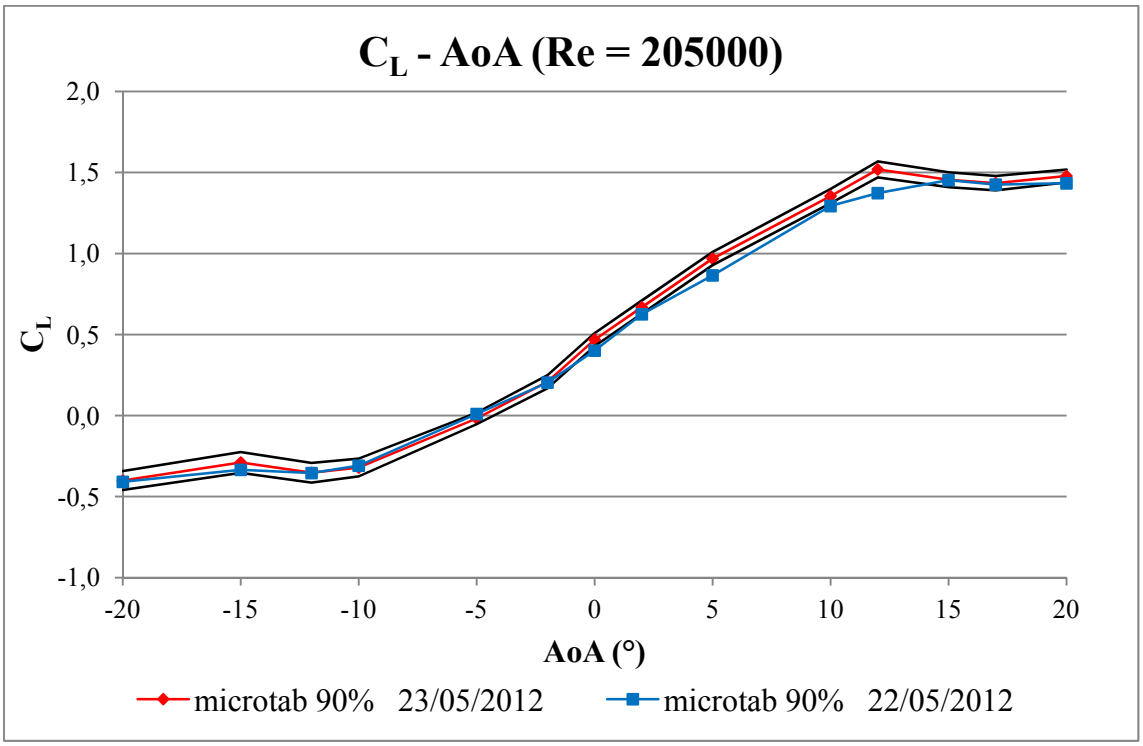

Figure Appendix 6.1. Results of tests performed in different days and similar conditions.

upna Universidad Pública de Navarra Nafarroako Unibertsitate Publikoa
Todos los derechos reservados
Eskubide guztiak erresalbatu dira

Bibliography

[1] Anderson, J.D. (2008). "*Introduction to Flight"*. McGraw-Hill, 6th edition.

[2] European Wind Energy Association (2012). "*Wind in Power"*. *2011 European Statistics*.

[3] J.F. Manwell, J.G. Mcgowan, A.L. Rogers (2009). "*Wind Energy Explained. Theory, Design and Application"*. Wiley

[4] S.J. Johnson, C.P. Van dam, D. Berg (2008). "*Active Load Control Techniques for Wind Turbines"*. Technical report, SANDIA National Laboratories.

[5] S.J. Johnson, C.P. Van dam, D. Berg (2010). "*An Overview of Active Load Control Techniques for Wind Turbines with an Emphasis on Microtabs"*. Wind Energy, 13:239-253.

[6] J.P. Baker, K.J Standish, C.P. Van Dam (2007). "*Two-Dimensional Wind Tunnel and Computational Investigation of a Microtab Modified Airfoil"*. Journal of Aircraft, 44(2):563-572.

[7] J. Ripa (2009). "*Energía Eólica. Tecnología Energética"*. Universidad Pública de Navarra.

[8] R. Tassinari (1995). "*El Producto Adecuado"*. Ed. Alfaomega.

[9] D.W Lobitz., P.S Veers, G.R. Eisler, D.J. Laino, P.G. Migliore, and G. Bir (2001). *"The Use of Twisted-Coupled Blades to Enhance the Performance of Horizontal Axis Wind Turbines".* SAND01-1303, Sandia National Laboratories, Albuquerque, NM, 2001.

[10] GE Wind Energy, LLC (2006). *"Advanced Wind Turbine Program Next Generation Turbine Development Project".* Subcontract Report NREL/SR-5000-38752, 2006.

[11] D.T. Yen, C.P. van Dam, F. Bräuchle, R.L. Smith , and S.D. Collins (2000). "*Active Load Control and Lift Enhancement Using MEM Translational Tabs*" Fluids 2000*,* AIAA-2000-2422, Denver, CO, June 2000.

[12] R.A. McD. Galbraith (1985). *"The aerodynamic characteristics of a GU25-5(11)8 aerofoil for low Reynolds numbers".* Experiments in Fluids 3, 253-256; Springer-Verlag (1985).

upna Universidad Pública de Navarra Nafarroako Unibertsitate Publikoa
Todos los derechos reservados
Eskubide guztiak erresalbatu dira

WEB SITES:

[13] W.J. Devenport and B.Vadapalli. *Panel Method Applet*. Department of Aerospace and Ocean Engineering, Virginia Tech. (http://www.engapplets.vt.edu/fluids/vpm/)

[14] UIUC *Airfoil Coordinates Database*. Department of Aerospace Engineering. University of Illinois. (http://www.ae.illinois.edu/m-selig/ads/coord_database.html)

[15] *Airfoil Investigation Database*. (http://www.worldofkrauss.com/)

[16] M. Hepperle. *Javafoil.* (http://www.mh-aerotools.de/airfoils/javafoil.htm)

upna Universidad Pública de Navarra Nafarroako Unibertsitate Publikoa
Todos los derechos reservados
Eskubide guztiak erresalbatu dira